N 62 10100
55/201-78
NASA TN D-1209

NASA TN D-1209

TECHNICAL NOTE

D-1209

ANALYSIS OF SOLAR-RADIATION SHIELDS FOR TEMPERATURE CONTROL OF SPACE VEHICLES SUBJECTED TO LARGE CHANGES IN SOLAR ENERGY

By George J. Nothwang, John C. Arvesen, and Frank M. Hamaker

Ames Research Center
Moffett Field, Calif.

NATIONAL AERONAUTICS AND SPACE ADMINISTRATION
WASHINGTON March 1962

NATIONAL AERONAUTICS AND SPACE ADMINISTRATION

TECHNICAL NOTE D-1209

ANALYSIS OF SOLAR-RADIATION SHIELDS FOR TEMPERATURE CONTROL OF SPACE VEHICLES SUBJECTED TO LARGE CHANGES IN SOLAR ENERGY

By George J. Nothwang, John C. Arvesen, and Frank M. Hamaker

SUMMARY

An analysis has been made of a passive temperature control system for a space vehicle which is subjected to variable solar energy. This system effectively isolates the capsule from the incident solar energy by the use of solar-radiation shields. The desired temperature level of the capsule could then be maintained by a constant internal heat load. The analysis was developed on the basis of diffusely reflecting isothermal surfaces and permits evaluation of the temperatures of various shield-capsule configurations. Several shield-capsule configurations were studied and parameters were established which indicate the important criteria for achieving the desired temperature control.

The analysis was applied to two specific vehicle configurations suitable for solar probe applications, and shield and capsule temperatures were calculated as the probe traveled from 1.0 to 0.1 astronomical unit from the sun. Typical results were obtained with a solar absorptance and thermal emittance and absorptance of 0.20 for all surfaces. For the conical capsule with a single shield, it was found that the temperature of the shield increased from 590° to 1900° R while the corresponding temperature of the conical capsule increased from 500° to 526° R. For a conical capsule with a double shield, the temperature of the first shield again increased from 590° to 1900° R but the corresponding temperature of the capsule rose only from 500° to 502° R. Thus, it is demonstrated that the temperature of a capsule can be controlled effectively with shield and capsule materials which have no unusually high or low absorptance and emittance characteristics.

The effects of specularly reflecting (instead of diffusely reflecting) surfaces and the effects of shield thermal conductivity on capsule temperature were also studied. Results from these studies were applied to the single-shield, conical-capsule configuration and it was found that these effects did not significantly alter the magnitude of temperature control achieved.

INTRODUCTION

All known materials, even those considered to be good reflectors, will absorb a fraction of incident radiation. Thus, any space vehicle subjected to solar radiation must absorb a certain amount of energy which (if the vehicle is in thermal equilibrium) must in turn be radiated from the vehicle. The amount of energy radiated, according to the Stefan-Boltzmann law, is proportional to the fourth power of the temperature of the surface. Thus, if the amount of incident solar energy varies over wide ranges, the temperature of the vehicle may also vary over an undesirably large range.

A535

This problem was exemplified in a report by Dugan (ref. 1) for a solar probe which traveled to within 0.1 astronomical unit of the sun. For the configuration studied, probe temperature changes on the order of hundreds of degrees Fahrenheit were calculated. However, the allowable temperature variations of such a vehicle are restricted by the temperature limits of the instrumentation. It is indicated in reference 2 that instruments may have to be maintained in the temperature range of 60° to 78° F (15° to 25° C) at all times. Thus, thermal control of such a vehicle is mandatory.

In general, two types of temperature control systems are used: active and passive (see ref. 2). Active systems generally involve mechanical devices, such as shutters, rotating fan blades, etc., to expose different surface materials with different surface properties to the incident radiation (see ref. 3). These systems may be complex and heavy and their reliability is always less than perfect. Therefore, a passive temperature control system is usually preferred if the desired temperature limits can be maintained.

One type of passive system that appears to have possible application is the use of solar radiation shields to completely isolate the instrument capsule from direct solar radiation. In this case, the ambient temperature of the capsule is a function of only the internal power of the capsule, the capsule surface area, and the thermal emittance. The use of such shields was mentioned briefly by Cornog (ref. 4), and Nichols (ref. 5) studied the use of disc-type solar shields in an active control system.

It is the purpose of the present study to evaluate the effectiveness of solar radiation shields for passive temperature control of vehicles subjected to large changes in solar energy. First, an analysis is made of the radiant heat-transfer processes which influence the temperatures of the shields and the shielded capsule. Then, several simple axially symmetric shield-capsule configurations are studied and parameters are established which indicate the important criteria for achieving the desired temperature control. For illustration, the results are applied to two solar probes that travel to within 0.1 astronomical unit of the sun.

The authors wish to thank Mr. Harvard Lomax of this Center for obtaining the numerical solutions for the cases of finite thermal conductivity in solar shields.

NOTATION

A	surface area, sq ft
A_x	projected surface area normal to direct solar radiation, sq ft
A_c'	area of capsule "seen" by the shield, sq ft
$B_1, B_2, \ldots, B_5$	constants defined by equations (32) through (36)
b	shield thickness, ft
$C_1, C_2, \ldots, C_8$	constants defined by equations (59) through (66)
$D(\varphi)$	intensity distribution function
E	solar flux at earth's distance from the sun, (129 watts/sq ft)
F	radiative heat-transfer configuration factor
$H(l)$	outgoing radiant flux from inner surface of the cone (appendix C), watts/sq ft
$I(l)$	incoming radiant flux to inner surface of the cone (appendix C), watts/sq ft
I_{av}	average intensity over all angles (eq. (5)), watts/sq ft steradian
$I(\varphi)$	directional intensity at viewing angle φ, watts/sq ft steradian
i, j, k	unit vectors along x, y, and z axes, respectively
K	kernel of integral equation (eq. (C10))
k	thermal conductivity, watts/$^{\circ}$R ft
L	slant length of cone, ft
l	distance along cone from apex to surface area dA, ft

m	exponent (eq. (B1))
n	number of reflections
$\bar{n}$	unit vector normal to dA, ft
Q	radiant energy, watts
Q_i	internal power of capsule, watts
R	radius of base of cone and radius of sphere, ft
$\bar{r}$	distance from the sun, astronomical units
S	distance between dA_a and dA_b, ft
T	temperature, $^{\circ}R$
T_{Qi}	capsule temperature due to internal power (eq. (44)), $^{\circ}R$
V	volume, cu ft
X, Y, Z	dimensionless integration parameters
x	distance between shield and capsule, ft
x, y, z	axes in Cartesian coordinate system
α	thermal absorptance
α_s	solar absorptance
$(\alpha_{s1})_{EFF}$	effective solar absorptance of first shield
β	semiapex angle of a cone, deg
δ	separation between apexes of two cones, between center of sphere and apex of cone (figs. 14 and 15), ft
ϵ	total hemispherical emittance
ζ	conical shield orientation parameter (appendix C)
θ	angle in the y-z plane as seen in figure 14, deg
ξ	Fredholm integration parameter (eqs. (C13) and (C17))
ρ	distance from apex of cone to elemental surface area or distance from center of sphere to elemental surface area, ft

σ Stefan-Boltzmann constant (502×10^{-12} watts/ft^2 $^{\circ}R^4$)

τ energy transfer factor (eqs. (51) and (68))

φ angle between the normal to an elemental area and a line connecting this elemental area with another, deg

ψ angle from x axis to position vector $\bar{\rho}$ as seen in figure 15, deg

ω solid angle, steradians

Subscripts

a surface a

b surface b

c capsule

INITIAL radiation transfer with no reflections

L lower limit of integration

max, min limits for specular reflections

n number of reflections

s solar energy

u upper limit of integration

o earth's distance from the sun (i.e., $\bar{r} = 1$)

1 front surface of first shield

2 back surface of first shield

3 front surface of second shield

4 back surface of second shield

1st first reflection

2nd second reflection

Superscripts

*	energy emitted
$(\bar{\ })$	vector notation

ANALYSIS

General Considerations

As the analysis of the radiative heat transfer associated with a capsule shielded from solar radiation is developed, a number of "ground rules" and assumptions are introduced. For clarity, these are collected in the following list:

1. The vehicle, which is composed of a capsule and one or more solar radiation shields, is oriented in the spatial environment so that solar radiation is incident on only the first shield and does not strike any other shield or the capsule.

2. The incident solar energy is composed of parallel rays and the flux varies as the inverse square of the distance from the sun.

3. Solar energy is the only source of incident radiation. (Other amounts of energy either reflected or emitted from planets are considered negligible.)

4. The capsule has an internal heat load, Q_1, which is constant.

5. The capsule has no concavity toward the shield.

6. The vehicle can be considered to be in thermal equilibrium at all times.

7. No heat is <u>conducted</u> from shield to shield or from shield to capsule or vice versa.

8. All surfaces emit energy diffusely, that is, the intensity distribution has a Lambertian or cosine variation.

9. All surfaces absorb a fraction of the incident energy and this fraction is independent of the angle of incidence.

10. The energy reflected from all surfaces is reflected diffusely, that is, the reflected intensity distribution has a cosine variation.

11. The surfaces of each shield or capsule are isothermal, that is, the thermal conductance is infinite.

Radiant Heat-Transfer Processes

General equations of radiative heat transfer from one surface element to another.- When two surface elements, dA_a and dA_b, located upon surfaces a and b, are situated so that they can "see" one another (see sketch) each will radiate energy to the other and a net exchange of energy from the hotter to the cooler area will result. The net amount of energy exchanged will be determined by the geometry, surface properties, and the absolute temperatures of the areas.

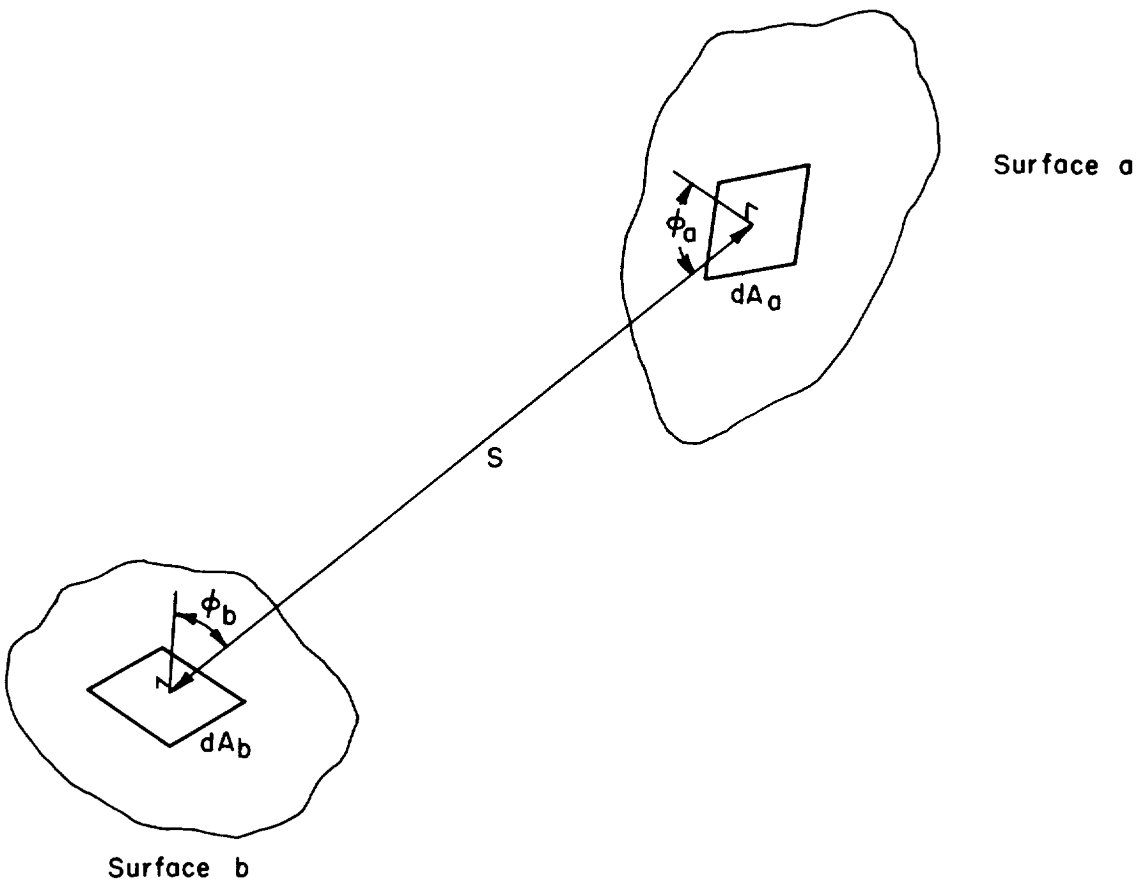

It can be seen from the sketch that the energy emitted from surface dA_a through the solid angle subtending dA_b is

$$d^2Q^*_{dA_a - dA_b} = I(\varphi_a) d\omega_a \cos \varphi_a \, dA_a \tag{1}$$

where $I(\varphi_a)$ is the directional intensity of radiation from surface dA_a at angle φ_a from the normal, and $d\omega_a$ is the solid angle to dA_b from dA_a. This angle may be expressed as

$$d\omega_a = \frac{\cos\varphi_b \, dA_b}{S^2} \tag{2}$$

Upon the substitution of equation (2), equation (1) becomes

$$d^2Q^*_{dA_a - dA_b} = I(\varphi_a) \frac{\cos\varphi_a \cos\varphi_b \, dA_a \, dA_b}{S^2} \tag{3}$$

$I(\varphi_a)$ may be expressed in terms of the average intensity, I_{av}, over surface dA_a by the relationship (ref. 6)

$$D(\varphi_a) = \frac{I(\varphi_a)}{I_{av}} \tag{4}$$

The average intensity over dA_a is defined as

$$I_{av} \equiv \frac{\epsilon_a \sigma T_a^4}{\pi} \tag{5}$$

Substitution of equations (4) and (5) into equation (3) will yield an expression for the energy incident upon dA_b due to energy emitted from dA_a at temperature T_a:

$$d^2Q^*_{dA_a - dA_b} = \epsilon_a \sigma T_a^4 D(\varphi_a) \frac{\cos\varphi_a \cos\varphi_b \, dA_a \, dA_b}{\pi S^2} \tag{6}$$

It should be pointed out that this equation yields only the amount of emitted energy from dA_a that is initially incident on dA_b and it does not consider any reflected energy between the two areas.

At this point the configuration factor, $dF_{dA_a - dA_b}$, is introduced and is defined as the fraction of the energy emitted by dA_a that is incident upon dA_b (see ref. 6). Since the energy emitted by dA_a is $\epsilon_a \sigma T_a^4 dA_a$ and the amount incident upon dA_b is given by equation (6), the configuration factor from dA_a to dA_b may be written as

$$dF_{dA_a - dA_b} = \frac{1}{dA_a} D(\varphi_a) \frac{\cos\varphi_a \cos\varphi_b \, dA_a \, dA_b}{\pi S^2} \tag{7}$$

and equation (6) may then be rewritten as

$$d^2Q^*_{dA_a - dA_b} = \epsilon_a \sigma T_a{}^4 dF_{dA_a - dA_b}\, dA_a \tag{8}$$

Radiant heat transfer between two finite surfaces.- It is possible to compute an average configuration factor for any two finite surfaces and any given intensity distribution, $D(\varphi_a)$, by integration of equation (7). For the present analysis, all surfaces will be assumed to emit energy with a Lambertian or cosine variation (i.e., $D(\varphi) = 1$) and the resulting equation is

$$F_{a-b} = \frac{1}{A_a} \int_{A_a} \int_{A_b} \frac{\cos \varphi_a \cos \varphi_b \, dA_a \, dA_b}{\pi S^2} \tag{9}$$

Integration of equation (9) can be accomplished with the use of high-speed electronic computers, and the techniques for several geometric configurations are given in appendix A.

If it is assumed that the surfaces are isothermal (i.e., the material has infinite thermal conductivity), the energy emitted by surface a that is initially incident on surface b can be expressed as (from eq. (8))

$$(Q^*_{a-b})_{INITIAL} = \epsilon_a \sigma T_a{}^4 F_{a-b} A_a \tag{10}$$

If the absorptance of surface b is assumed to be independent of the angle of incident radiation and is a constant, α_b, the amount of energy emitted by surface a that is initially absorbed by surface b is

$$(Q_{a-b})_{INITIAL} = \alpha_b \epsilon_a \sigma T_a{}^4 F_{a-b} A_a \tag{11}$$

Since no surface is a perfect absorber (i.e., $\alpha < 1$), the reflected energy must be included in the analysis. Following the method proposed by Christianson (see ref. 7) the reflected energy is considered as follows: Equation (11) gives the initial amount of energy absorbed by surface b. The fraction $(1 - \alpha_b)$ of the amount given in equation (10) is reflected. Assuming this energy is reflected in the same manner as energy is emitted (namely, with a Lambertian or cosine distribution) then the amount

$$(Q_{a-b-a})_{1st} = F_{b-a}(1 - \alpha_b) \epsilon_a \sigma T_a{}^4 F_{a-b} A_a \tag{12}$$

is incident on surface a. The fraction, α_a, of this energy is absorbed by surface a and again $(1 - \alpha_a)$ times this energy is reflected. Thus, a second amount of energy will be absorbed by surface b and it will be

$$(Q_{a-b-a-b})_{2nd} = \alpha_b \epsilon_a \sigma T_a^4 A_a F_{a-b}^2 F_{b-a}(1 - \alpha_b)(1 - \alpha_a) \tag{13}$$

Again some energy is reflected from surface b and it can be seen that for an infinite number of reflections the total energy absorbed by surface b is

$$Q_{a-b} = \alpha_b \epsilon_a \sigma T_a^4 F_{a-b} A_a \sum_{n=0}^{\infty} (1 - \alpha_a)^n (1 - \alpha_b)^n F_{a-b}^n F_{b-a}^n \tag{14}$$

A
5
3
5

Since all terms in the summation have values less than 1, the binomial theorem can be used to reduce equation (14) to the closed form

$$Q_{a-b} = \frac{\alpha_b \epsilon_a \sigma T_a^4 F_{a-b} A_a}{1 - (1 - \alpha_a)(1 - \alpha_b) F_{a-b} F_{b-a}} \tag{15}$$

Equation (15) is an expression for only the heat transfer from surface a to surface b. In order to perform a heat balance, a similar equation for heat transfer from surface b to surface a would have to be written.

<u>Energy emitted by a single concave surface</u>.- If any surface, called surface a, can "see itself" (such as the concave surface of a right circular cone), the surface will have an average configuration factor to itself, F_{a-a} (see appendix A). Thus, the amount of energy emitted by surface a that is initially incident on itself is

$$(Q_{a-a})_{INITIAL} = \epsilon_a \sigma T_a^4 F_{a-a} A_a \tag{16}$$

With the use of an analysis similar to that presented in the previous section, the total energy incident on surface a, considering an infinite number of reflections, can be shown to be

$$Q_{a-a} = \frac{\epsilon_a \sigma T_a^4 F_{a-a} A_a}{1 - (1 - \alpha_a) F_{a-a}} \tag{17}$$

and, therefore, the energy radiated from the entire concave surface is

$$Q_a{}^* = \frac{(1 - F_{a-a}) \epsilon_a \sigma T_a^4 A_a}{1 - (1 - \alpha_a) F_{a-a}} \tag{18}$$

Solar energy absorbed by a single concave surface.- The amount of solar radiation incident upon a concave surface is $(E/\bar{r}^2)A_x$. Again, there will be reflections within the concavity which can be summed in the same manner as in the two previous sections and the total energy absorbed by surface a can be shown to be

$$Q_{sa} = \frac{\alpha_{sa}(E/\bar{r}^2)A_x}{1 - (1 - \alpha_{sa})F_{a-a}} \tag{19}$$

where α_{sa} is the solar absorptance of surface a. It can be seen from the above equation that as F_{a-a} approaches 1 (the interior surface of a long slender cone approximates this case), surface a absorbs energy more nearly like a perfect absorber ($\alpha_s = 1$), regardless of the value of solar absorptance.

Applications to Shield-Capsule Configurations

Single shield configuration.- It is now possible to apply the derived equations of radiant heat transfer to the case of a single solar radiation shield between a capsule and the incident solar energy.

Let subscripts 1 and 2 refer to the shield's sunlit (front) and shaded (back) surfaces, respectively, and let the subscript c refer to the surface of the capsule. From equation (19) the total solar energy absorbed by surface 1 is

$$Q_{s1} = \frac{\alpha_{s1}(E/\bar{r}^2)A_x}{1 - (1 - \alpha_{s1})F_{1-1}} \tag{20}$$

The energy emitted by surface 1 (from eq. (18)) is then

$$Q_1{}^* = \frac{(1 - F_{1-1})A_1\epsilon_1\sigma T_1{}^4}{1 - (1 - \alpha_1)F_{1-1}} \tag{21}$$

The heat balance between the shield and capsule is not easily analyzed by the methods presented here if either the shield or capsule has a concavity. The present study is therefore simplified by assuming no concavity on the capsule. In addition, to simplify the analysis of the case where the shield has a concavity toward the capsule ($F_{2-2} > 0$), the analysis as presented also neglects the relatively small amount of energy that is reflected from the capsule back to the shield, is then reflected from one part of the shield to another, and is then eventually either absorbed in the shield or capsule or dissipated to space.

The energy emitted from the back surface of the shield can be determined in a manner similar to that required for equation (21).

$$Q_2{}^* = \frac{(1 - F_{2-2})A_2\epsilon_2\sigma T_2{}^4}{1 - (1 - \alpha_2)F_{2-2}} \tag{22}$$

The energy emitted from the shield, reflected from the capsule, and reabsorbed by the shield will consist of two components. The first will be the energy that is emitted directly to the capsule, is reflected from the capsule, and is reflected back and forth between the shield and capsule.

$$Q_{2-c-2} = \frac{\alpha_2 F_{2-c}F_{c-2}(1 - \alpha_c)\epsilon_2 A_2\sigma T_2{}^4}{1 - (1 - \alpha_2)(1 - \alpha_c)F_{2-c}F_{c-2}} \tag{23}$$

The second component will be the energy that is emitted from the shield directly to itself, is reflected within itself any number of times, and is then reflected an infinite number of times between shield and capsule.

$$Q_{2-2-c-2} = \frac{\alpha_2 F_{2-2}F_{2-c}F_{c-2}(1 - \alpha_2)(1 - \alpha_c)\epsilon_2 A_2\sigma T_2{}^4}{[1 - (1 - \alpha_2)(1 - \alpha_c)F_{2-c}F_{c-2}][1 - (1 - \alpha_2)F_{2-2}]} \tag{24}$$

The capsule has its own temperature, T_c, and will radiate energy to the shield. The amount absorbed is

$$\begin{aligned} Q_{c-2} = {} & \frac{\alpha_2 F_{c-2}A_c'\epsilon_c\sigma T_c{}^4}{1 - (1 - \alpha_2)(1 - \alpha_c)F_{2-c}F_{c-2}} + \frac{\alpha_2(1 - \alpha_2)F_{2-2}F_{c-2}A_c'\epsilon_c\sigma T_c{}^4}{1 - (1 - \alpha_2)F_{2-2}} \\ & + \frac{\alpha_2 F_{2-2}F_{2-c}F_{c-2}^2(1 - \alpha_2)^2(1 - \alpha_c)A_c'\epsilon_c\sigma T_c{}^4}{[1 - (1 - \alpha_2)(1 - \alpha_c)F_{2-c}F_{c-2}][1 - (1 - \alpha_2)F_{2-2}]} \end{aligned} \tag{25}$$

where A_c' is the area of the capsule "seen" by the shield. By the reciprocity theorem (ref. 7)

$$F_{c-2}A_c' = F_{2-c}A_2 \tag{26}$$

Equation (25) may now be rewritten as

$$Q_{c-2} = \frac{\alpha_2 F_{2-c} A_2 \epsilon_c \sigma T_c^4}{1 - (1 - \alpha_2)(1 - \alpha_c)F_{2-c}F_{c-2}} + \frac{\alpha_2 F_{2-2} F_{2-c}(1 - \alpha_2) A_2 \epsilon_c \sigma T_c^4}{1 - (1 - \alpha_2)F_{2-2}}$$

$$+ \frac{\alpha_2 F_{2-2} F_{2-c}^2 F_{c-2}(1 - \alpha_2)^2 (1 - \alpha_c) A_2 \epsilon_c \sigma T_c^4}{[1 - (1 - \alpha_2)(1 - \alpha_c)F_{2-c}F_{c-2}][1 - (1 - \alpha_2)F_{2-2}]} \qquad (27)$$

A heat balance may now be made upon the shield. Since there is no internally generated heat:

HEAT ABSORBED = HEAT EMITTED

In most practical configurations, the shield will be thin so that $A_1 = A_2$ and $T_1 = T_2$. The heat balance may now be evaluated from equations (20), (21), (22), (23), (24), and (27):

$$\frac{\alpha_{s1}(E/\bar{r}^2)A_x}{1 - (1 - \alpha_{s1})F_{1-1}} + \frac{\alpha_2 F_{2-c} F_{c-2}(1 - \alpha_c)\epsilon_2 A_2 \sigma T_2^4 + \alpha_2 F_{2-c} A_2 \epsilon_c \sigma T_c^4}{1 - (1 - \alpha_2)(1 - \alpha_c)F_{2-c}F_{c-2}} + \frac{\alpha_2 F_{2-2} F_{2-c}(1 - \alpha_2) A_2 \epsilon_c \sigma T_c^4}{1 - (1 - \alpha_2)F_{2-2}}$$

$$+ \frac{\alpha_2 F_{2-2} F_{2-c} F_{c-2}(1 - \alpha_2)(1 - \alpha_c)\epsilon_2 A_2 \sigma T_2^4 + \alpha_2 F_{2-2} F_{2-c}^2 F_{c-2}(1 - \alpha_2)^2 (1 - \alpha_c) A_2 \epsilon_c \sigma T_c^4}{[1 - (1 - \alpha_2)(1 - \alpha_c)F_{2-c}F_{c-2}][1 - (1 - \alpha_2)F_{2-2}]}$$

$$= \frac{(1 - F_{1-1})A_2 \epsilon_1 \sigma T_2^4}{1 - (1 - \alpha_1)F_{1-1}} + \frac{(1 - F_{2-2})A_2 \epsilon_2 \sigma T_2^4}{1 - (1 - \alpha_2)F_{2-2}} \qquad (28)$$

Similarly, a heat balance on the capsule may be made and evaluated to give

HEAT ABSORBED + INTERNAL HEAT = HEAT EMITTED

or

$$\frac{\alpha_c F_{2-c} A_2 \epsilon_2 \sigma T_2^4 + \alpha_c F_{2-c}^2 (1 - \alpha_2) A_2 \epsilon_c \sigma T_c^4}{[1 - (1 - \alpha_2)F_{2-2}][1 - (1 - \alpha_2)(1 - \alpha_c)F_{2-c}F_{c-2}]} + Q_i = \epsilon_c A_c \sigma T_c^4 \qquad (29)$$

Equations (28) and (29) may be solved simultaneously for capsule temperature and shield temperature as a function of surface properties, geometric configuration, internal heat, and distance from the sun:

$$T_c = \left[\frac{(B_1B_4/\bar{r}^2) + B_2Q_i}{B_2B_5 - B_3B_4}\right]^{1/4} \tag{30}$$

$$T_2 = \left[\frac{(B_1B_5/\bar{r}^2) + B_3Q_i}{B_2B_5 - B_3B_4}\right]^{1/4} \tag{31}$$

where

$$B_1 = \frac{\alpha_{s1}A_xE}{1 - (1 - \alpha_{s1})F_{1-1}} \tag{32}$$

A535

$$\begin{aligned} B_2 = {} & \frac{(1 - F_{1-1})A_2\epsilon_1\sigma}{1 - (1 - \alpha_1)F_{1-1}} + \frac{(1 - F_{2-2})A_2\epsilon_2\sigma}{1 - (1 - \alpha_2)F_{2-2}} \\ & - \frac{\alpha_2F_{2-2}F_{2-c}F_{c-2}(1 - \alpha_2)(1 - \alpha_c)\epsilon_2A_2\sigma}{[1 - (1 - \alpha_2)(1 - \alpha_c)F_{2-c}F_{c-2}][1 - (1 - \alpha_2)F_{2-2}]} \\ & - \frac{\alpha_2F_{2-c}F_{c-2}(1 - \alpha_c)\epsilon_2A_2\sigma}{1 - (1 - \alpha_2)(1 - \alpha_c)F_{2-c}F_{c-2}} \end{aligned} \tag{33}$$

$$\begin{aligned} B_3 = {} & \frac{\alpha_2F_{2-c}A_2\epsilon_c\sigma}{1 - (1 - \alpha_2)(1 - \alpha_c)F_{2-c}F_{c-2}} + \frac{\alpha_2F_{2-2}F_{2-c}(1 - \alpha_2)A_2\epsilon_c\sigma}{1 - (1 - \alpha_2)F_{2-2}} \\ & + \frac{\alpha_2F_{2-2}F_{2-c}^2F_{c-2}(1 - \alpha_2)^2(1 - \alpha_c)A_2\epsilon_c\sigma}{[1 - (1 - \alpha_2)(1 - \alpha_c)F_{2-c}F_{c-2}][1 - (1 - \alpha_2)F_{2-2}]} \end{aligned} \tag{34}$$

$$B_4 = \frac{\alpha_cF_{2-c}A_2\epsilon_2\sigma}{[1 - (1 - \alpha_2)F_{2-2}][1 - (1 - \alpha_2)(1 - \alpha_c)F_{2-c}F_{c-2}]} \tag{35}$$

$$B_5 = \epsilon_cA_c\sigma - \frac{\alpha_cF_{2-c}^2(1 - \alpha_2)A_2\epsilon_c\sigma}{[1 - (1 - \alpha_2)F_{2-2}][1 - (1 - \alpha_2)(1 - \alpha_c)F_{2-c}F_{c-2}]} \tag{36}$$

The total energy absorbed by the capsule may now be found by the substitution of equation (30) for the capsule temperature into equation (29) for the heat balance on the capsule:

$$\text{TOTAL HEAT ABSORBED} = Q_c = \epsilon_cA_c\sigma\left[\frac{(B_1B_4/\bar{r}^2) + B_2Q_i}{B_2B_5 - B_3B_4}\right] - Q_i \tag{37}$$

This absorbed energy consists of two components, (a) that due to solar irradiation and (b) that due to reflection and reradiation by the shield of the internal energy, Q_i. These two components may be evaluated by eliminating first, the effect of internal energy (i.e., $Q_i = 0$) and second, the effect of solar energy (i.e., $\bar{r} = \infty$). The energy absorbed as a result of solar irradiation is found to be

$$Q_{cs} = \epsilon_c A_c \sigma \left(\frac{B_1 B_4/\bar{r}^2}{B_2 B_5 - B_3 B_4}\right) \tag{38}$$

or for $\bar{r} = 1.0$

$$Q_{cso} = \epsilon_c A_c \sigma \left(\frac{B_1 B_4}{B_2 B_5 - B_3 B_4}\right) \tag{39}$$

The absorbed energy due to reflection and reradiation from the shield of emitted internal energy is

$$Q_{ci} = \epsilon_c A_c \sigma \left(\frac{B_2 Q_i}{B_2 B_5 - B_3 B_4}\right) - Q_i \tag{40}$$

or

$$\frac{Q_{ci}}{Q_i} = \epsilon_c A_c \sigma \left(\frac{B_2}{B_2 B_5 - B_3 B_4}\right) - 1 \tag{41}$$

From equations (30), (38), and (40) the temperature of the capsule can be written

$$T_c = \left(\frac{1}{\epsilon_c A_c \sigma}\right)^{1/4} \left(Q_{cs} + Q_{ci} + Q_i\right)^{1/4} \tag{42}$$

or

$$T_c = \left(\frac{Q_i}{\epsilon_c A_c \sigma}\right)^{1/4} \left[\left(\frac{Q_{cso}}{Q_i}\right)\left(\frac{1}{\bar{r}^2}\right) + \frac{Q_{ci}}{Q_i} + 1\right]^{1/4} \tag{43}$$

Let

$$T_{Qi} = \left(\frac{Q_i}{\epsilon_c A_c \sigma}\right)^{1/4} \tag{44}$$

which is the temperature the capsule would attain with no incident solar energy and no shield attached to the capsule. Therefore, equation (43) can be written in dimensionless form as

$$\frac{T_c}{T_{Qi}} = \left[\left(\frac{Q_{cso}}{Q_i}\right)\left(\frac{1}{\bar{r}^2}\right) + \frac{Q_{ci}}{Q_i} + 1\right]^{1/4} \tag{45}$$

If one wishes to compute a fractional capsule temperature change from the capsule temperature at the earth's distance from the sun ($\bar{r}$ = 1.0), the equation becomes

$$\frac{T_c - T_{co}}{T_{Qi}} = \left[\left(\frac{Q_{cso}}{Q_i}\right)\left(\frac{1}{\bar{r}^2}\right) + \frac{Q_{ci}}{Q_i} + 1\right]^{1/4} - \left(\frac{Q_{cso}}{Q_i} + \frac{Q_{ci}}{Q_i} + 1\right)^{1/4} \tag{46}$$

For a specific value of $\bar{r}$ the capsule temperature change is dependent on the magnitude of Q_{cso}/Q_i. If equation (39) is divided by Q_i, the resulting equation is

$$\frac{Q_{cso}}{Q_i} = \frac{\epsilon_c A_c \sigma}{Q_i}\left(\frac{B_1 B_4}{B_2 B_5 - B_3 B_4}\right) \tag{47}$$

It becomes convenient to define an effective solar absorptance of the solar shield as

$$(\alpha_{s1})_{EFF} = \frac{\alpha_{s1}}{1 - (1 - \alpha_{s1})F_{1-1}} \tag{48}$$

which, when substituted into equation (32), yields

$$B_1 = (\alpha_{s1})_{EFF} A_x E \tag{49}$$

Substitution of equation (49) in (47) yields

$$\frac{Q_{cso}}{Q_i} = (\alpha_{s1})_{EFF}\left(\frac{A_x E}{Q_i}\right)\left[\epsilon_c A_c \sigma \left(\frac{B_4}{B_2 B_5 - B_3 B_4}\right)\right] \tag{50}$$

The product of the first two quantities on the right side of the equation is the ratio of the solar energy absorbed by the shield at $\bar{r}$ = 1.0 to the internal power of the capsule. Therefore, the last term must be the ratio of the energy absorbed by the capsule (due only to solar irradiation) to the solar energy absorbed by the shield, and is a function of only the shield-capsule configuration and the thermal emittances and absorptances of each of the surfaces. (The same ratio can be obtained from equations (20), (48), (32), and (38).) This ratio is a measure of the ability

2A

of a shield-capsule configuration to transfer absorbed solar energy from the shield to the capsule and is termed the energy transfer factor, τ. Thus,

$$\tau = \epsilon_c A_c \sigma \left(\frac{B_4}{B_2 B_5 - B_3 B_4}\right) \tag{51}$$

and with this substitution, equation (50) becomes

$$\frac{Q_{cso}}{Q_i} = (\alpha_{s1})_{EFF} \left(\frac{A_x E}{Q_i}\right) \tau \tag{52}$$

The above equation shows the relationship of parameters that will, in turn, affect the temperature change of a capsule (eq. (46)) subjected to various amounts of solar energy.

Double-shield configuration.- The energy incident upon the capsule may be further decreased by the use of multiple shields. Because of the increased complexity of the resulting equations, only the effects of placing a flat shield (disc) between the primary shield and the capsule will be studied. The methods used to determine capsule temperature are similar to those used in the preceding section for the single shield. Again for thin shields $A_1 = A_2$, $T_1 = T_2$, $A_3 = A_4$, and $T_3 = T_4$. A heat balance on the first shield yields

$$\frac{\alpha_{s1}(E/\bar{r}^2)A_x}{1 - (1 - \alpha_{s1})F_{1-1}} + \frac{\alpha_2 F_{2-2} F_{3-2}(1 - \alpha_2)\epsilon_3 A_4 \sigma T_4^4}{1 - (1 - \alpha_2)F_{2-2}} + \frac{\alpha_2 F_{3-2}\epsilon_3 A_4 \sigma T_4^4 + \alpha_2 F_{2-3} F_{3-2}(1 - \alpha_3)\epsilon_2 A_2 \sigma T_2^4}{1 - (1 - \alpha_2)(1 - \alpha_3)F_{2-3}F_{3-2}}$$

$$+ \frac{\alpha_2 F_{2-2} F_{2-3} F_{3-2}(1 - \alpha_2)(1 - \alpha_3)\epsilon_2 A_2 \sigma T_2^4 + \alpha_2 F_{2-2} F_{2-3} F_{3-2}^2 (1 - \alpha_2)^2 (1 - \alpha_3)\epsilon_3 A_4 \sigma T_4^4}{[1 - (1 - \alpha_2)(1 - \alpha_3)F_{2-3}F_{3-2}][1 - (1 - \alpha_2)F_{2-2}]}$$

$$= \frac{(1 - F_{1-1})A_2 \epsilon_1 \sigma T_2^4}{1 - (1 - \alpha_1)F_{1-1}} + \frac{(1 - F_{2-2})A_2 \epsilon_2 \sigma T_2^4}{1 - (1 - \alpha_2)F_{2-2}} \tag{53}$$

Similarly, the heat balance on the intermediate shield will give

$$\frac{\alpha_3 F_{2-3} A_2 \epsilon_2 \sigma T_2^4 + \alpha_3 F_{2-3}(1 - \alpha_2)F_{3-2}\epsilon_3 A_4 \sigma T_4^4}{[1 - (1 - \alpha_2)F_{2-2}][1 - (1 - \alpha_2)(1 - \alpha_3)F_{2-3}F_{3-2}]}$$

$$+ \frac{\alpha_4 F_{4-c}\epsilon_c A_4 \sigma T_c^4 + \alpha_4 F_{c-4}(1 - \alpha_c)F_{4-c} A_4 \epsilon_4 \sigma T_4^4}{1 - (1 - \alpha_4)(1 - \alpha_c)F_{4-c}F_{c-4}} = A_4 \sigma T_4^4(\epsilon_3 + \epsilon_4) \tag{54}$$

Finally, the heat balance on the capsule will yield

$$\frac{\alpha_c F_{4-c} A_4 \epsilon_4 \sigma T_4^{\,4} + \alpha_c F_{4-c}^2 (1 - \alpha_4) A_4 \epsilon_c \sigma T_c^{\,4}}{1 - (1 - \alpha_4)(1 - \alpha_c) F_{4-c} F_{c-4}} + Q_i = \epsilon_c A_c \sigma T_c^{\,4} \tag{55}$$

Upon solving the three heat balance equations simultaneously for the temperatures of the capsule and the shields, the following equations are obtained:

$$T_c = \left[\frac{(C_1 C_4 C_7/\bar{r}^2) + (C_3 C_8 - C_2 C_4) Q_i}{C_3 C_6 C_8 - C_3 C_5 C_7 - C_2 C_4 C_8}\right]^{1/4} \tag{56}$$

$$T_4 = \left[\frac{(C_1 C_4 C_8/\bar{r}^2) + C_3 C_5 Q_i}{C_3 C_6 C_8 - C_3 C_5 C_7 - C_2 C_4 C_8}\right]^{1/4} \tag{57}$$

$$T_2 = \left\{\frac{[(C_1 C_6 C_8 - C_1 C_5 C_7)/\bar{r}^2] + C_2 C_5 Q_i}{C_3 C_6 C_8 - C_3 C_5 C_7 - C_2 C_4 C_8}\right\}^{1/4} \tag{58}$$

where the constants C_1 through C_8 have the values

$$C_1 = \frac{\alpha_{s1} A_x E}{1 - (1 - \alpha_{s1}) F_{1-1}} \tag{59}$$

$$C_2 = \frac{\alpha_2 F_{3-2} \epsilon_3 A_4 \sigma}{1 - (1 - \alpha_2)(1 - \alpha_3) F_{2-3} F_{3-2}} + \frac{\alpha_2 F_{2-2} F_{3-2} (1 - \alpha_2) \epsilon_3 A_4 \sigma}{1 - (1 - \alpha_2) F_{2-2}}$$
$$+ \frac{\alpha_2 F_{2-2} F_{2-3} F_{3-2}^2 (1 - \alpha_2)^2 (1 - \alpha_3) \epsilon_3 A_4 \sigma}{[1 - (1 - \alpha_2)(1 - \alpha_3) F_{2-3} F_{3-2}][1 - (1 - \alpha_2) F_{2-2}]} \tag{60}$$

$$C_3 = \frac{(1 - F_{1-1}) A_2 \epsilon_1 \sigma}{1 - (1 - \alpha_1) F_{1-1}} + \frac{(1 - F_{2-2}) A_2 \epsilon_2 \sigma}{1 - (1 - \alpha_2) F_{2-2}} - \frac{\alpha_2 F_{2-3} F_{3-2} (1 - \alpha_3) \epsilon_2 A_2 \sigma}{1 - (1 - \alpha_2)(1 - \alpha_3) F_{2-3} F_{3-2}}$$
$$- \frac{\alpha_2 F_{2-2} F_{2-3} F_{3-2} (1 - \alpha_2)(1 - \alpha_3) \epsilon_2 A_2 \sigma}{[1 - (1 - \alpha_2)(1 - \alpha_3) F_{2-3} F_{3-2}][1 - (1 - \alpha_2) F_{2-2}]} \tag{61}$$

$$C_4 = \frac{\alpha_3 F_{2-3} A_2 \epsilon_2 \sigma}{[1 - (1 - \alpha_2) F_{2-2}][1 - (1 - \alpha_2)(1 - \alpha_3) F_{2-3} F_{3-2}]} \tag{62}$$

$$C_5 = \frac{\alpha_4 F_{4-c} \epsilon_c A_4 \sigma}{1 - (1 - \alpha_4)(1 - \alpha_c) F_{4-c} F_{c-4}} \tag{63}$$

$$C_6 = A_4(\epsilon_3 + \epsilon_4)\sigma - \frac{\alpha_3 F_{2-3}(1 - \alpha_2)F_{3-2}\epsilon_3 A_4 \sigma}{[1 - (1 - \alpha_2)F_{2-2}][1 - (1 - \alpha_2)(1 - \alpha_3)F_{2-3}F_{3-2}]}$$

$$- \frac{\alpha_4 F_{c-4}(1 - \alpha_c)F_{4-c}A_4 \epsilon_4 \sigma}{1 - (1 - \alpha_4)(1 - \alpha_c)F_{4-c}F_{c-4}} \tag{64}$$

$$C_7 = \frac{\alpha_c F_{4-c} A_4 \epsilon_4 \sigma}{1 - (1 - \alpha_4)(1 - \alpha_c)F_{4-c}F_{c-4}} \tag{65}$$

$$C_8 = \epsilon_c A_c \sigma - \frac{\alpha_c F_{4-c}^2 (1 - \alpha_4) A_4 \epsilon_c \sigma}{1 - (1 - \alpha_4)(1 - \alpha_c)F_{4-c}F_{c-4}} \tag{66}$$

The temperature change of a double-shielded capsule is again given in terms of energies by equation (46) where

$$\frac{Q_{ci}}{Q_i} = \epsilon_c A_c \sigma \left(\frac{C_3 C_6 - C_2 C_4}{C_3 C_6 C_8 - C_3 C_5 C_7 - C_2 C_4 C_8}\right) - 1 \tag{67}$$

and Q_{cso}/Q_i is given by equation (52). The energy transfer factor is now

$$\tau = \epsilon_c A_c \sigma \left(\frac{C_4 C_7}{C_3 C_6 C_8 - C_3 C_5 C_7 - C_2 C_4 C_8}\right) \tag{68}$$

and $(\alpha_{s1})_{EFF}$ is given by equation (48).

RESULTS AND DISCUSSION

The equations presented in the Analysis section of this report provide the tools required for evaluating solar-shield-type passive temperature control systems. First, the effects of shield-capsule configuration, solar absorptance, and thermal emittance and absorptance on system performance will be studied. Second, the analysis will be applied to the temperature control problem of a solar probe to demonstrate the effectiveness of the solar-shield-type temperature control system. Third, the limitations of the analysis will be discussed.

Capsule Temperature Change

The purpose of any spacecraft temperature control system is to minimize the changes in capsule temperature while the vehicle is traveling in a prescribed trajectory. Equation (46) expresses the capsule temperature change (the reference temperature, T_{co}, is the capsule temperature when the vehicle is 1 astronomical unit from the sun) in terms of the parameters, Q_{cso}/Q_i, Q_{ci}/Q_i, and $\bar{r}$. For the more practical configurations studied, the parameter Q_{ci}/Q_i (eq. (41)), is very much less than 1. (The magnitude of Q_{ci}/Q_i will be shown later for various configurations.) Therefore, equation (46) can be reduced to

$$\frac{T_c - T_{co}}{T_{Qi}} = \left[\left(\frac{Q_{cso}}{Q_i}\right)\left(\frac{1}{\bar{r}^2}\right) + 1\right]^{1/4} - \left(\frac{Q_{cso}}{Q_i} + 1\right)^{1/4} \qquad (69)$$

A535

Results from the above equation are shown in figure 1 to indicate capsule temperature change as a function of the parameter, Q_{cso}/Q_i, for vehicles which travel from the earth to various distances from the sun. It can be seen that for a prescribed temperature change of the capsule, the value of the parameter Q_{cso}/Q_i must become smaller if the mission requires that the vehicle travel closer to the sun. Thus, the parameter Q_{cso}/Q_i is a measure of the temperature-control-system performance.

Equation (52) shows that Q_{cso}/Q_i is simply the product of the parameters $(\alpha_{s1})_{EFF}$, $(A_X E/Q_i)$, and τ. The quantity, $A_X E/Q_i$, is the ratio of the amount of solar energy incident on a vehicle at the earth's distance from the sun to the internal power of the capsule. Generally, the frontal area of the vehicle is chosen as a design parameter and the internal power is dictated by the payload instrumentation. Thus, one will not generally have a wide choice of the value of $A_X E/Q_i$ for any specific vehicle. Minimization of Q_{cso}/Q_i will then require minimization of the product of $(\alpha_{s1})_{EFF}$ and τ. The effect of shield-capsule geometry on these parameters is discussed in the next two sections.

Effective solar absorptance.- The effective solar absorptance is given by equation (48). For a shield which has a concavity toward the sun, there will be a configuration factor to itself, F_{1-1} (see appendix A), and the effective solar absorptance will be greater than the solar absorptance of the material by itself. In the case of a conical shield with the open end (base of the cone) toward the sun, the configuration factor to itself becomes

$$F_{1-1} = 1 - \frac{A_X}{A_1} = 1 - \sin\beta \qquad (70)$$

where β is the semiapex angle of the cone, and the effective solar absorptance from equation (48) becomes

$$(\alpha_{s1})_{EFF} = \frac{\alpha_{s1}}{1 - (1 - \alpha_{s1})(1 - \sin \beta)} \tag{71}$$

Results from this equation are presented in figure 2. It can be seen that for small cone angles the effective solar absorptance approaches 1. This exemplifies the ability of a long slender cone to absorb energy more nearly like a black body even though the absorptance of the material is relatively low. Thus, it is seen that the effective solar absorptance can be several times the solar absorptance of the material.

Energy transfer factor.- The energy transfer factor, τ, for a single-shield configuration is expressed in equation (51). It is the fraction of the solar energy absorbed by the first shield that is absorbed by the capsule. As indicated by this equation, the energy transfer factor is dependent only on the shield-capsule configuration and on the thermal emittance and absorptance of the shields and capsule. The effects of these parameters for typical configurations are shown in figures 3 through 5.

Energy transfer factors are shown in figure 3 for a conical-shield, conical-capsule configuration with various conical-shield semiapex angles and several values of thermal emittance and absorptance. The configuration is shown on the top of the figure and the radius of the base of the conical shield is chosen to be equal to the radius of the base of the conical capsule for all shield semiapex angles. In addition, these results are for the case where the thermal emittance and absorptance for all surfaces of the shield and capsule were identical (i.e., $\alpha_1 = \epsilon_1 = \alpha_2 = \epsilon_2 = \alpha_c = \epsilon_c$).

It can be seen from figure 3 that for this particular configuration and the range of α and ϵ presented, the energy transfer factor, τ, varies by four orders of magnitude. The highest values of τ occur at $\beta = 169^o$ where the shield completely encloses the front of the capsule. The lowest values of τ occur at the lowest values of β, α, and ϵ.

In order to show the effects of capsule configuration, τ was also computed for a conical-shield, spherical-capsule configuration and the results are compared with the conical-capsule configuration in figure 4. At particular values of β and $\alpha = \epsilon$, τ is at least twice as great for the spherical capsule as it is for the conical capsule. This results from the higher configuration factors between the shield and spherical capsule.

The configurations studied so far have had a fixed distance between the apex of the conical shield and the capsule. Effects of variation of this distance on τ are shown in figure 5 for two conical-shield angles and two values of α and ϵ. It can be seen that τ decreases with an increase in distance between shield and capsule. Also note that the change in τ due to increasing x/R from 0 to 1.0 is of the same order of magnitude as that due to changing β from 90° to 45°.

Multiple-shield configurations can be expected to yield smaller values of τ than the single-shield types. Thus, the analysis was extended to the double-shield capsule configuration where the first shield can be of arbitrary shape and the second shield is a disc. Energy transfer factor, τ, is expressed by equation (68) and results from this equation for the configurations chosen are shown in figure 6. It can be seen that for $\beta = 45^{\circ}$ and $\alpha = \epsilon = 1.0$ or 0.1, the position of the disc
does not appreciably change τ. Even with $\beta = 90^{\circ}$ and $\alpha = \epsilon = 1.0$, the A
position of the disc has little effect on τ. However, for $\beta = 90^{\circ}$ 5
and $\alpha = \epsilon = 0.1$, the position of the disc has a pronounced effect on τ 3
because, as the two parallel discs approach each other, the reflected 5
energy suffers more reflections, and thus more absorption, between the parallel discs and less energy is dissipated to space.

A comparison of figures 5 and 6 indicates that, for given values of β, α, and ϵ, the double-shield configuration has substantially smaller values of τ than does the single-shield configuration. The greatest decrease occurs for the lower values of α and ϵ. In general, the combination of highly reflecting surfaces and multiple-shield arrangements will yield the lowest values of τ.

The foregoing results presented in figures 3 through 6 were taken from a complete set of calculations made with an IBM 7090 computer for single- and double-shield configurations and both conical and spherical capsules. The input variables were conical shield angle, distance from the shield to capsule, and thermal emittance and absorptance. These calculations yielded configuration factors, τ and Q_{ci}/Q_i, which are tabulated in tables I through IV. The configuration is shown at the top of each table and, in these calculations, the thermal emittance and absorptance of the shields were chosen to be the same as those for the capsule. Note that for most practical configurations, the ratio Q_{ci}/Q_i is very much less than 1.0 and, therefore, as mentioned before, equation (69) can be used to calculate capsule temperature change.

Equilibrium Temperatures of a Solar Probe

It was indicated in the Introduction that one of the most severe thermal control problems of space vehicles was that associated with a solar probe which would travel from the earth to within 0.1 astronomical unit of the sun. Results from the foregoing analysis are applied to this problem to demonstrate the use of solar radiation shields in a passive temperature control system for a space vehicle subjected to variable solar energy. The configurations chosen are only typical and have not been optimized in any respect.

Figure 7 shows the configurations that were studied. The probe is assumed to be a vehicle with a total capsule volume of 4.0 cubic feet and an internal heat load, Q_i, of 100 watts. The conical capsule has a length to diameter ratio of 2 and its total surface area (including the base) is 15.61 square feet. The emittance of the capsule surface is chosen so that the surface temperature is 500° R when no external energy is absorbed by the capsule and no shield is attached, that is, T_{Qi} is 500° R. The resulting thermal emittance of the capsule, ϵ_c, is 0.20. For simplicity in this analysis, thermal absorptance, α, and thermal emittance, ϵ, of the shields are chosen to be the same as ϵ_c. Two values of solar absorptance, α_{s1}, of 0.2 and 1.0 were chosen since most materials have solar absorptances in this range.

Equilibrium temperatures of the capsule were computed from equations (30) and (56) as a function of distance of the probe from the sun, and the results are plotted in figure 8. It can be seen that for $\bar{r}$ in the range from 0.1 to 1.0 and $\alpha_{s1} = 0.2$ the capsule temperature change is 26° F for the single-shield configuration and only 2° F for the double-shield configuration. For $\alpha_{s1} = 1.0$, the corresponding capsule temperature changes are only 80° F and 7° F, respectively.

For comparison, the equilibrium temperature of the same capsule without solar radiation shields is

$$T_c = \left[\left(\frac{\alpha_{sc}}{\epsilon_c}\right)\left(\frac{A_x}{A_c}\right)\left(\frac{E}{\sigma\bar{r}^2}\right) + \frac{Q_i}{\epsilon_c A_c \sigma}\right]^{1/4} \qquad (72)$$

where ϵ_c is again 0.20 and ratios of α_{sc}/ϵ_c are set equal to 5.0, 1.0, and 0.1. The results are shown in figure 9. For α_{sc}/ϵ_c equal to 5.0 and for $\bar{r}$ in the range from 0.1 to 1.0, the temperature change is about 1490° F. Even for α_{sc}/ϵ_c equal to 0.1, the capsule temperature change is about 360° F.

Thus, for this example, the use of solar shields can reduce the capsule temperature variation by at least one to two orders of magnitude from that attainable with an unshielded capsule. Moreover these low temperature variations can be achieved with conventional materials with no unusual emissive or absorptive properties.

Shield materials will be chosen not only for their absorptive and emissive properties but also for their ability to withstand the temperatures they will reach in the spatial environment. The shield temperatures for the solar probe configurations were computed from equations (31), (57), and (58) and are shown in figure 10 as a function of distance from the sun. At $\bar{r} = 0.1$ the maximum shield temperature is about 2620° R for the 45° conical shield with $\alpha_{s1} = 1.0$; the corresponding shield temperature with $\alpha_{s1} = 0.2$ is only 1900° R. These temperatures are below the maximum allowable temperatures of various materials but indicate that care in selection of the first shield material is necessary. The temperature of the second shield (disc) is appreciably lower than that of the first shield and should present no unusual problems in material selection. Also note that the temperature of the 45° conical shield is the same whether the shield is the only shield (as in the single shield configuration) or the first shield of the double-shield configuration. These results indicate that, for these configurations, the presence of the capsule with its internal power and/or the intermediate shield has a negligible effect on the first shield temperature.

It should be noted that the above results are for α_{s1}/ϵ of the shields of 1.0 and 5.0 with the highest shield temperatures corresponding to the highest α_{s1}/ϵ. Thus, lower shield temperatures will be obtained with materials which have lower values of α_{s1}/ϵ.

The results of the equilibrium temperatures of a solar probe have been shown for the specific sizes shown in figure 7. These results are also applicable to any other size of vehicle which is geometrically scaled and where the ratio of internal power to capsule surface area is the same.

The equilibrium temperatures of a solar probe have been presented for the case where the frontal area of the first shield is the same as that for the capsule. It is recognized that when the probe approaches the sun, the first shield frontal area will have to be larger than the capsule frontal area to shade the capsule completely. For the single-shield, conical-capsule configuration shown in figure 7(a), complete shading of the capsule at 0.1 astronomical unit requires the radius of the first shield to be increased to 1.255 feet; the frontal area of the shield would then be increased by 63 percent. As this probe travels in the range of $0.1 \leq \bar{r} \leq 1.0$, the capsule temperature changes are 36° and 110° F for $\alpha_{s1} = 0.2$ and 1.0, respectively. The corresponding capsule temperature changes for the probe with the smaller shield (see fig. 8) are 26° and 80° F, respectively. Therefore, an increase in shield frontal area relative to capsule frontal area does increase the temperature change of the capsule but does not significantly alter the magnitude of temperature control achieved.

Limitations of Analysis

One basic assumption used throughout the Analysis section of this report is that the shield and capsule surfaces emit energy in a Lambertian or cosine distribution (i.e., $D(\varphi) = 1$). If one wishes to use a different intensity distribution function, equation (9) must include this function under the integral (see eq. (7)) and the method of determining configuration factors given in appendix A must be modified.

Two additional assumptions made in the analysis deserve consideration in terms of their influence on the magnitude of temperature control which can be achieved. These assumptions are (a) that the surfaces reflect diffusely and (b) that the thermal conductivity of the shields and capsule is infinite. The effects of these assumptions are evaluated by comparing results of the foregoing analysis to the analyses for the cases of specular reflections and zero thermal conductivity. These analyses are presented in appendixes B and C, respectively, and the results are applied to the single-shield, solar-probe configuration as an example.

Specular reflectance.- Because of the complexity of a specular reflection analysis, it was possible to evaluate only the limiting cases of maximum and minimum energy transferred to the capsule and the corresponding maximum and minimum capsule temperatures. These temperatures were calculated for the single-shield, solar-probe configuration (see fig. 7(a)) as a function of $\bar{r}$ and are presented in figure 11 along with the results of the diffuse reflection analysis. At $\bar{r} = 0.1$, the maximum capsule temperature is 537° R for the specular reflection case as compared to 526° R for the diffuse reflection case. It can also be seen that at a particular value of $\bar{r}$, both the maximum and minimum capsule temperatures for the specular reflection case are higher than that for the diffuse reflection case. This is a result of the relatively high $(\alpha_{s1})_{EFF}$ for specular reflections in the 45° conical shield example. (See appendix B.) Thus, it can be seen that differences in capsule temperature can result which might be significant between the cases of specular and diffuse reflections.

The results in appendix B indicate that $(\alpha_{s1})_{EFF}$ and τ for the case of specular reflections vary considerably from those for the case of diffuse reflections as the conical shield angle is changed. Therefore, capsule temperatures will also vary between the two cases. The temperature changes of the conical capsule with a single conical shield of various semiapex angles were computed for the specular and diffuse reflection cases as the vehicle traveled from $\bar{r}$ of 1.0 to 0.1. The results are shown in figure 12. It is evident that for β less than 50°, the percentage temperature differences between the specular and diffuse reflection analyses are substantial although the actual temperature differences are only about 10° F. For $50^\circ \leq \beta \leq 90^\circ$, the specular analysis indicates capsule temperature changes slightly smaller than those for the diffuse case. For $\beta > 90^\circ$, the large differences in capsule temperature change result from the differences in energy transfer factor for the diffuse and specular analyses as discussed in appendix B.

Shield thermal conductance.- From the practical viewpoint, the capsule of a solar probe can be considered to be isothermal whereas a shield constructed from thin materials may not be able to conduct heat along the shield and appreciable temperature gradients may exist. Appendix C contains an analysis for computing the temperature distribution along a radial line of the cone which has a finite thermal conductance and is exposed to solar radiation. In order to determine the effects of thermal conductance on the capsule temperature of the single-shield, solar-probe configuration, the analysis was applied to a 45° cone of zero thermal conductance to determine the maximum and minimum temperatures the conical shield could attain. It was then assumed that the entire shield was maintained at these extreme temperatures and the corresponding capsule temperatures were computed. The results are shown in figure 13 along with the infinite thermal conductance results. At $\bar{r} = 0.1$, it can be seen that with zero conductance the maximum capsule temperature is approximately 542° R and the minimum is 523° R; whereas the infinite conductance results show a capsule temperature of about 526° R. Thus, when one considers that these results are for extreme limits, it appears that the analysis as presented in this report yields reasonable approximations for capsule temperatures even when low-conductance shields are used.

A
5
3
5

CONCLUDING REMARKS

It has been shown that shields can be used to effectively isolate a capsule from direct solar radiation and, thereby, achieve passive temperature control of a space vehicle subjected to variable solar energy. The ambient capsule temperature is then primarily a function of internal power, surface area, and thermal emittance.

An analysis of the radiative heat-transfer processes for simple axially symmetric shield-capsule configurations indicates that the required temperature range of an instrumented capsule may be maintained with materials that have no unusually high or low absorptance and emittance characteristics.

Examination of two basic assumptions made in the analysis, (a) diffusely reflecting surfaces and (b) isothermal surfaces (infinite thermal conductance), indicates that no serious changes in magnitude of temperature control will be incurred if the analysis is applied to vehicles that have specularly reflecting surfaces or thin shields (i.e., zero thermal conductance).

The analysis of the radiative heat transfer associated with a capsule shielded from solar-radiation was applied to configurations with only conical and flat-disc first shields whose frontal areas were the same as the frontal area of the capsule. However, the analysis can be applied to any first-shield configuration for which configuration factors can be calculated and for which direct solar radiation is incident on only the first shield (i.e., the capsule and/or additional shields are in shadow at all times). Thus, if a space vehicle requires the use of a parabolic solar collector, this collector can also be used as a solar radiation shield for other components of the vehicle.

Ames Research Center
National Aeronautics and Space Administration
Moffett Field, Calif., Dec. 27, 1961

APPENDIX A

DETERMINATION OF CONFIGURATION FACTORS

FOR CONES AND SPHERES

The calculations for the configuration factors between two cones and a cone and a sphere were performed with an I.B.M. 704 computer. The necessary equations for these computations are derived in this appendix.

CONFIGURATION FACTOR BETWEEN TWO CONES

The geometric configuration for two cones is shown in figure 14. The coordinate positions of points on each cone, the distance between the points, and the unit normals to the cone surfaces at the points are shown as vectors. These vectors may be expressed in component form as

$$\left.\begin{aligned}
\bar{\rho}_a &= \rho_a(i \cos \beta_a + j \sin \beta_a \sin \theta_a + k \sin \beta_a \cos \theta_a) \\
\bar{\rho}_b &= \rho_b(i \cos \beta_b + j \sin \beta_b \sin \theta_b + k \sin \beta_b \cos \theta_b) \\
\bar{n}_a &= -i \sin \beta_a + j \cos \beta_a \sin \theta_a + k \cos \beta_a \cos \theta_a \\
\bar{n}_b &= i \sin \beta_b - j \cos \beta_b \sin \theta_b - k \cos \beta_b \cos \theta_b \\
\bar{\delta} &= i\delta
\end{aligned}\right\} \tag{A1}$$

The distance vector between the two points is

$$\bar{S} = \bar{\delta} + \bar{\rho}_a - \bar{\rho}_b \tag{A2}$$

The angles, φ_a and φ_b, between the distance vector and the normals to the surfaces can be obtained from the scalar product relationships:

$$\left.\begin{aligned}
\cos \varphi_a &= -\frac{\bar{n}_a \cdot \bar{S}}{|n||S|} = -\frac{\bar{n}_a \cdot \bar{\delta} + \bar{n}_a \cdot \bar{\rho}_b}{|S|} \\
\cos \varphi_b &= \frac{\bar{n}_b \cdot \bar{\delta} + \bar{n}_b \cdot \bar{\rho}_a}{|S|}
\end{aligned}\right\} \tag{A3}$$

The elemental areas located at $\overline{\rho}_a$ and $\overline{\rho}_b$ are given by

$$\left.\begin{aligned} dA_a &= \rho_a \sin \beta_a \, d\rho_a \, d\theta_a \\ dA_b &= \rho_b \sin \beta_b \, d\rho_b \, d\theta_b \end{aligned}\right\} \qquad \text{(A4)}$$

Equations (A1) are substituted into equations (A2) and (A3) and the resulting equations together with equations (A4) are substituted into the expression for the configuration factor, equation (9):

$$F_{a-b} = \frac{1}{\pi A_a} \iiiint \left\{\delta \sin \beta_a - \rho_b \left[\sin \beta_a \cos \beta_b - \sin \beta_b \cos \beta_a \cos(\theta_a - \theta_b)\right]\right\}$$
$$\left(\frac{\left\{\delta \sin \beta_b - \rho_a \left[\sin \beta_a \cos \beta_b \cos(\theta_a - \theta_b) - \sin \beta_b \cos \beta_a\right]\right\} \rho_a \rho_b \sin \beta_a \sin \beta_b \, d\rho_a \, d\rho_b \, d\theta_a \, d\theta_b}{\left\{\delta^2 + 2\delta(\rho_a \cos \beta_a - \rho_b \cos \beta_b) + \rho_a^2 + \rho_b^2 - 2\rho_a\rho_b \left[\cos \beta_a \cos \beta_b + \sin \beta_a \sin \beta_b \cos(\theta_a - \theta_b)\right]\right\}^2}\right) \qquad \text{(A5)}$$

Because of axial symmetry, one integration can be readily performed and equation (A5) reduces to

$$F_{a-b} = \frac{4 \sin \beta_a \sin \beta_b}{A_a} \int_0^{L_a} \int_0^{L_b} \int_0^{\theta_u} \left[\delta \sin \beta_a - \rho_b(\sin \beta_a \cos \beta_b - \sin \beta_b \cos \beta_a \cos \theta)\right]$$
$$\left\{\frac{\left[\delta \sin \beta_b - \rho_a(\sin \beta_a \cos \beta_b \cos \theta - \sin \beta_b \cos \beta_a)\right] \rho_a \rho_b \, d\rho_a \, d\rho_b \, d\theta}{\left[\delta^2 + 2\delta(\rho_a \cos \beta_a - \rho_b \cos \beta_b) + \rho_a^2 + \rho_b^2 - 2\rho_a\rho_b(\cos \beta_a \cos \beta_b + \sin \beta_a \sin \beta_b \cos \theta)\right]^2}\right\} \qquad \text{(A6)}$$

where $\theta = (\theta_a - \theta_b)$ and L_a and L_b are the slant heights of the respective cones. The largest value that θ_u (θ_u is the upper limit of θ) can take is π radians and this limit will be restricted by the situation where the distance vector, $\overline{S}$, becomes tangent to one of the conical surfaces. This condition is equivalent to $\cos \varphi_a = 0$ or $\cos \varphi_b = 0$ which gives, from equations (A3), two possible values for θ_u:

$$\left.\begin{aligned} \cos \theta_u &= \frac{\tan \beta_a}{\sin \beta_b}\left(\cos \beta_b - \frac{\delta}{\rho_b}\right) \\ \cos \theta_u &= \frac{\tan \beta_b}{\sin \beta_a}\left(\cos \beta_a + \frac{\delta}{\rho_a}\right) \end{aligned}\right\} \qquad \text{(A7)}$$

If both of these cosines are greater than unity in absolute value, then $\theta_u = \pi$. If one of the two cosines is less than unity in absolute value, then that one will determine the value of θ_u. If both of the cosines are within the unity limits, then the equation giving the smallest value of θ_u is the deciding one.

To facilitate computation the equations can be put into dimensionless forms:

$$F_{a-b} = \frac{4\sin\beta_b}{\pi}\int_0^1\int_0^{\frac{\sin\beta_a}{\sin\beta_b}}\int_0^{\theta_u}\left[\frac{Z}{Y}\sin\beta_a - (\sin\beta_a\cos\beta_b - \sin\beta_b\cos\beta_a\cos\theta)\right]$$
$$\left\{\frac{\left[\frac{Z}{X}\sin\beta_b - (\sin\beta_a\cos\beta_b\cos\theta - \sin\beta_b\cos\beta_a)\right]d\theta\,dY\,dX}{\left[\frac{Z^2}{XY} + 2Z\left(\frac{\cos\beta_a}{Y} - \frac{\cos\beta_b}{X}\right) + \frac{X}{Y} + \frac{Y}{X} - 2(\cos\beta_a\cos\beta_b - \sin\beta_a\sin\beta_b\cos\theta)\right]^2}\right\} \tag{A8}$$

A535

$$\left.\begin{aligned}\cos\theta_u &= \frac{\tan\beta_a}{\sin\beta_b}\left(\cos\beta_b - \frac{Z}{Y}\right)\\ \cos\theta_u &= \frac{\tan\beta_b}{\sin\beta_a}\left(\cos\beta_a + \frac{Z}{X}\right)\end{aligned}\right\} \tag{A9}$$

where

$$\left.\begin{aligned}X &= \frac{\rho_a}{L_a}\\ Y &= \frac{\rho_b}{L_a}\\ Z &= \frac{\delta}{L_a}\end{aligned}\right\} \tag{A10}$$

CONFIGURATION FACTOR BETWEEN A CONE AND A SPHERE

The equations for the configuration factors between a cone and a sphere are derived in a manner similar to the preceding section with reference to figure 15.

$$F_{a-b} = \frac{4}{\pi}\left(\frac{R}{L}\right)^2\int_0^1\int_{\psi_L}^{\psi_u}\int_0^{\theta_u}\left[\frac{\delta}{L}\sin\beta - \frac{R}{L}(\sin\beta\cos\psi + \cos\beta\sin\psi\cos\theta)\right]$$
$$\left\{\frac{\left[\frac{\delta}{L}\cos\psi - \frac{R}{L} - X(\cos\beta\cos\psi - \sin\beta\sin\psi\cos\theta)\right]X\sin\psi\,d\theta\,d\psi\,dX}{\left[X^2 + \left(\frac{R}{L}\right)^2 + \left(\frac{\delta}{L}\right)^2 - 2\frac{\delta}{L}\left(X\cos\beta + \frac{R}{L}\cos\psi\right) + 2X\frac{R}{L}(\cos\beta\cos\psi - \sin\beta\sin\psi\cos\theta)\right]^2}\right\} \tag{A11}$$

$$\psi_u = \tan^{-1}\left[\frac{X \sin \beta}{(\delta/L) - X \cos \beta}\right] + \cos^{-1}\left\{\frac{R/L}{[(\delta/L)^2 - 2X(\delta/L) \cos \beta + X^2]^{1/2}}\right\} \tag{A12}$$

The lower limit, ψ_L, is determined as the greater of the two values:

$$\left.\begin{aligned} &\psi_L = 0 \\ &\text{or} \\ &\psi_L = \tan^{-1}\left[\frac{X \sin \beta}{(\delta/L) - X \cos \beta}\right] - \cos^{-1}\left\{\frac{R/L}{[(\delta/L)^2 - 2X(\delta/L) \cos \beta + X^2]^{1/2}}\right\}\end{aligned}\right\} \tag{A13}$$

Equations (A12) and (A13) have the additional restriction that $\tan^{-1}\{X \sin \beta/[(\delta/L) - X \cos \beta]\} > 0$. The two expressions for θ_u are of the same form as in the previous case:

$$\left.\begin{aligned} \cos \theta_u &= -\frac{\tan \beta}{\sin \psi}\left(\cos \psi - \frac{\delta/L}{R/L}\right) \\ \cos \theta_u &= \frac{1}{\sin \beta \sin \psi}\left[\cos \beta \cos \psi + \frac{1}{X}\left(\frac{R}{L} - \frac{\delta}{L} \cos \psi\right)\right]\end{aligned}\right\} \tag{A14}$$

The method of determining which expression gives the desired value of θ_u is exactly the same as in the case of equation (A9) for the two cones.

CONFIGURATION FACTOR FROM A CONCAVE SURFACE TO ITSELF

The configuration factor from a concave surface to itself may be readily calculated from simple relationships between surface areas. When a plane surface is placed over the open end of a concave surface, as shown in the sketch for the special case of a cone, the reciprocity theorem states that

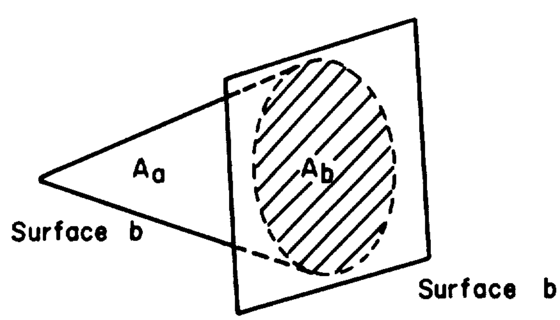

$$F_{a-b}A_a = F_{b-a}A_b \tag{A15}$$

It is apparent that $F_{b-a} = 1$ since all radiant energy from surface b is incident upon surface a and thus equation (A15) may be written

$$F_{a-b} = \frac{A_b}{A_a} \tag{A16}$$

Since all energy leaving surface a strikes either itself again or surface b, the summation of configuration factors from surface a must be unity:

$$F_{a-a} + F_{a-b} = 1 \tag{A17}$$

Thus from equations (A16) and (A17) the configuration factor from surface a to itself is determined as

A
5
3
5

$$F_{a-a} = 1 - \frac{A_b}{A_a} \tag{A18}$$

If an obstructing surface is located within the concave surface, resulting in a partial shielding effect, the preceding analysis is not valid and the basic configuration factor, equation (9), must be used with the limits of integration decreased accordingly. In the case of a cone with a conical obstruction, the configuration factor equation is found by previous methods to be

$$F_{a-a} = \frac{4}{\pi \sin \beta} \int_0^1 \int_0^1 \int_0^{\theta_u} \frac{(1 - \cos \theta)^2 \sin^4 \beta_a \cos^2 \beta_a \left(\frac{l_{a1}}{L}\right)^2 \left(\frac{l_{a2}}{L}\right)^2 d\left(\frac{l_{a1}}{L}\right) d\left(\frac{l_{a2}}{L}\right) d\theta}{\left[\left(\frac{l_{a1}}{L}\right)^2 + \left(\frac{l_{a2}}{L}\right)^2 - 2\left(\frac{l_{a1}}{L}\right)\left(\frac{l_{a2}}{L}\right)(\cos^2 \beta_a + \sin^2 \beta_a \cos \theta)\right]^2} \tag{A19}$$

where l_{a1} and l_{a2} are distances from the apex of cone a to dA_{a1} and dA_{a2}, respectively, on the surface and θ_u is now determined by the degree of obstruction by surface b.

$$\theta_u = \cos^{-1}\left[\frac{\tan \beta_b}{\sin \beta_a}\left(\cos \beta_a - \frac{\delta}{l_{a2}}\right)\right] + \cos^{-1}\left[\frac{\tan \beta_b}{\sin \beta_a}\left(\cos \beta_a - \frac{\delta}{l_{a1}}\right)\right] \tag{A20}$$

For no obstructing inner cone the upper limit of integration of θ will be

$$\theta_u = \pi \tag{A21}$$

APPENDIX B

EFFECTS OF SPECULAR REFLECTIONS

The analytic study of the radiative heat transfer due to specular reflections for the general class of shapes considered in the text is, in general, not possible. The problem is one of not being able to express analytically the process of reflections between two surfaces which "see" each other. It is possible, however, to evaluate the lower and upper limits of the energy which can be transferred to these surfaces as a result of those reflections. For illustration and for comparison with the diffuse reflection results, these limits will be evaluated for the case of the single-shield, conical-capsule configuration. It will also be assumed that the surfaces still emit diffusely, which is a valid assumption for many engineering materials. (See ref. 8.)

One exception to the above limitations occurs for the parallel solar radiation incident on the shield. For this case, the effective solar absorptance, $(\alpha_{s1})_{EFF}$, can be evaluated analytically by tracing an incident ray through the number of reflections which occur for any shield angle. For a specular surface the incident ray of energy will be reflected at an angle of reflection equal to the angle of incidence and may or may not strike the surface again, depending upon the geometry of the surface and the position of the ray with respect to the apex of the cone. Upon each succeeding reflection the angle of incidence is seen to increase by 2β (see sketch) until the ray is reflected out of the cone.

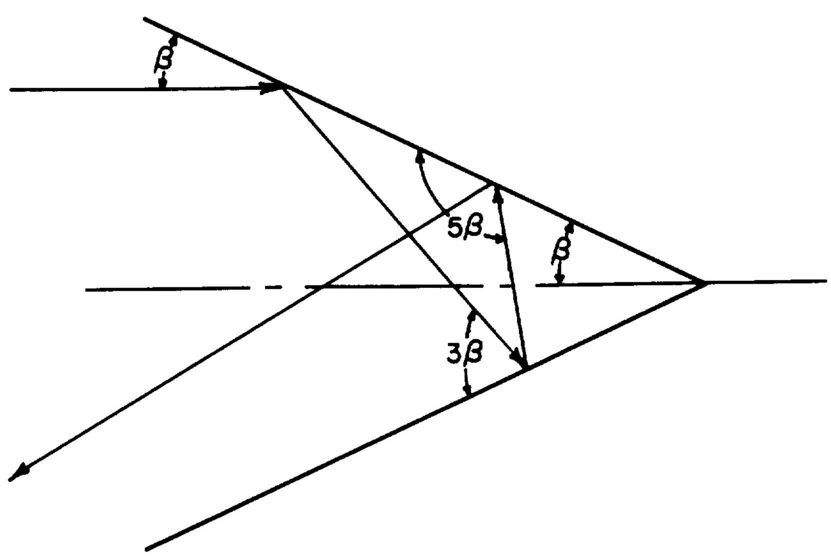

After n reflections the fraction of the ray's energy that is absorbed is

$$\alpha_{s1} \sum_{m=0}^{m=n-1} (1 - \alpha_{s1})^m$$

It can be shown that the initially incident rays near the apex may be reflected one more time than those near the edge of the cone. Thus, the effective absorptance of the entire surface must be weighted by the surface areas associated with the local effective absorptances. If A_n is the area over which the initially incident rays experience n reflections and A_{n-1} is the area over which the initially incident rays experience n-1 reflections, the expression for specular effective solar absorptance for the entire surface may be written

A535

$$(\alpha_{s1})_{EFF} = \frac{\alpha_{s1}}{A_1}\left[A_n \sum_{m=0}^{m=n-1} (1 - \alpha_{s1})^m + A_{n-1} \sum_{m=0}^{m=n-2} (1 - \alpha_{s1})^m\right] \tag{B1}$$

A_n, A_{n-1} and n may be easily determined graphically by ray tracing for any conical shield of interest. Figure 16 shows the effective solar absorptance as a function of shield semiapex angle, β, at various values of surface absorptance for both specular and diffuse surfaces. The flat portions of the specular curve occur between $2n\beta = 180^\circ$ and $2n\beta + \beta = 180^\circ$; that is, after n reflections all rays are parallel to incident radiation and parallel to the surface, respectively. It can be seen that some rather large differences between $(\alpha_{s1})_{EFF}$ for the two cases occur, particularly when small cone angles and low solar absorptance materials are combined.

For the example configuration, the limits of the specular reflection analysis are determined from the consideration of reflected thermal energy between surfaces. To obtain the lower limit of the energy which can be transferred when specularly reflecting materials are concerned, only the energy emitted by one surface that is initially absorbed in the other surface will be considered (i.e., all emitted energy which is reflected is assumed to be dissipated to space). The pertinent equations for this case can be developed from equations (11), (16), and (19).

The amount of solar energy absorbed by the first shield can again be written as

$$Q_{s1} = (\alpha_{s1})_{EFF} A_x \frac{E}{r^2} \tag{B2}$$

where $(\alpha_{s1})_{EFF}$ for specularly reflecting surfaces is given in figure 16.

The equations for energies emitted and absorbed for the shield are

$$Q_1^* = \epsilon_1 A_1 \sigma T_1{}^4 \tag{B3}$$

$$Q_2^* = \epsilon_2 A_2 \sigma T_2{}^4 \tag{B4}$$

$$Q_{1-1} = \alpha_1 F_{1-1} \epsilon_1 A_1 \sigma T_1{}^4 \tag{B5}$$

$$Q_{2-2} = \alpha_2 F_{2-2} \epsilon_2 A_2 \sigma T_2{}^4 \tag{B6}$$

$$Q_{c-2} = \alpha_2 F_{c-2} A_c' \epsilon_c \sigma T_c{}^4 = \alpha_2 F_{2-c} A_2 \epsilon_c \sigma T_c{}^4 \tag{B7}$$

The equations for energies emitted and absorbed for the capsule are

$$Q_c^* = \epsilon_c A_c \sigma T_c{}^4 \tag{B8}$$

$$Q_{2-c} = \alpha_c F_{2-c} \epsilon_2 A_2 \sigma T_2{}^4 \tag{B9}$$

$$Q_i = \text{internal power of the capsule} \tag{B10}$$

Since the shield and capsule are in thermal equilibrium, heat balances (utilizing equations (B2) through (B10)) on the shield and capsule yield (as in the text)

$$T_c = \left[\frac{(B_1 B_4/\bar{r}^2) + B_2 Q_i}{B_2 B_5 - B_3 B_4}\right]^{1/4} \tag{B11}$$

and

$$T_2 = \left[\frac{(B_1 B_5/\bar{r}^2) + B_3 Q_i}{B_2 B_5 - B_3 B_4}\right]^{1/4} \tag{B12}$$

where

$$B_1 = (\alpha_{s1})_{EFF} A_x E \tag{B13}$$

$$(B_2)_{min} = \epsilon_1 A_2 \sigma (1 - \alpha_1 F_{1-1}) + \epsilon_2 A_2 \sigma (1 - \alpha_2 F_{2-2}) \tag{B14}$$

$$B_3 = \alpha_2 F_{2-c} \epsilon_c A_2 \sigma \tag{B15}$$

$$(B_4)_{min} = \alpha_c F_{2-c} \epsilon_2 A_2 \sigma \tag{B16}$$

$$(B_5)_{min} = \epsilon_c A_c \sigma \tag{B17}$$

To determine the upper limit of capsule temperature due to specular reflections, equations (B2) to (B10) will be modified as necessary to maximize the total energy which could possibly be transferred to the capsule. Of these, only equations (B5) and (B9) need to be modified.

Equation (B5) is modified to maximize the portion of that energy emitted by the front face of the shield which is reabsorbed. This maximum occurs when $\alpha_1 = 1$, which, in effect, implies that this portion of the emitted energy is subjected to an infinite number of reflections within the concave shield. Equation (B5) then becomes

$$Q_{1-1} = F_{1-1}\epsilon_1 A_1 \sigma T_1^4 \tag{B18}$$

The equation (B9) is modified by assuming that all energy reflected from the back of the shield (the quantity $(1 - \alpha_2)F_{2-c}A_2\epsilon_c\sigma T_c^4 + (1 - \alpha_2)F_{2-2}\epsilon_2 A_2\sigma T_2^4$) is incident on the capsule and a fraction, α_c, of this incident energy is absorbed. The energy reflected from the capsule is assumed to be dissipated to space. (This assumption is correct for the single conical shield, 14.04° conical-capsule configuration for $0^\circ \leq \beta \leq 127^\circ$.) Thus, equation (B9) is modified to

A535

$$Q_{2-c} = \alpha_c[F_{2-c} + (1 - \alpha_2)F_{2-2}]\epsilon_2 A_2\sigma T_2^4 + \alpha_c(1 - \alpha_2)F_{2-c}A_2\epsilon_c\sigma T_c^4 \tag{B19}$$

A heat balance on the capsule and shield utilizing equations (B2), (B3), (B4), (B6), (B7), (B8), (B10), (B18), and (B19) yields the usual equations for the capsule and shield temperatures given by equations (B11) and (B12) where

$$B_1 = (\alpha_{s1})_{EFF}A_x E \tag{B20}$$

$$(B_2)_{max} = \epsilon_1 A_2\sigma(1 - F_{1-1}) + \epsilon_2 A_2\sigma(1 - \alpha_2 F_{2-2}) \tag{B21}$$

$$B_3 = \alpha_2 F_{2-c}A_2\epsilon_c\sigma \tag{B22}$$

$$(B_4)_{max} = \alpha_c[F_{2-c} + (1 - \alpha_2)F_{2-2}]\epsilon_2 A_2\sigma \tag{B23}$$

$$(B_5)_{max} = \epsilon_c A_c\sigma - \alpha_c(1 - \alpha_2)F_{2-c}A_2\epsilon_c\sigma \tag{B24}$$

Energy transfer factors, τ, were calculated from equation (51) for the two cases of maximum and minimum energy transfer using equations (B21) through (B24) and equations (B14) through (B17), respectively. The results are shown in figure 17 as a function of shield semiapex angle along with the diffuse reflection results. It is seen that the diffuse case falls within the limits of the specular case and at $\alpha = \epsilon = 1$ all analyses agree. The region of greatest difference occurs at values of β greater than 90° and at $\alpha = \epsilon < 1$. This difference results primarily from the limits imposed on Q_{2-c}. In the lower limit, only the energy emitted by the shield directly to the capsule may be absorbed (see eq. (B9)). For the upper limit, all reflected energy from the back of the shield is also included (see eq. (B19)). In the region of $\beta < 90^\circ$, it can be seen that the diffuse reflection analysis can be used as a reasonable approximation of the energy transfer factor for specular reflecting surfaces. For $\beta > 90^{o}$, the large differences between the diffuse reflection analysis and the limits of the specular reflection analysis indicate that, in this region, the diffuse reflection analysis may not be a good approximation for the specular case.

APPENDIX C

EFFECTS OF THERMAL CONDUCTIVITY ON THE TEMPERATURE DISTRIBUTION OF A CONICAL SHIELD

In the foregoing analysis the assumption of an isothermal shield surface might possibly introduce serious errors into the calculated energy radiated back to the capsule if either the shield conductivity is low or the thickness is small. The temperature of the apex of a conical shield in this case will be somewhat higher than the temperature of the edge as a result of reflections and the restricted "view" of space that the inside surface has near the apex.

The temperature gradient along the slant length of a cone isolated in space subjected to solar radiation parallel to its axis will be determined as a function of thermal conductivity, thickness, semiapex angle, α and ϵ, and distance from the sun. The method of analysis will be similar to that given by Nichols in reference 5.

At equilibrium there will be a balance between the net energy emitted from a given volume element of the cone due to radiation and the heat conducted along the cone into the element. Since the cone temperature is assumed to be axisymmetric, the net heat conducted into the volume element (see fig. 18) is given by

$$\text{Net } Q \text{ conducted in} = -kb\,d\theta\,l \sin\beta\left(\frac{dT}{dl}\right) - \left[-kb\,d\theta\,(l + dl)\sin\beta\left(\frac{dT}{dl} + \frac{d^2T}{dl^2}dl\right)\right]$$

$$= kb\,d\theta \sin\beta\,dl\,\frac{d}{dl}\left(l\,\frac{dT}{dl}\right) \tag{C1}$$

The energy emitted from the outside surface of the cone is, of course, determined from the temperature of the cone element. On the inside surface, however, the problem is complicated by interactions between the emitted and absorbed energies. To differentiate, let $I(l)$ be the incident radiant flux and $H(l)$ be the emitted radiant flux, respectively, for the inner surface of any given element; these items are exclusive of the initially incident solar flux. The <u>net</u> energy leaving the volume element will then be

$$\text{Net } Q \text{ emitted} = \left[H(l) + \epsilon\sigma T^4(l) - I(l) - \alpha_s\left(\frac{E}{r^2}\right)\sin\beta\right]d\theta\,l\sin\beta\,dl \tag{C2}$$

Since the volume element is in thermal equilibrium

$$\sum Q = 0 \tag{C3}$$

NET Q conducted in = NET Q emitted

$$kb\ d\theta \sin\beta\ dl \frac{d}{dl}\left(l \frac{dT}{dl}\right) = \left[H(l) + \epsilon\sigma T^4(l) - I(l) - \alpha_s \left(\frac{E}{\bar{r}^2}\right) \sin\beta\right] d\theta\ l \sin\beta\ dl \tag{C4}$$

or

$$\frac{kb}{l}\frac{d}{dl}\left(l \frac{dT}{dl}\right) = H(l) + \epsilon\sigma T^4(l) - I(l) - \alpha_s \left(\frac{E}{\bar{r}^2}\right) \sin\beta \tag{C5}$$

$H(l)$ is related to $I(l)$ by the relation

$$H(l) = \epsilon\sigma T^4(l) + (1 - \alpha)I(l) \tag{C6}$$

$I(l)$ is a result of flux emitted and reflected to the surface element (this element shall be denoted by the subscript 1) from all the other elements (any other element shall be noted by the subscript 2). The radiation from any surface element dA_2 upon dA_1 is (see fig. 18)

$$dI(l_1) = \left[H(l_2) + \zeta(1 - \alpha_s)\left(\frac{E}{\bar{r}^2}\right) \sin\beta\right] \frac{\cos\varphi_1 \cos\varphi_2}{\pi S^2} dA_2 \tag{C7}$$

The purpose of the symbol ζ is to allow for two distinct cases; (1) $\zeta = 0$ when the cone's vertex faces the sun and (2) $\zeta = 1$ when the cone's vertex faces away from the sun.

Using methods described in appendix A it is possible to rewrite $\cos\varphi_1$, $\cos\varphi_2$, S, and dA_2 into functions of variables l_1, l_2, and Q_2 where θ_1 is arbitrarily equal to zero. The radiation incident upon dA_1 from the entire cone is then

$$I(l_1) = \int_0^L \int_0^{2\pi} \left[H(l_2) + \zeta(1 - \alpha_s)\left(\frac{E}{\bar{r}^2}\right) \sin\beta\right] \frac{(1 - \cos\theta_2)^2 \cos^2\beta \sin^3\beta\ l_1 l_2^2\ dl_2\ d\theta_2}{\pi[l_1^2 + l_2^2 - 2l_1 l_2(\cos^2\beta + \sin^2\beta\cos\theta_2)]^2} \tag{C8}$$

which may be put in the form

$$I(l_1) = \int_0^L \left[H(l_2) + \zeta(1 - \alpha_s)\left(\frac{E}{\bar{r}^2}\right) \sin\beta\right] K(l_1, l_2)\ dl_2 \tag{C9}$$

where

$$K(l_1, l_2) = \frac{\cos^2 \beta \sin^3 \beta \; l_1 l_2^2}{\pi} \int_0^{2\pi} \frac{(1 - \cos \theta_2)^2 \, d\theta_2}{[l_1^2 + l_2^2 - 2 l_1 l_2 (\cos^2 \beta + \sin^2 \beta \cos \theta_2)]^2} \tag{C10}$$

Thus, there are now three unknowns (H, I, and T) and by solving simultaneously equations (C5), (C6), and (C9) an equation for T is obtained:

$$\begin{aligned} \frac{kb}{l_1} \frac{d}{dl_1}\left[l_1 \frac{dT(l_1)}{dl_1}\right] &= 2\epsilon\sigma T^4(l_1) - \alpha_s \left(\frac{E}{r^2}\right) \sin \beta \\ &+ (1 - \alpha) \int_0^L \left\{ \frac{kb}{l_2} \frac{d}{dl_2}\left[l_2 \frac{dT(l_2)}{dl_2}\right] - \frac{2-\alpha}{1-\alpha} \epsilon\sigma T^4(l_2) \right. \\ &\left. + \frac{\alpha_s - \zeta\alpha - (1 - \zeta)\alpha_s\alpha}{1 - \alpha} \left(\frac{E}{r^2}\right) \sin \beta \right\} K(l_1, l_2) \, dl_2 \end{aligned} \tag{C11}$$

For the purpose of the present report only the extreme limits of thermal conductivity (i.e., $k = 0$ and $k = \infty$) will be studied and compared with the analysis developed within the report. The resulting equation will be simplified by the assumption that the solar absorptance is the same as the thermal absorptance (i.e., $\alpha_s = \alpha$).

INFINITE CONDUCTIVITY

For the case of infinite conductivity T becomes a constant and, because $k \to \infty$,

$$\frac{kb}{l} \frac{d}{dl}\left(l \frac{dT}{dl}\right) \to \frac{Q}{l} \tag{C12}$$

even though $(dT/dl) \to 0$ where Q is a finite quantity representative of a rate of heat conduction into the elemental volume.

With the substitution

$$\xi = \frac{\frac{Q}{l} - \frac{2 - \alpha}{1 - \alpha} \epsilon\sigma T^4 + (1 - \zeta)\alpha \left(\frac{E}{r^2}\right) \sin \beta}{- \frac{1 - 2\alpha}{1 - \alpha} \epsilon\sigma T^4 - \zeta\alpha \left(\frac{E}{r^2}\right) \sin \beta} \tag{C13}$$

equation (C11) becomes a Fredholm integral equation

$$\xi(l_1) = 1 + (1 - \alpha)\int_0^L \xi(l_2)K(l_1, l_2)\, dl_2 \tag{C14}$$

If it is assumed that no heat is radiated from the edge of the cone, then the boundary condition for determining T is that the summation of Q must be zero over the entire cone and can be written

$$\int Q\, dl = 0 \tag{C15}$$

When this operation is performed upon equation (C13) the required equation for the isothermal temperature is obtained:

$$T^4 = \frac{(1 - \alpha)\left(\frac{E}{\bar{r}^2}\right)\sin\beta}{\epsilon\sigma}\left(\frac{\frac{1 - \zeta}{2} + \frac{\zeta}{L^2}\int_0^L l_1\xi\, dl_1}{\frac{2 - \alpha}{2} - \alpha\int_0^L l_1\xi\, dl_1}\right) \tag{C16}$$

ZERO CONDUCTIVITY

For the case of $k = 0$ the substitution

$$\xi = \frac{\frac{2\alpha(1 - \alpha)(1 - \zeta)}{2 - \alpha}\left(\frac{E}{\bar{r}^2}\right)\sin\beta - 2\epsilon\sigma T^4}{-\frac{\alpha}{2 - \alpha}[2\zeta + \alpha(1 - 2\zeta)]\left(\frac{E}{\bar{r}^2}\right)\sin\beta} \tag{C17}$$

will reduce equation (C11) to a Fredholm equation of the previous type:

$$\xi(l_1) = 1 + \left(1 - \frac{\alpha}{2}\right)\int_0^L \xi(l_2)K(l_1, l_2)\, dl_2 \tag{C18}$$

The temperature along the cone is then determined by equation (C17)

$$T^4(l_1) = \frac{\alpha(1 - \alpha)\left(\frac{E}{\bar{r}^2}\right)\sin\beta}{(2 - \alpha)\epsilon\sigma}\left[1 - \zeta + \frac{\zeta + (\alpha/2)(1 - 2\zeta)}{1 - \alpha}\xi(l_1)\right] \tag{C19}$$

The calculation of the solutions to equations (C14) and (C18) is, of course, the same since the two equations differ only by a constant. Numerical solutions to be presented were obtained on an IBM 704 computer using the iterative procedure developed in reference 9.

In figure 19 the results of equation (C16) for $k = \infty$ and equation (C19) for $k = 0$ are presented for the special case of a 45° cone whose apex faces away from the sun. These values of temperature are compared to the isothermal shield temperature obtained from equation (31) in the Analysis section when the shield is alone in space (i.e., $F_{2-c} = F_{c-2} = 0$). It is seen that the magnitude of the temperature difference over the length of the cone, for the case of zero conductivity, becomes less as $\alpha = \epsilon$ becomes larger. Thus, if a highly reflective shield material were used, the gradient experienced would be greater than if a highly absorptive one were used and the chance of locally exceeding the maximum allowable temperature is greater. The method of analysis presented in the text of the report compares very favorably to the infinite conductivity analysis presented herein.

An energy transfer factor, τ, may be calculated from equations (31) and (51) by finding the shield temperature due only to solar irradiation and equating with the expression for τ. The equation thus obtained,

$$\tau = \frac{\epsilon A_c \sigma T_2{}^4 \bar{r}^2}{B_1 B_5 / B_4} \tag{C20}$$

was applied to the single-shield, solar-probe configuration and the results are shown in figure 20. The limiting values of energy transfer factor for the case of zero conductivity were calculated using the apex temperature (maximum) and the edge temperature (minimum). The isothermal analysis developed within the text of the report is seen to fall between these two limits.

REFERENCES

1. Dugan, Duane W.: A Preliminary Study of the Solar-Probe Mission. NASA TN D-783, 1961.

2. Anon.: Materials Problems Associated With the Thermal Control of Space Vehicles. Materials Advisory Board of National Academy of Sciences - National Research Council. Rep. MAB-155-M, Oct. 20, 1959.

3. Acker, R. M., Lipkis, R. P., and Vehrencamp, J. E.: Temperature Control System for the Atlas Able-4 Lunar Satellite. For oral presentation at ASME 1960 Summer Annual Meeting and Aviation Conference, Dallas, Texas, June 5-9, 1960.

4. Cornog, R. A.: Temperature Equilibria in Space Vehicles. Jour. of the Astronautical Sciences, vol. 5, 1958, pp. 64-67. (Pub. also as Amer. Astron. Soc. preprint 58-22.)

5. Nichols, Lester D.: Effect of Shield Position and Absorptivity on Temperature Distribution of a Body Shielded From Solar Radiation in Space. NASA TN D-578, 1961.

6. Hamilton, D. C., and Morgan, W. R.: Radiant-Interchange Configuration Factors. NACA TN 2836, 1952.

7. Jakob, Max: Heat Transfer. Vol. II. N. Y., John Wiley and Sons, Inc., 1957, pp. 1-34.

8. Jakob, Max: Heat Transfer. Vol. I. N. Y., John Wiley and Sons, Inc., 1949, pp. 44-52.

9. Heaslet, Max. A., and Lomax, Harvard: Numerical Predictions of Radiative Interchange Between Conducting Fins With Mutual Irradiations. NASA TR R-116, 1962.

TABLE I.- CONFIGURATION FACTORS, ENERGY TRANSFER FACTORS, AND Q_{ci}/Q_i FOR SINGLE-SHIELD CONICAL-CAPSULE CONFIGURATION

(a) $x/R = 0$

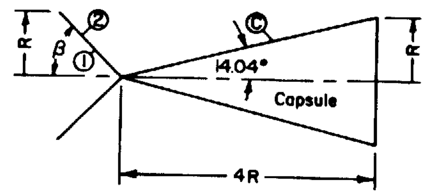

		$\beta = 15°$	$\beta = 30°$	$\beta = 45°$	$\beta = 60°$	$\beta = 75°$	$\beta = 90°$	$\beta = 105°$	$\beta = 120°$	$\beta = 135°$	$\beta = 150°$	$\beta = 166°$
F_{1-1}		0.741	0.500	0.293	0.134	0.034	0	0	0	0	0	0
F_{2-2}		0	0	0	0	0	0	.032	.118	.229	.304	0
F_{2-c}		.004	.016	.034	.059	.089	.126	.171	.230	.316	.474	1.000
F_{c-2}		.004	.008	.012	.016	.022	.031	.043	.064	.108	.230	1.000
$\alpha=\epsilon=$ 0.05	τ	$.112 \times 10^{-3}$	$.405 \times 10^{-3}$	$.862 \times 10^{-3}$	$.147 \times 10^{-2}$	$.223 \times 10^{-2}$	$.316 \times 10^{-2}$	$.445 \times 10^{-2}$	$.659 \times 10^{-2}$	$.105 \times 10^{-1}$	$.189 \times 10^{-1}$	.725
	Q_{ci}/Q_i	0	0	0	0	0	0	0	.001	.002	.007	1.138
$\alpha=\epsilon=$ 0.1	τ	$.236 \times 10^{-3}$	$.828 \times 10^{-3}$	$.174 \times 10^{-2}$	$.296 \times 10^{-2}$	$.447 \times 10^{-2}$	$.632 \times 10^{-2}$	$.888 \times 10^{-2}$	$.131 \times 10^{-1}$	$.209 \times 10^{-1}$	$.373 \times 10^{-1}$	.730
	Q_{ci}/Q_i	0	0	0	0	0	0	.001	.001	.003	.013	1.117
$\alpha=\epsilon=$ 0.2	τ	$.513 \times 10^{-3}$	$.172 \times 10^{-2}$	$.355 \times 10^{-2}$	$.595 \times 10^{-2}$	$.896 \times 10^{-2}$	$.126 \times 10^{-1}$	$.177 \times 10^{-1}$	$.261 \times 10^{-1}$	$.411 \times 10^{-1}$	$.728 \times 10^{-1}$	.740
	Q_{ci}/Q_i	0	0	0	0	0	.001	.001	.002	.006	.024	1.073
$\alpha=\epsilon=$ 0.3	τ	$.819 \times 10^{-3}$	$.268 \times 10^{-2}$	$.542 \times 10^{-2}$	$.900 \times 10^{-2}$	$.135 \times 10^{-1}$	$.190 \times 10^{-1}$	$.265 \times 10^{-1}$	$.388 \times 10^{-1}$	$.607 \times 10^{-1}$	.106	.751
	Q_{ci}/Q_i	0	0	0	0	0	.001	.002	.003	.009	.034	1.028
$\alpha=\epsilon=$ 0.5	τ	$.149 \times 10^{-2}$	$.474 \times 10^{-2}$	$.933 \times 10^{-2}$	$.152 \times 10^{-1}$	$.225 \times 10^{-1}$	$.316 \times 10^{-1}$	$.440 \times 10^{-1}$	$.638 \times 10^{-1}$	$.979 \times 10^{-1}$	.168	.774
	Q_{ci}/Q_i	0	0	0	0	.001	.001	.002	.005	.013	.047	.935
$\alpha=\epsilon=$ 0.75	τ	$.239 \times 10^{-2}$	$.754 \times 10^{-2}$	$.145 \times 10^{-1}$	$.232 \times 10^{-1}$	$.339 \times 10^{-1}$	$.473 \times 10^{-1}$	$.657 \times 10^{-1}$	$.939 \times 10^{-1}$	.141	.236	.804
	Q_{ci}/Q_i	0	0	0	0	.001	.001	.003	.006	.015	.055	.810
$\alpha=\epsilon=$ 1.0	τ	$.334 \times 10^{-2}$	$.105 \times 10^{-1}$	$.200 \times 10^{-1}$	$.314 \times 10^{-1}$	$.454 \times 10^{-1}$	$.631 \times 10^{-1}$	$.872 \times 10^{-1}$	.123	.181	.295	.837
	Q_{ci}/Q_i	0	0	0	0	.001	.002	.003	.006	.016	.055	.674

TABLE I.- CONFIGURATION FACTORS, ENERGY TRANSFER FACTORS, AND Q_{ci}/Q_i FOR SINGLE-SHIELD CONICAL-CAPSULE CONFIGURATION - Continued

(b) x/R = 0.50

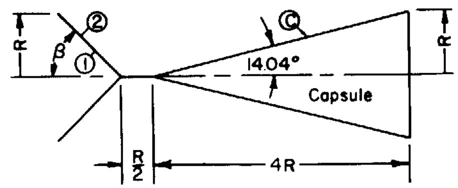

		β = 15°	β = 30°	β = 45°	β = 60°	β = 75°	β = 90°	β = 105°	β = 120°	β = 135°	β = 150°	β = 165°	β = 167°
F_{1-1}		0.740	0.500	0.293	0.134	0.034	0	0	0	0	0	0	0
F_{2-2}		0	0	0	0	0	0	.034	.134	.285	.427	.270	.104
F_{2-c}		.004	.013	.025	.040	.055	.073	.093	.120	.170	.290	.717	.896
F_{c-2}		.003	.006	.009	.011	.014	.018	.023	.038	.058	.141	.672	1.000
α=ε=	τ	$.986\times10^{-4}$	$.328\times10^{-3}$	$.637\times10^{-3}$	$.994\times10^{-3}$	$.139\times10^{-2}$	$.182\times10^{-2}$	$.240\times10^{-2}$	$.347\times10^{-2}$	$.594\times10^{-2}$	$.130\times10^{-1}$	$.464\times10^{-1}$	.194
0.05	Q_{ci}/Q_i	0	0	0	0	0	0	0	0	.001	.003	.049	.305
α=ε=	τ	$.208\times10^{-3}$	$.671\times10^{-3}$	$.129\times10^{-2}$	$.200\times10^{-2}$	$.278\times10^{-2}$	$.364\times10^{-2}$	$.480\times10^{-2}$	$.690\times10^{-2}$	$.118\times10^{-1}$	$.255\times10^{-1}$	$.908\times10^{-1}$	.324
0.1	Q_{ci}/Q_i	0	0	0	0	0	0	0	0	.001	.005	.093	.496
α=ε=	τ	$.452\times10^{-3}$	$.140\times10^{-2}$	$.262\times10^{-2}$	$.402\times10^{-2}$	$.557\times10^{-2}$	$.728\times10^{-2}$	$.958\times10^{-2}$	$.137\times10^{-1}$	$.231\times10^{-1}$	$.491\times10^{-1}$	.173	.484
0.2	Q_{ci}/Q_i	0	0	0	0	0	0	0	.001	.002	.010	.168	.703
α=ε=	τ	$.721\times10^{-3}$	$.217\times10^{-2}$	$.400\times10^{-2}$	$.608\times10^{-2}$	$.837\times10^{-2}$	$.109\times10^{-1}$	$.143\times10^{-1}$	$.204\times10^{-1}$	$.340\times10^{-1}$	$.711\times10^{-1}$	.245	.576
0.3	Q_{ci}/Q_i	0	0	0	0	0	0	0	.001	.003	.014	.225	.790
α=ε=	τ	$.131\times10^{-2}$	$.384\times10^{-2}$	$.689\times10^{-2}$	$.103\times10^{-1}$	$.140\times10^{-1}$	$.182\times10^{-1}$	$.238\times10^{-1}$	$.335\times10^{-1}$	$.545\times10^{-1}$	.111	.361	.673
0.5	Q_{ci}/Q_i	0	0	0	0	0	0	.001	.001	.004	.019	.293	.814
α=ε=	τ	$.210\times10^{-2}$	$.611\times10^{-2}$	$.107\times10^{-1}$	$.157\times10^{-1}$	$.211\times10^{-1}$	$.273\times10^{-1}$	$.356\times10^{-1}$	$.492\times10^{-1}$	$.781\times10^{-1}$	.153	.464	.730
0.75	Q_{ci}/Q_i	0	0	0	0	0	0	.001	.002	.005	.022	.313	.736
α=ε=	τ	$.294\times10^{-2}$	$.853\times10^{-2}$	$.148\times10^{-1}$	$.212\times10^{-1}$	$.282\times10^{-1}$	$.364\times10^{-1}$	$.472\times10^{-1}$	$.644\times10^{-1}$	$.996\times10^{-1}$	.188	.534	.763
1.0	Q_{ci}/Q_i	0	0	0	0	0	.001	.001	.002	.005	.021	.288	.615

TABLE I.- CONFIGURATION FACTORS, ENERGY TRANSFER FACTORS, AND Q_{ci}/Q_i FOR SINGLE-SHIELD CONICAL-CAPSULE CONFIGURATION - Concluded

(c) x/R = 1.0

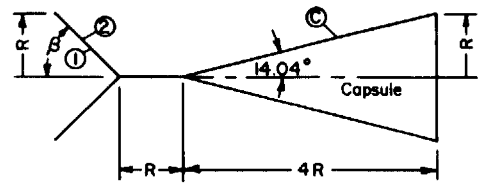

		β = 15°	β = 30°	β = 45°	β = 60°	β = 75°	β = 90°	β = 105°	β = 120°	β = 135°	β = 150°	β = 169°
F_{1-1}		0.740	0.500	0.293	0.134	0.034	0	0	0	0	0	0
F_{2-2}		0	0	0	0	0	0	.034	.134	.293	.484	.192
F_{2-c}		.003	.011	.020	.030	.039	.048	.057	.068	.089	.162	.808
F_{c-2}		.003	.005	.007	.008	.010	.012	.014	.019	.031	.078	1.000
α=ε=	τ	$.880\times10^{-4}$	$.277\times10^{-3}$	$.503\times10^{-3}$	$.743\times10^{-3}$	$.976\times10^{-3}$	$.121\times10^{-2}$	$.146\times10^{-2}$	$.196\times10^{-2}$	$.313\times10^{-2}$	$.777\times10^{-2}$	.119
0.05	Q_{ci}/Q_i	0	0	0	0	0	0	0	0	0	.001	.188
α=ε=	τ	$.186\times10^{-3}$	$.566\times10^{-3}$	$.102\times10^{-2}$	$.149\times10^{-2}$	$.195\times10^{-2}$	$.241\times10^{-2}$	$.293\times10^{-2}$	$.389\times10^{-2}$	$.620\times10^{-2}$	$.152\times10^{-1}$	.219
0.1	Q_{ci}/Q_i	0	0	0	0	0	0	0	0	0	.002	.335
α=ε=	τ	$.403\times10^{-3}$	$.118\times10^{-2}$	$.207\times10^{-2}$	$.301\times10^{-2}$	$.391\times10^{-2}$	$.482\times10^{-2}$	$.584\times10^{-2}$	$.773\times10^{-2}$	$.121\times10^{-1}$	$.291\times10^{-1}$	.371
0.2	Q_{ci}/Q_i	0	0	0	0	0	0	0	0	.001	.003	.538
α=ε=	τ	$.643\times10^{-3}$	$.183\times10^{-2}$	$.316\times10^{-2}$	$.454\times10^{-2}$	$.588\times10^{-2}$	$.723\times10^{-2}$	$.875\times10^{-2}$	$.115\times10^{-1}$	$.179\times10^{-1}$	$.418\times10^{-1}$	.476
0.3	Q_{ci}/Q_i	0	0	0	0	0	0	0	0	.001	.005	.652
α=ε=	τ	$.117\times10^{-2}$	$.324\times10^{-2}$	$.544\times10^{-2}$	$.768\times10^{-2}$	$.984\times10^{-2}$	$.121\times10^{-1}$	$.145\times10^{-1}$	$.189\times10^{-1}$	$.286\times10^{-1}$	$.643\times10^{-1}$	.598
0.5	Q_{ci}/Q_i	0	0	0	0	0	0	0	0	.001	.006	.722
α=ε=	τ	$.188\times10^{-2}$	$.515\times10^{-2}$	$.847\times10^{-2}$	$.117\times10^{-1}$	$.148\times10^{-1}$	$.181\times10^{-1}$	$.217\times10^{-1}$	$.278\times10^{-1}$	$.410\times10^{-1}$	$.879\times10^{-1}$	.666
0.75	Q_{ci}/Q_i	0	0	0	0	0	0	0	.001	.001	.007	.671
α=ε=	τ	$.262\times10^{-2}$	$.720\times10^{-2}$	$.117\times10^{-1}$	$.159\times10^{-1}$	$.198\times10^{-1}$	$.241\times10^{-1}$	$.288\times10^{-1}$	$.364\times10^{-1}$	$.523\times10^{-1}$	.108	.698
1.0	Q_{ci}/Q_i	0	0	0	0	0	0	0	.001	.001	.007	.562

A 535

TABLE II.- CONFIGURATION FACTORS, ENERGY TRANSFER FACTORS, AND Q_{ci}/Q_i FOR DOUBLE-SHIELD CONICAL-CAPSULE CONFIGURATION

(a) $x/R = 0$

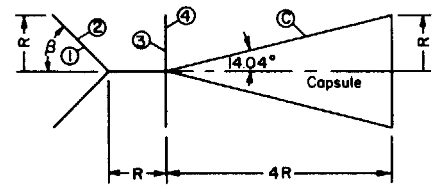

		β = 15°	β = 30°	β = 45°	β = 60°	β = 75°	β = 90°	β = 105°	β = 120°	β = 135°
F_{1-1}		0.741	0.500	0.293	0.134	0.034	0	0	0	0
F_{2-2}		0	0	0	0	0	0	.034	.134	.293
F_{2-3}		.013	.055	.121	.204	.292	.382	.472	.569	.707
F_{3-2}		.052	.109	.172	.235	.303	.382	.488	.657	1.000
F_{4-c}		.126	.126	.126	.126	.126	.126	.126	.126	.126
F_{c-4}		.031	.031	.031	.031	.031	.031	.031	.031	.031
$\alpha=\epsilon=$ 0.05	τ	$.113\times10^{-5}$	$.445\times10^{-5}$	$.988\times10^{-5}$	$.169\times10^{-4}$	$.252\times10^{-4}$	$.351\times10^{-4}$	$.494\times10^{-4}$	$.806\times10^{-4}$	$.231\times10^{-3}$
	Q_{ci}/Q_i	0	0	0	0	0	0	0	0	0
$\alpha=\epsilon=$ 0.1	τ	$.477\times10^{-5}$	$.182\times10^{-4}$	$.399\times10^{-4}$	$.678\times10^{-4}$	$.100\times10^{-3}$	$.139\times10^{-3}$	$.195\times10^{-3}$	$.313\times10^{-3}$	$.858\times10^{-3}$
	Q_{ci}/Q_i	0	0	0	0	0	0	0	0	0
$\alpha=\epsilon=$ 0.2	τ	$.207\times10^{-4}$	$.758\times10^{-4}$	$.162\times10^{-3}$	$.272\times10^{-3}$	$.399\times10^{-3}$	$.548\times10^{-3}$	$.758\times10^{-3}$	$.119\times10^{-2}$	$.298\times10^{-2}$
	Q_{ci}/Q_i	.001	.001	.001	.001	.001	.001	.001	.001	.001
$\alpha=\epsilon=$ 0.3	τ	$.496\times10^{-4}$	$.177\times10^{-3}$	$.371\times10^{-3}$	$.613\times10^{-3}$	$.892\times10^{-3}$	$.121\times10^{-2}$	$.166\times10^{-2}$	$.254\times10^{-2}$	$.585\times10^{-2}$
	Q_{ci}/Q_i	.001	.001	.001	.001	.001	.001	.001	.001	.001
$\alpha=\epsilon=$ 0.5	τ	$.150\times10^{-3}$	$.520\times10^{-3}$	$.106\times10^{-2}$	$.171\times10^{-2}$	$.245\times10^{-2}$	$.329\times10^{-2}$	$.440\times10^{-2}$	$.643\times10^{-2}$	$.127\times10^{-1}$
	Q_{ci}/Q_i	.001	.001	.001	.001	.001	.001	.001	.001	.001
$\alpha=\epsilon=$ 0.75	τ	$.361\times10^{-3}$	$.124\times10^{-2}$	$.247\times10^{-2}$	$.389\times10^{-2}$	$.544\times10^{-2}$	$.719\times10^{-2}$	$.943\times10^{-2}$	$.131\times10^{-1}$	$.222\times10^{-1}$
	Q_{ci}/Q_i	.001	.001	.001	.001	.001	.001	.002	.002	.002
$\alpha=\epsilon=$ 1.0	τ	$.672\times10^{-3}$	$.231\times10^{-2}$	$.451\times10^{-2}$	$.697\times10^{-2}$	$.959\times10^{-2}$	$.125\times10^{-1}$	$.161\times10^{-1}$	$.214\times10^{-1}$	$.323\times10^{-1}$
	Q_{ci}/Q_i	.002	.002	.002	.002	.002	.002	.002	.002	.002

TABLE II.- CONFIGURATION FACTORS, ENERGY TRANSFER FACTORS, AND Q_{ci}/Q_i FOR DOUBLE-SHIELD CONICAL-CAPSULE CONFIGURATION - Continued

(b) x/R = 0.5

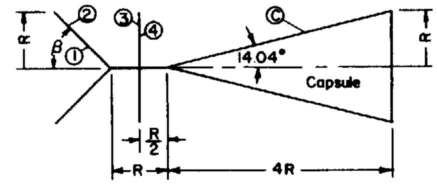

		β = 15°	β = 30°	β = 45°	β = 60°	β = 75°	β = 90°	β = 105°	β = 117°
F_{1-1}		0.741	0.500	0.293	0.134	0.034	0	0	0
F_{2-2}		0	0	0	0	0	0	.034	.134
F_{2-3}		.020	.081	.180	.309	.456	.610	766	.866
F_{3-2}		.078	.163	.254	.375	.472	.610	.793	1.000
F_{4-c}		.073	.073	.073	.073	.073	.073	.073	.073
F_{c-4}		.018	.018	.018	.018	.018	.018	.018	.018
α=ε= 0.05	τ	$.982 \times 10^{-6}$	$.384 \times 10^{-5}$	$.865 \times 10^{-5}$	$.159 \times 10^{-4}$	$.261 \times 10^{-4}$	$.429 \times 10^{-4}$	$.855 \times 10^{-4}$	$.266 \times 10^{-3}$
	Q_{ci}/Q_i	0	0	0	0	0	0	0	0
α=ε= 0.1	τ	$.414 \times 10^{-5}$	$.157 \times 10^{-4}$	$.349 \times 10^{-4}$	$.633 \times 10^{-4}$	$.103 \times 10^{-3}$	$.167 \times 10^{-3}$	$.320 \times 10^{-3}$	$.873 \times 10^{-3}$
	Q_{ci}/Q_i	0	0	0	0	0	0	0	0
α=ε= 0.2	τ	$.180 \times 10^{-4}$	$.653 \times 10^{-4}$	$.141 \times 10^{-3}$	$.252 \times 10^{-3}$	$.403 \times 10^{-3}$	$.636 \times 10^{-3}$	$.114 \times 10^{-2}$	$.257 \times 10^{-2}$
	Q_{ci}/Q_i	0	0	0	0	0	0	0	0
α=ε= 0.3	τ	$.431 \times 10^{-4}$	$.152 \times 10^{-3}$	$.323 \times 10^{-3}$	$.565 \times 10^{-3}$	$.889 \times 10^{-3}$	$.137 \times 10^{-2}$	$.232 \times 10^{-2}$	$.459 \times 10^{-2}$
	Q_{ci}/Q_i	0	0	0	0	0	0	0	0
α=ε= 0.5	τ	$.130 \times 10^{-3}$	$.447 \times 10^{-3}$	$.920 \times 10^{-3}$	$.156 \times 10^{-2}$	$.238 \times 10^{-2}$	$.351 \times 10^{-2}$	$.547 \times 10^{-2}$	$.907 \times 10^{-2}$
	Q_{ci}/Q_i	0	0	0	0	0	0	0	0
α=ε= 0.75	τ	$.314 \times 10^{-3}$	$.106 \times 10^{-2}$	$.213 \times 10^{-2}$	$.350 \times 10^{-2}$	$.516 \times 10^{-2}$	$.730 \times 10^{-2}$	$.106 \times 10^{-1}$	$.152 \times 10^{-1}$
	Q_{ci}/Q_i	0	0	0	0	.001	.001	.001	.001
α=ε= 1.0	τ	$.584 \times 10^{-3}$	$.198 \times 10^{-2}$	$.389 \times 10^{-2}$	$.622 \times 10^{-2}$	$.892 \times 10^{-2}$	$.122 \times 10^{-1}$	$.168 \times 10^{-1}$	$.220 \times 10^{-1}$
	Q_{ci}/Q_i	.001	.001	.001	.001	.001	.001	.001	.001

TABLE II.- CONFIGURATION FACTORS, ENERGY TRANSFER FACTORS, AND Q_{ci}/Q_i FOR DOUBLE-SHIELD CONICAL-CAPSULE CONFIGURATION - Concluded

(c) $x/R = 1.0$

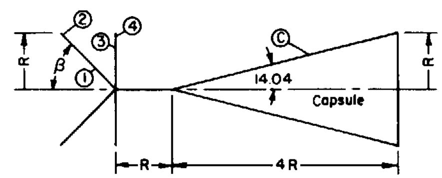

		$\beta = 15°$	$\beta = 30°$	$\beta = 45°$	$\beta = 60°$	$\beta = 75°$	$\beta = 90°$
F_{1-1}		0.741	0.500	0.293	0.134	0.340	0
F_{2-2}		0	0	0	0	0	0
F_{2-3}		.035	.138	.299	.509	.745	1.000
F_{3-2}		.135	.276	.423	.588	.772	1.000
F_{4-c}		.048	.048	.048	.048	.048	.048
F_{c-4}		.012	.012	.012	.012	.012	.012
$\alpha = \epsilon =$ 0.05	τ	$.113 \times 10^{-5}$	$.442 \times 10^{-5}$	$.103 \times 10^{-4}$	$.215 \times 10^{-4}$	$.496 \times 10^{-4}$	$.610 \times 10^{-3}$
	Q_{ci}/Q_i	0	0	0	0	0	0
$\alpha = \epsilon =$ 0.1	τ	$.476 \times 10^{-5}$	$.181 \times 10^{-4}$	$.415 \times 10^{-4}$	$.847 \times 10^{-4}$	$.187 \times 10^{-3}$	$.124 \times 10^{-2}$
	Q_{ci}/Q_i	0	0	0	0	0	0
$\alpha = \epsilon =$ 0.2	τ	$.207 \times 10^{-4}$	$.749 \times 10^{-4}$	$.167 \times 10^{-3}$	$.329 \times 10^{-3}$	$.675 \times 10^{-3}$	$.254 \times 10^{-2}$
	Q_{ci}/Q_i	0	0	0	0	0	0
$\alpha = \epsilon =$ 0.3	τ	$.496 \times 10^{-4}$	$.174 \times 10^{-3}$	$.378 \times 10^{-3}$	$.721 \times 10^{-3}$	$.139 \times 10^{-2}$	$.391 \times 10^{-2}$
	Q_{ci}/Q_i	0	0	0	0	0	0
$\alpha = \epsilon =$ 0.5	τ	$.150 \times 10^{-3}$	$.511 \times 10^{-3}$	$.106 \times 10^{-2}$	$.192 \times 10^{-2}$	$.335 \times 10^{-2}$	$.689 \times 10^{-2}$
	Q_{ci}/Q_i	0	0	0	0	0	0
$\alpha = \epsilon =$ 0.75	τ	$.361 \times 10^{-3}$	$.121 \times 10^{-2}$	$.243 \times 10^{-2}$	$.414 \times 10^{-2}$	$.661 \times 10^{-2}$	$.111 \times 10^{-1}$
	Q_{ci}/Q_i	0	0	0	0	0	0
$\alpha = \epsilon =$ 1.0	τ	$.671 \times 10^{-3}$	$.225 \times 10^{-2}$	$.438 \times 10^{-2}$	$.715 \times 10^{-2}$	$.107 \times 10^{-1}$	$.161 \times 10^{-1}$
	Q_{ci}/Q_i	0	0	0	0	0	0

TABLE III.- CONFIGURATION FACTORS, ENERGY TRANSFER FACTORS, AND Q_{ci}/Q_i FOR SINGLE-SHIELD SPHERICAL-CAPSULE CONFIGURATION

(a) $x/R = 0$

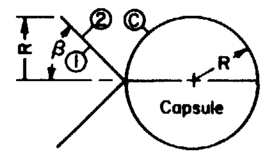

		β = 10°	β = 20°	β = 30°	β = 50°	β = 60°	β = 70°	β = 90°
F_{1-1}		0.826	0.658	0.500	0.234	0.134	0.060	0
F_{2-2}		0	0	0	0	0	0	0
F_{2-c}		.011	.029	.067	.185	.268	.363	.542
F_{c-2}		.016	.043	.067	.121	.155	.193	.300
$\alpha=\epsilon=$	τ	$.304\times10^{-3}$	$.772\times10^{-3}$	$.172\times10^{-2}$	$.476\times10^{-2}$	$.700\times10^{-2}$	$.974\times10^{-2}$	$.160\times10^{-1}$
0.05	Q_{c1}/Q_1	0	0	0	.001	.001	.002	.004
$\alpha=\epsilon=$	τ	$.656\times10^{-3}$	$.161\times10^{-2}$	$.352\times10^{-2}$	$.958\times10^{-2}$	$.140\times10^{-1}$	$.194\times10^{-1}$	$.317\times10^{-1}$
0.1	Q_{c1}/Q_1	0	0	0	.001	.002	.004	.008
$\alpha=\epsilon=$	τ	$.145\times10^{-2}$	$.343\times10^{-2}$	$.734\times10^{-2}$	$.194\times10^{-1}$	$.282\times10^{-1}$	$.387\times10^{-1}$	$.623\times10^{-1}$
0.2	Q_{c1}/Q_1	0	0	0	.002	.004	.007	.015
$\alpha=\epsilon=$	τ	$.234\times10^{-2}$	$.542\times10^{-2}$	$.114\times10^{-1}$	$.294\times10^{-1}$	$.424\times10^{-1}$	$.579\times10^{-1}$	$.919\times10^{-1}$
0.3	Q_{c1}/Q_1	0	0	.001	.003	.005	.009	.021
$\alpha=\epsilon=$	τ	$.424\times10^{-2}$	$.979\times10^{-2}$	$.202\times10^{-1}$	$.502\times10^{-1}$	$.712\times10^{-1}$	$.960\times10^{-1}$	.149
0.5	Q_{c1}/Q_1	0	0	.001	.004	.008	.014	.030
$\alpha=\epsilon=$	τ	$.677\times10^{-2}$	$.157\times10^{-1}$	$.320\times10^{-1}$	$.772\times10^{-1}$	.108	.143	.216
0.75	Q_{c1}/Q_1	0	0	.001	.006	.010	.017	.037
$\alpha=\epsilon=$	τ	$.937\times10^{-2}$	$.220\times10^{-1}$	$.447\times10^{-1}$	.105	.145	.191	.281
1.0	Q_{c1}/Q_1	0	0	.001	.006	.011	.018	.038

A535

TABLE III.- CONFIGURATION FACTORS, ENERGY TRANSFER FACTORS, AND Q_{ci}/Q_i FOR SINGLE-SHIELD SPHERICAL-CAPSULE CONFIGURATION - Continued

(b) $x/R = 0.5$

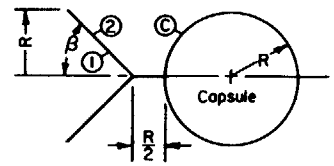

		$\beta = 15°$	$\beta = 30°$	$\beta = 45°$	$\beta = 60°$	$\beta = 90°$	$\beta = 120°$
F_{1-1}		0.741	0.500	0.293	0.134	0	0
F_{2-2}		0	0	0	0	0	.134
F_{2-c}		.011	.045	.101	.171	.336	.558
F_{c-2}		.021	.045	.072	.099	.168	.322
$\alpha=\epsilon=$ 0.05	τ	$.291\times10^{-3}$	$.114\times10^{-2}$	$.257\times10^{-2}$	$.436\times10^{-2}$	$.888\times10^{-2}$	$.194\times10^{-1}$
	Q_{ci}/Q_i	0	0	0	0	.001	.006
$\alpha=\epsilon=$ 0.1	τ	$.613\times10^{-3}$	$.234\times10^{-2}$	$.519\times10^{-2}$	$.875\times10^{-2}$	$.177\times10^{-1}$	$.383\times10^{-1}$
	Q_{ci}/Q_i	0	0	0	.001	.003	.012
$\alpha=\epsilon=$ 0.2	τ	$.133\times10^{-2}$	$.487\times10^{-2}$	$.106\times10^{-1}$	$.176\times10^{-1}$	$.352\times10^{-1}$	$.746\times10^{-1}$
	Q_{ci}/Q_i	0	0	.001	.002	.005	.022
$\alpha=\epsilon=$ 0.3	τ	$.213\times10^{-2}$	$.757\times10^{-2}$	$.161\times10^{-1}$	$.266\times10^{-1}$	$.525\times10^{-1}$	.109
	Q_{ci}/Q_i	0	0	.001	.002	.008	.030
$\alpha=\epsilon=$ 0.5	τ	$.386\times10^{-2}$	$.134\times10^{-1}$	$.277\times10^{-1}$	$.448\times10^{-1}$	$.868\times10^{-1}$	.174
	Q_{ci}/Q_i	0	0	.001	.003	.011	.042
$\alpha=\epsilon=$ 0.75	τ	$.620\times10^{-2}$	$.213\times10^{-1}$	$.431\times10^{-1}$	$.681\times10^{-1}$	.129	.247
	Q_{ci}/Q_i	0	.001	.002	.004	.014	.050
$\alpha=\epsilon=$ 1.0	τ	$.866\times10^{-2}$	$.298\times10^{-1}$	$.593\times10^{-1}$	$.921\times10^{-1}$	.170	.314
	Q_{ci}/Q_i	0	.001	.002	.005	.014	.051

TABLE III.- CONFIGURATION FACTORS, ENERGY TRANSFER FACTORS, AND Q_{ci}/Q_i FOR SINGLE-SHIELD SPHERICAL-CAPSULE CONFIGURATION - Concluded

(c) x/R = 1.0

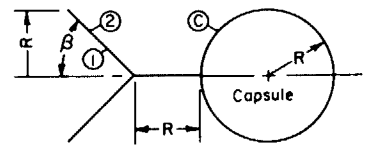

		β = 15°	β = 30°	β = 45°	β = 60°	β = 90°	β = 120°	β = 135°
F_{1-1}		0.741	0.500	0.293	0.134	0	0	0
F_{2-2}		0	0	0	0	0	.134	.293
F_{2-c}		.008	.034	.073	.117	.211	.315	.414
F_{c-2}		.016	.034	.051	.068	.106	.182	.293
α=ε= 0.05	τ	$.221\times10^{-3}$	$.874\times10^{-3}$	$.184\times10^{-2}$	$.296\times10^{-2}$	$.539\times10^{-2}$	$.958\times10^{-2}$	$.164\times10^{-1}$
	Q_{ci}/Q_i	0	0	0	0	.001	.002	.005
α=ε= 0.1	τ	$.467\times10^{-3}$	$.179\times10^{-2}$	$.372\times10^{-2}$	$.594\times10^{-2}$	$.108\times10^{-1}$	$.190\times10^{-1}$	$.324\times10^{-1}$
	Q_{ci}/Q_i	0	0	0	0	.001	.003	.009
α=ε= 0.2	τ	$.101\times10^{-2}$	$.372\times10^{-2}$	$.757\times10^{-2}$	$.120\times10^{-1}$	$.215\times10^{-1}$	$.376\times10^{-1}$	$.629\times10^{-1}$
	Q_{ci}/Q_i	0	0	0	.001	.002	.006	.017
α=ε= 0.3	τ	$.162\times10^{-2}$	$.579\times10^{-2}$	$.116\times10^{-1}$	$.181\times10^{-1}$	$.322\times10^{-1}$	$.557\times10^{-1}$	$.916\times10^{-1}$
	Q_{ci}/Q_i	0	0	0	.001	.003	.009	.023
α=ε= 0.5	τ	$.294\times10^{-2}$	$.102\times10^{-1}$	$.199\times10^{-1}$	$.305\times10^{-1}$	$.534\times10^{-1}$	$.907\times10^{-1}$	.144
	Q_{ci}/Q_i	0	0	.001	.002	.004	.012	.032
α=ε= 0.75	τ	$.472\times10^{-2}$	$.163\times10^{-1}$	$.309\times10^{-1}$	$.464\times10^{-1}$	$.798\times10^{-1}$	.132	.201
	Q_{ci}/Q_i	0	0	.001	.002	.005	.015	.037
α=ε= 1.0	τ	$.659\times10^{-2}$	$.227\times10^{-1}$	$.426\times10^{-1}$	$.628\times10^{-1}$	.106	.171	.251
	Q_{ci}/Q_i	0	0	.001	.002	.006	.016	.037

A535

TABLE IV.- CONFIGURATION FACTORS, ENERGY TRANSFER FACTORS, AND Q_{ci}/Q_i FOR DOUBLE-SHIELD SPHERICAL-CAPSULE CONFIGURATION

(a) $x/R = 0$

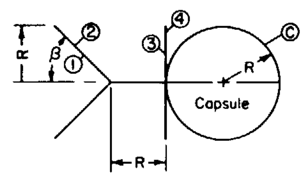

		$\beta = 15°$	$\beta = 30°$	$\beta = 45°$	$\beta = 60°$	$\beta = 75°$	$\beta = 90°$	$\beta = 105°$	$\beta = 120°$	$\beta = 135°$
F_{1-1}		0.741	0.500	0.293	0.134	0.034	0	0	0	0
F_{2-2}		0	0	0	0	0	0	.034	.134	.293
F_{2-3}		.013	.055	.121	.204	.292	.382	.472	.569	.707
F_{3-2}		.052	.109	.172	.235	.303	.382	.488	.657	1.000
F_{4-c}		.542	.542	.542	.542	.542	.542	.542	.542	.542
F_{c-4}		.300	.300	.300	.300	.300	.300	.300	.300	.300
$\alpha = \epsilon =$ 0.05	τ	$.573 \times 10^{-5}$	$.226 \times 10^{-4}$	$.501 \times 10^{-4}$	$.858 \times 10^{-4}$	$.128 \times 10^{-3}$	$.178 \times 10^{-3}$	$.250 \times 10^{-3}$	$.408 \times 10^{-3}$	$.117 \times 10^{-2}$
	Q_{ci}/Q_i	.004	.004	.004	.004	.004	.004	.004	.004	.004
$\alpha = \epsilon =$ 0.1	τ	$.239 \times 10^{-4}$	$.914 \times 10^{-4}$	$.200 \times 10^{-3}$	$.340 \times 10^{-3}$	$.504 \times 10^{-3}$	$.698 \times 10^{-3}$	$.978 \times 10^{-3}$	$.157 \times 10^{-2}$	$.431 \times 10^{-2}$
	Q_{ci}/Q_i	.008	.008	.008	.008	.008	.008	.008	.008	.008
$\alpha = \epsilon =$ 0.2	τ	$.102 \times 10^{-3}$	$.374 \times 10^{-3}$	$.800 \times 10^{-3}$	$.134 \times 10^{-2}$	$.197 \times 10^{-2}$	$.270 \times 10^{-2}$	$.374 \times 10^{-2}$	$.586 \times 10^{-2}$	$.147 \times 10^{-1}$
	Q_{ci}/Q_i	.015	.015	.015	.015	.015	.015	.015	.015	.016
$\alpha = \epsilon =$ 0.3	τ	$.240 \times 10^{-3}$	$.856 \times 10^{-3}$	$.180 \times 10^{-2}$	$.297 \times 10^{-2}$	$.432 \times 10^{-2}$	$.589 \times 10^{-2}$	$.806 \times 10^{-2}$	$.123 \times 10^{-1}$	$.285 \times 10^{-1}$
	Q_{ci}/Q_i	.021	.021	.021	.021	.021	.021	.021	.021	.022
$\alpha = \epsilon =$ 0.5	τ	$.706 \times 10^{-3}$	$.245 \times 10^{-2}$	$.499 \times 10^{-2}$	$.807 \times 10^{-2}$	$.115 \times 10^{-1}$	$.155 \times 10^{-1}$	$.207 \times 10^{-1}$	$.304 \times 10^{-1}$	$.606 \times 10^{-1}$
	Q_{ci}/Q_i	.030	.030	.030	.030	.030	.031	.031	.031	.033
$\alpha = \epsilon =$ 0.75	τ	$.165 \times 10^{-2}$	$.566 \times 10^{-2}$	$.113 \times 10^{-1}$	$.178 \times 10^{-1}$	$.249 \times 10^{-1}$	$.329 \times 10^{-1}$	$.431 \times 10^{-1}$	$.599 \times 10^{-1}$	.103
	Q_{ci}/Q_i	.037	.037	.037	.037	.307	.037	.038	.039	.043
$\alpha = \epsilon =$ 1.0	τ	$.300 \times 10^{-2}$	$.103 \times 10^{-1}$	$.201 \times 10^{-1}$	$.311 \times 10^{-1}$	$.428 \times 10^{-1}$	$.558 \times 10^{-1}$	$.719 \times 10^{-1}$	$.957 \times 10^{-1}$	.145
	Q_{ci}/Q_i	.038	.038	.038	.039	.039	.040	.041	.043	.048

TABLE IV.- CONFIGURATION FACTORS, ENERGY TRANSFER FACTORS, AND Q_{ci}/Q_i FOR DOUBLE-SHIELD SPHERICAL-CAPSULE CONFIGURATION - Continued

(b) x/R = 0.5

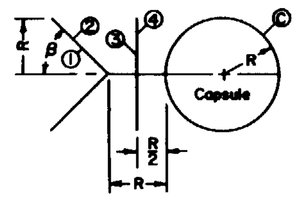

		β = 15°	β = 30°	β = 45°	β = 60°	β = 75°	β = 90°	β = 105°	β = 117°
F_{1-1}		0.741	0.500	0.293	0.134	0.034	0	0	0
F_{2-2}		0	0	0	0	0	0	.034	.134
F_{2-3}		.020	.081	.180	.309	.456	.610	.766	.866
F_{3-2}		.078	.163	.254	.375	.472	.610	.793	1.000
F_{4-c}		.336	.336	.336	.336	.336	.336	.336	.336
F_{c-4}		.168	.168	.168	.168	.168	.168	.168	.168
$\alpha=\epsilon=$ 0.05	τ	$.479\times10^{-5}$	$.187\times10^{-4}$	$.422\times10^{-4}$	$.774\times10^{-4}$	$.127\times10^{-3}$	$.209\times10^{-3}$	$.417\times10^{-3}$	$.130\times10^{-2}$
	Q_{ci}/Q_i	.001	.001	.001	.001	.001	.001	.001	.001
$\alpha=\epsilon=$ 0.10	τ	$.201\times10^{-4}$	$.763\times10^{-4}$	$.170\times10^{-3}$	$.308\times10^{-3}$	$.502\times10^{-3}$	$.813\times10^{-3}$	$.156\times10^{-2}$	$.425\times10^{-2}$
	Q_{ci}/Q_i	.003	.003	.003	.003	.003	.003	.003	.003
$\alpha=\epsilon=$ 0.20	τ	$.871\times10^{-4}$	$.316\times10^{-3}$	$.684\times10^{-3}$	$.122\times10^{-2}$	$.195\times10^{-2}$	$.308\times10^{-2}$	$.552\times10^{-2}$	$.125\times10^{-1}$
	Q_{ci}/Q_i	.005	.005	.005	.005	.005	.005	.005	.006
$\alpha=\epsilon=$ 0.3	τ	$.207\times10^{-3}$	$.732\times10^{-3}$	$.155\times10^{-2}$	$.272\times10^{-2}$	$.428\times10^{-2}$	$.658\times10^{-2}$	$.112\times10^{-1}$	$.222\times10^{-1}$
	Q_{ci}/Q_i	.008	.008	.008	.008	.008	.008	.008	.008
$\alpha=\epsilon=$ 0.5	τ	$.621\times10^{-3}$	$.213\times10^{-2}$	$.439\times10^{-2}$	$.744\times10^{-2}$	$.114\times10^{-1}$	$.167\times10^{-1}$	$.261\times10^{-1}$	$.434\times10^{-1}$
	Q_{ci}/Q_i	.011	.011	.011	.011	.011	.011	.012	.012
$\alpha=\epsilon=$ 0.75	τ	$.148\times10^{-2}$	$.503\times10^{-2}$	$.101\times10^{-1}$	$.165\times10^{-1}$	$.244\times10^{-1}$	$.345\times10^{-1}$	$.500\times10^{-1}$	$.722\times10^{-1}$
	Q_{ci}/Q_i	.014	.014	.014	.014	.014	.014	.015	.016
$\alpha=\epsilon=$ 1.00	τ	$.274\times10^{-2}$	$.928\times10^{-2}$	$.182\times10^{-1}$	$.291\times10^{-1}$	$.418\times10^{-1}$	$.574\times10^{-1}$	$.787\times10^{-1}$	.103
	Q_{ci}/Q_i	.014	.014	.015	.015	.015	.016	.017	.019

TABLE IV. - CONFIGURATION FACTORS, ENERGY TRANSFER FACTORS, AND Q_{ci}/Q_i FOR DOUBLE-SHIELD SPHERICAL-CAPSULE CONFIGURATION - Concluded

(c) x/R = 1.0

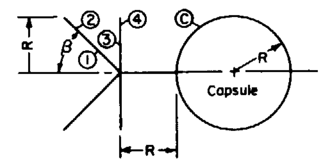

		β = 15°	β = 30°	β = 45°	β = 60°	β = 75°	β = 90°
F_{1-1}		0.741	0.500	0.293	0.134	0.034	0
F_{2-2}		0	0	0	0	0	0
F_{2-3}		.035	.138	.298	.509	.745	1.000
F_{3-2}		.135	.276	.423	.588	.772	1.000
F_{4-c}		.211	.211	.211	.211	.211	.211
F_{c-4}		.106	.106	.106	.106	.106	.106
$\alpha=\epsilon=$ 0.05	τ	$.505\times10^{-5}$	$.198\times10^{-4}$	$.463\times10^{-4}$	$.962\times10^{-4}$	$.222\times10^{-3}$	$.273\times10^{-2}$
	Q_{ci}/Q_i	.001	.001	.001	.001	.001	.001
$\alpha=\epsilon=$ 0.1	τ	$.213\times10^{-4}$	$.806\times10^{-4}$	$.185\times10^{-3}$	$.378\times10^{-3}$	$.836\times10^{-3}$	$.552\times10^{-2}$
	Q_{ci}/Q_i	.001	.001	.001	.001	.001	.001
$\alpha=\epsilon=$ 0.2	τ	$.923\times10^{-4}$	$.334\times10^{-3}$	$.745\times10^{-3}$	$.147\times10^{-2}$	$.301\times10^{-2}$	$.113\times10^{-1}$
	Q_{ci}/Q_i	.002	.002	.002	.002	.002	.002
$\alpha=\epsilon=$ 0.3	τ	$.220\times10^{-3}$	$.775\times10^{-3}$	$.168\times10^{-2}$	$.321\times10^{-2}$	$.619\times10^{-2}$	$.174\times10^{-1}$
	Q_{ci}/Q_i	.003	.003	.003	.003	.003	.003
$\alpha=\epsilon=$ 0.5	τ	$.664\times10^{-3}$	$.226\times10^{-2}$	$.471\times10^{-2}$	$.850\times10^{-2}$	$.149\times10^{-1}$	$.306\times10^{-1}$
	Q_{ci}/Q_i	.004	.004	.004	.004	.004	.005
$\alpha=\epsilon=$ 0.75	τ	$.159\times10^{-2}$	$.535\times10^{-2}$	$.107\times10^{-1}$	$.183\times10^{-1}$	$.292\times10^{-1}$	$.492\times10^{-1}$
	Q_{ci}/Q_i	.005	.005	.005	.006	.006	.006
$\alpha=\epsilon=$ 1.0	τ	$.295\times10^{-2}$	$.989\times10^{-2}$	$.193\times10^{-1}$	$.315\times10^{-1}$	$.471\times10^{-1}$	$.709\times10^{-1}$
	Q_{ci}/Q_i	.006	.006	.006	.006	.007	.007

A
5
3
5

A
5
3
5

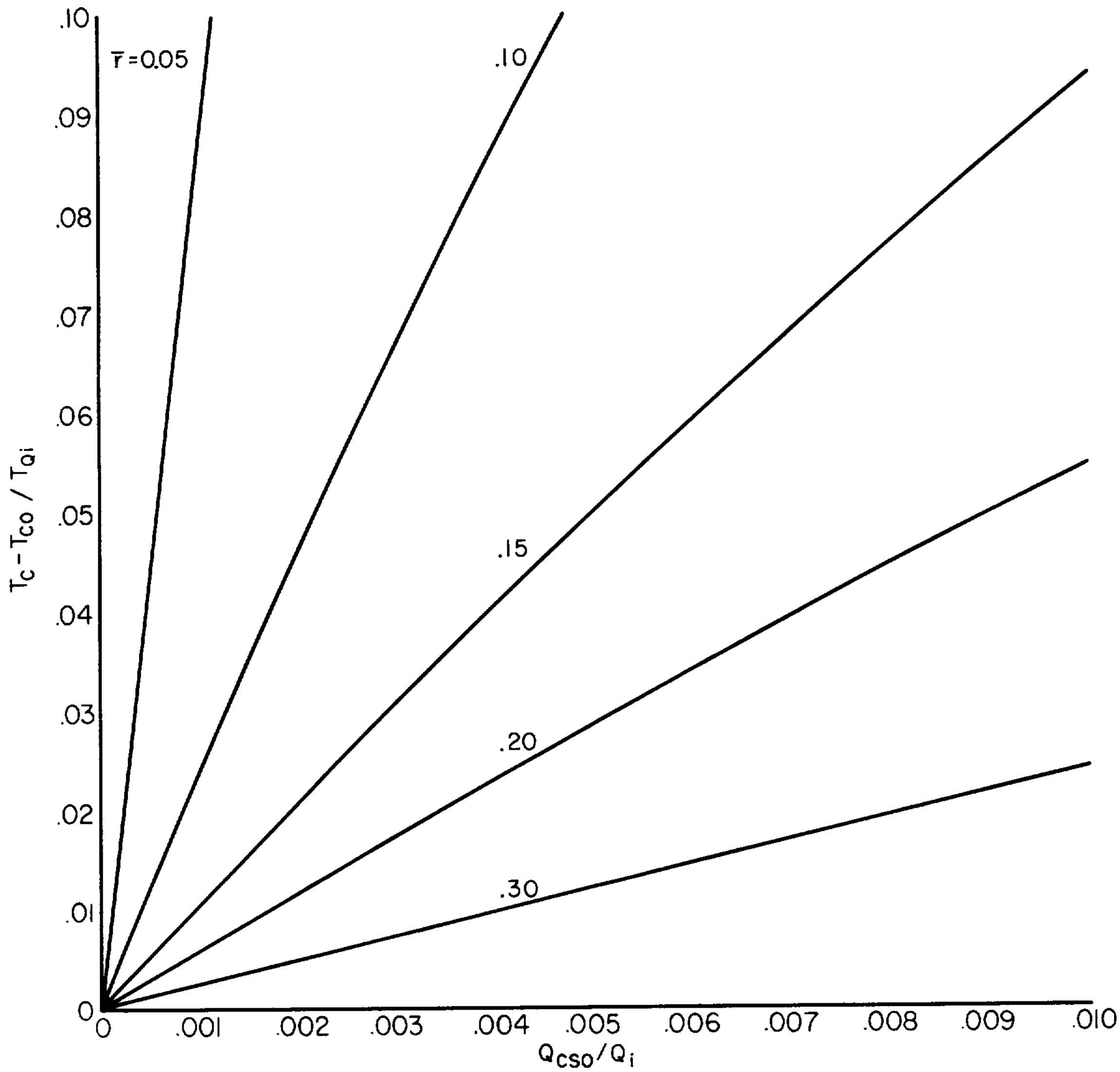

Figure 1.- Capsule temperature change as a function of the ratio Q_{cso}/Q_i for vehicles which travel from the earth to various distances from the sun.

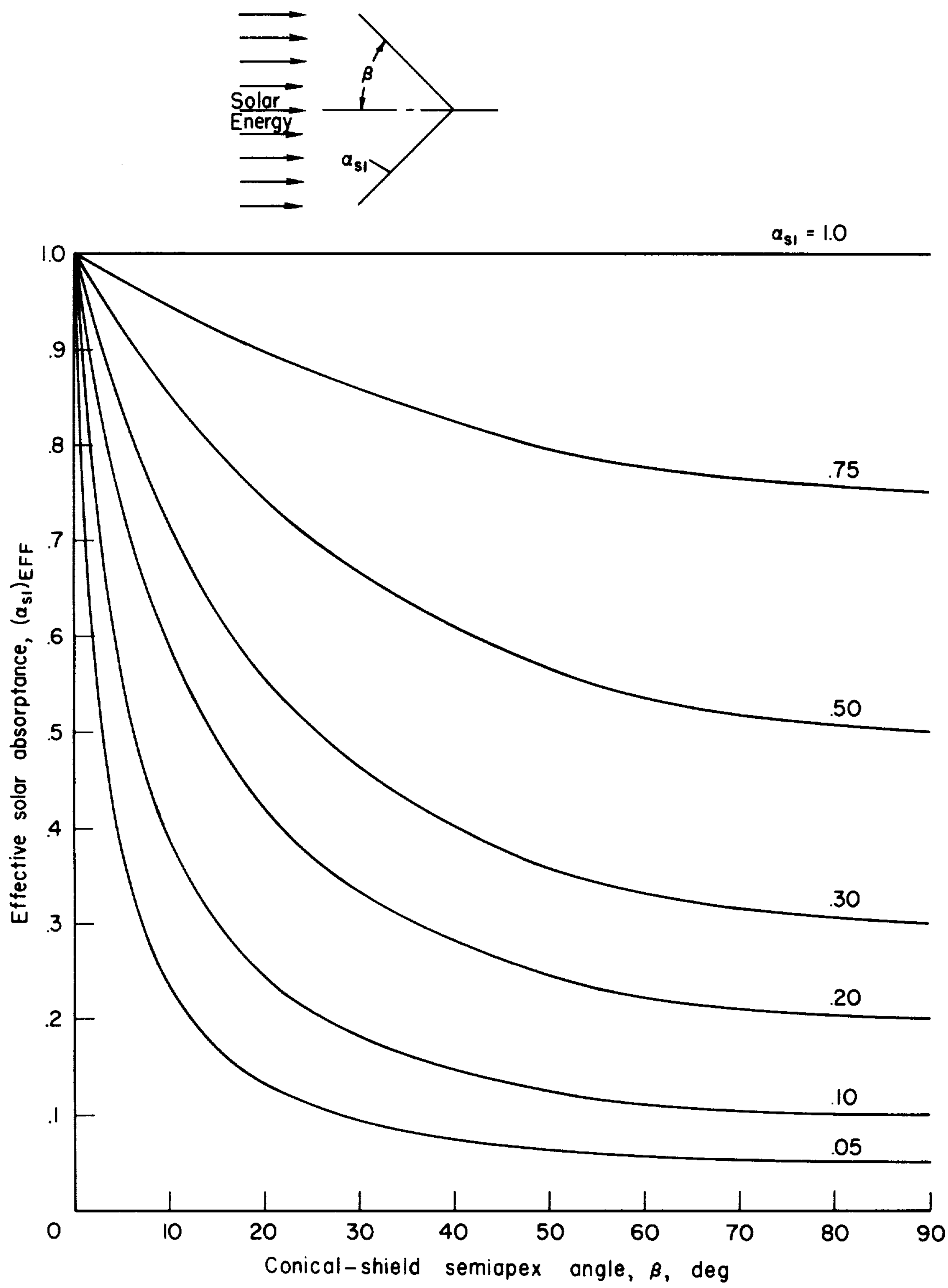

Figure 2.- Effective solar absorptance as a function of conical-shield semiapex angle for various solar absorptances.

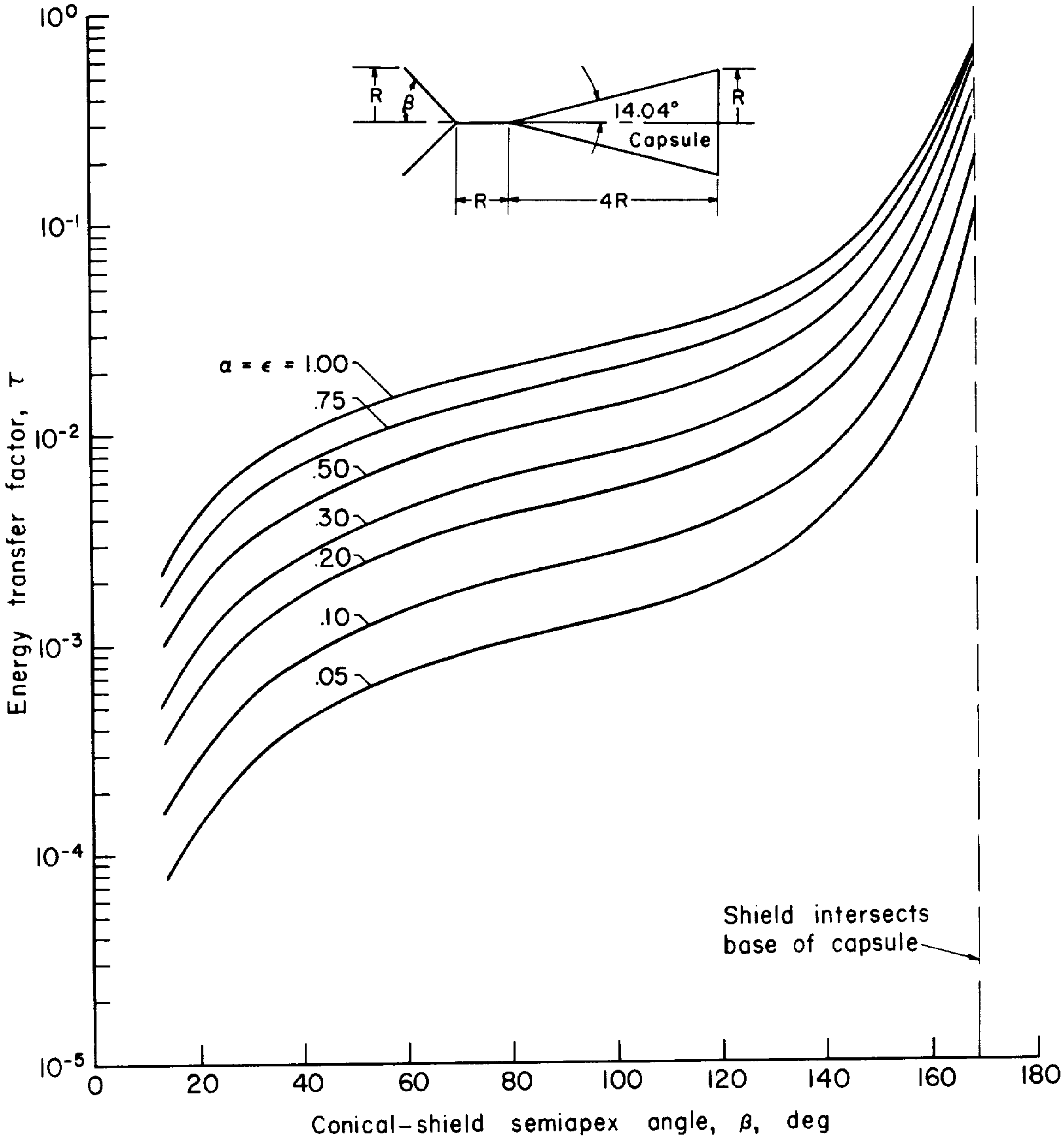

Figure 3.- Energy transfer factor as a function of conical-shield semiapex angle for various values of thermal emittance and absorptance.

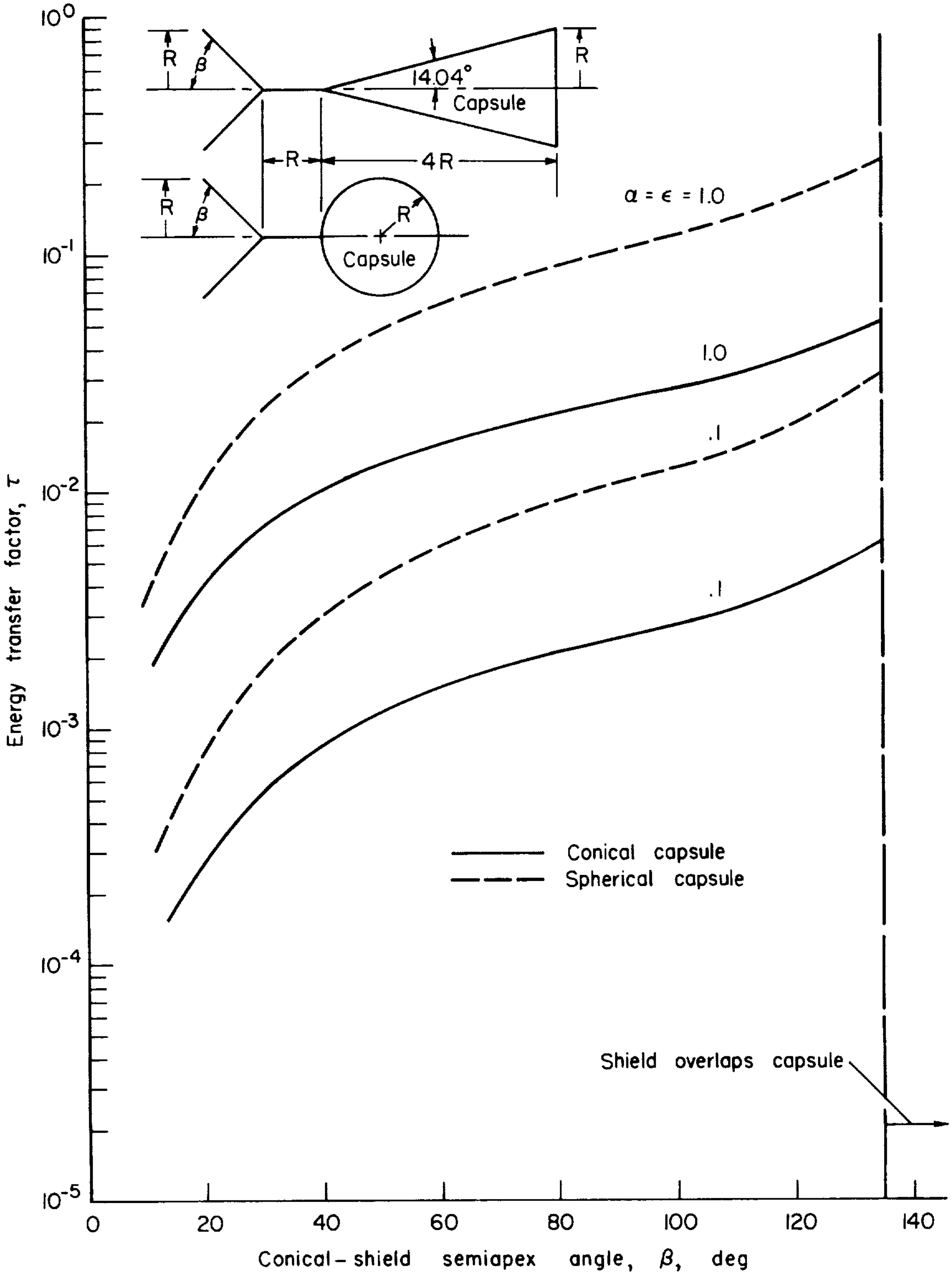

Figure 4.- Comparison of energy transfer factors for conical and spherical capsules and single conical shields.

A
5
3
5

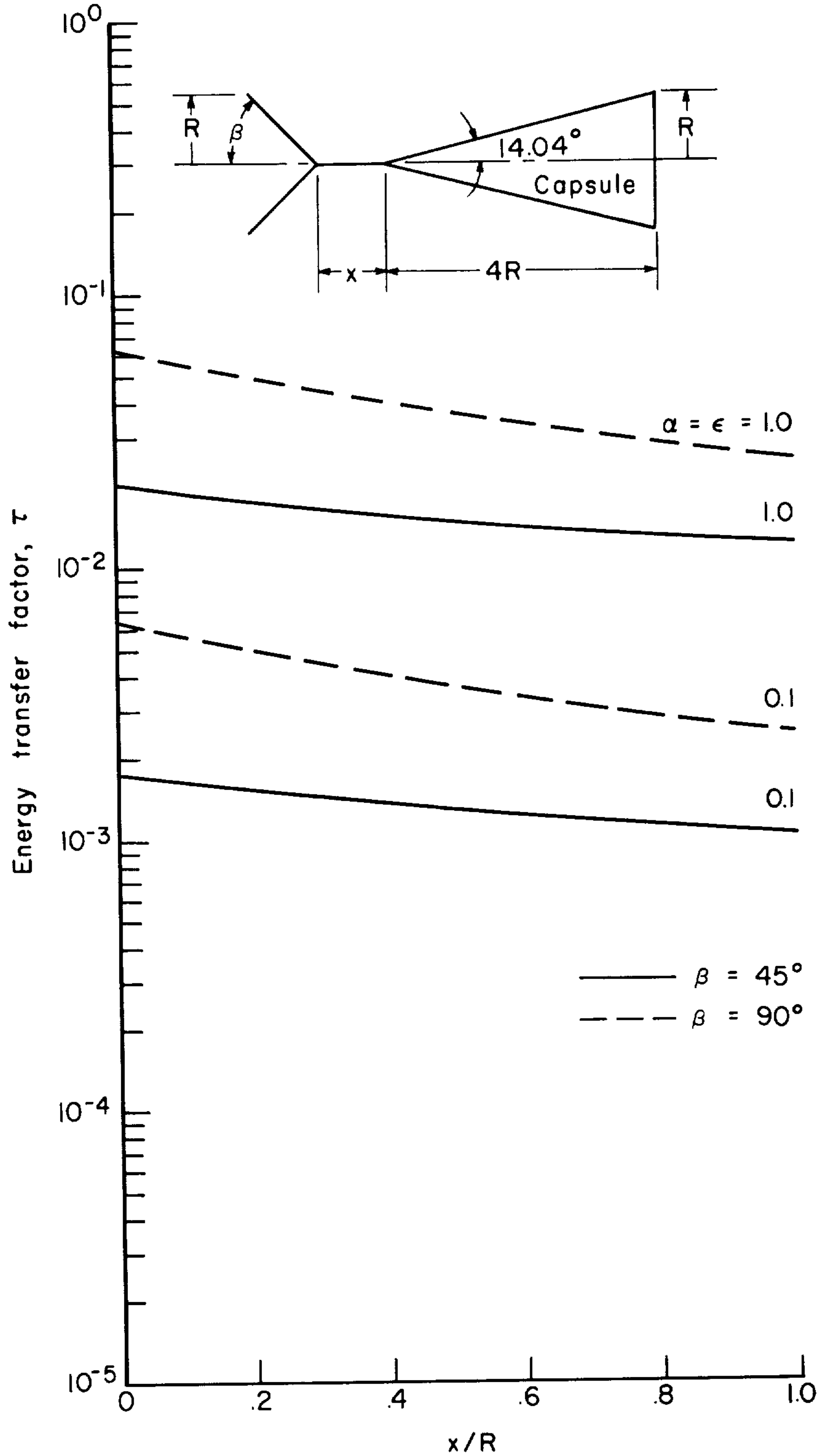

Figure 5.- Energy transfer factor as a function of distance between the shield and capsule.

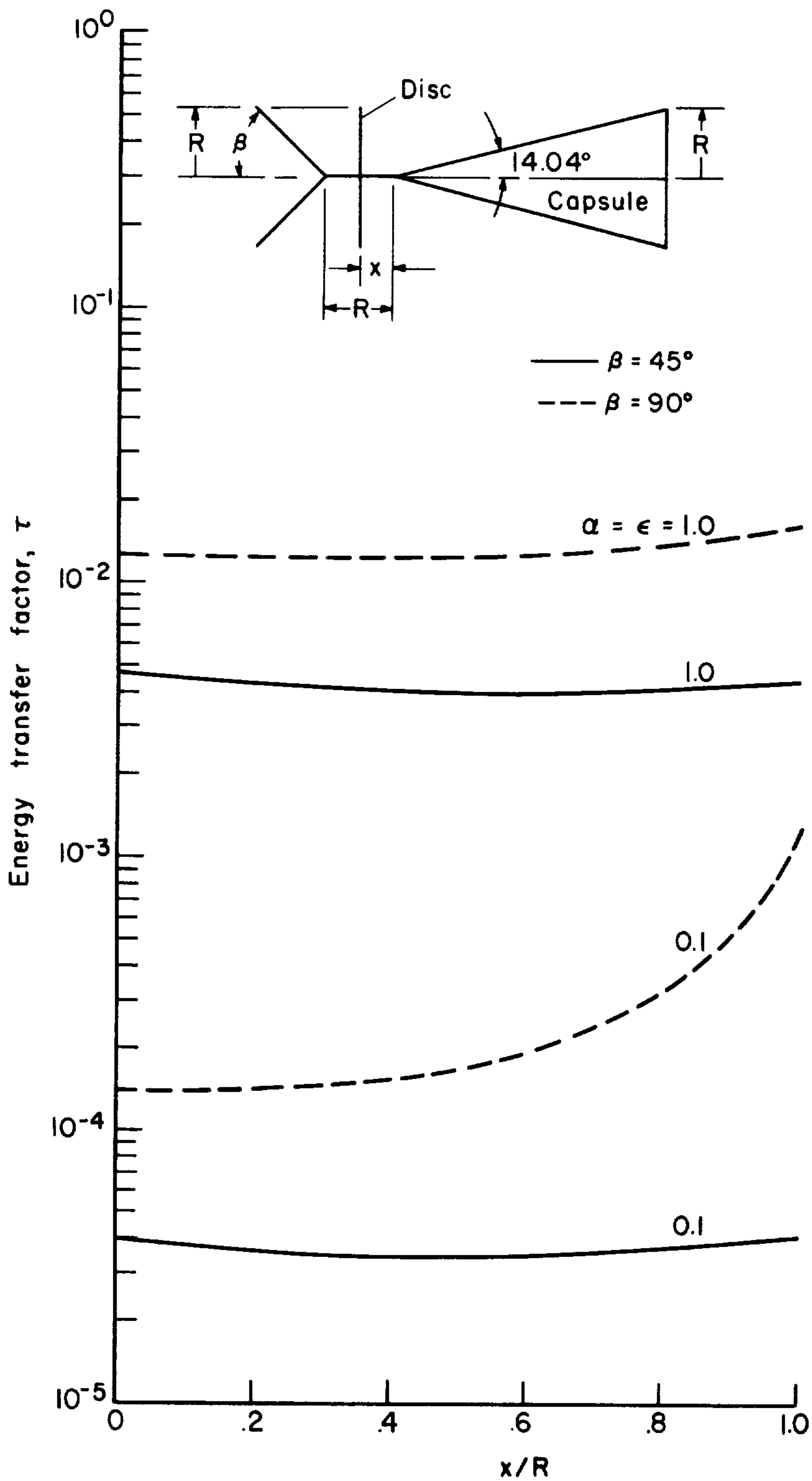

Figure 6.- Energy transfer factor as a function of position of disc between a conical shield and capsule.

A
5
3
5

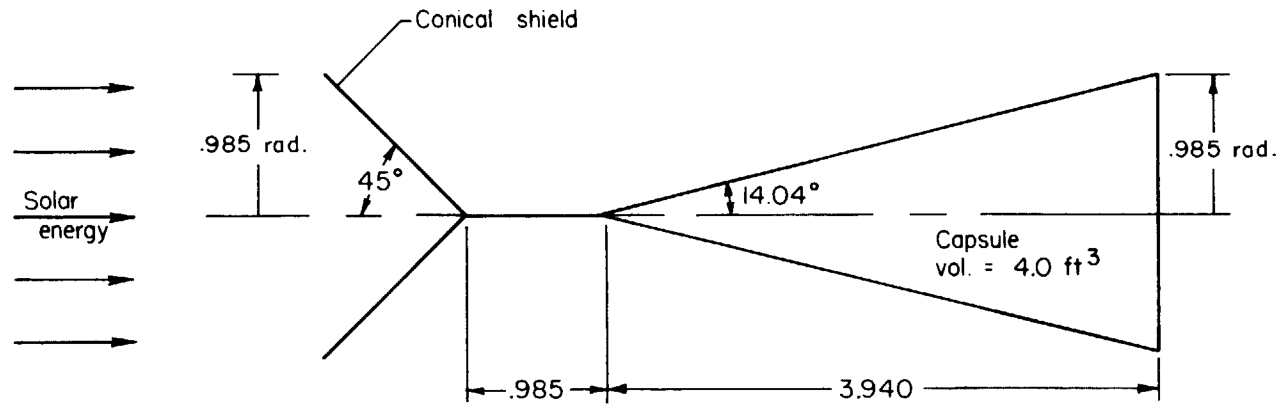

(a.) Single - shield configuration

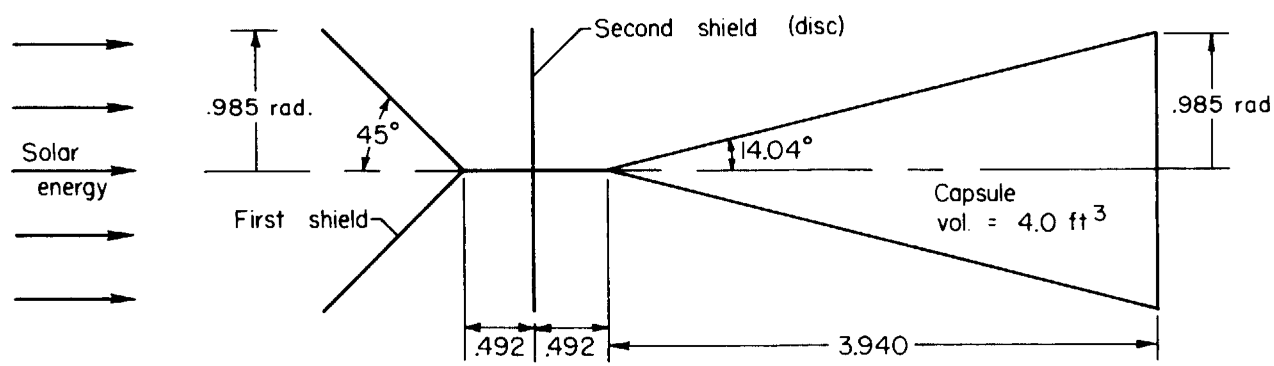

(b.) Double - shield configuration

Note: All dimensions in feet.

Figure 7.- Solar probe configurations.

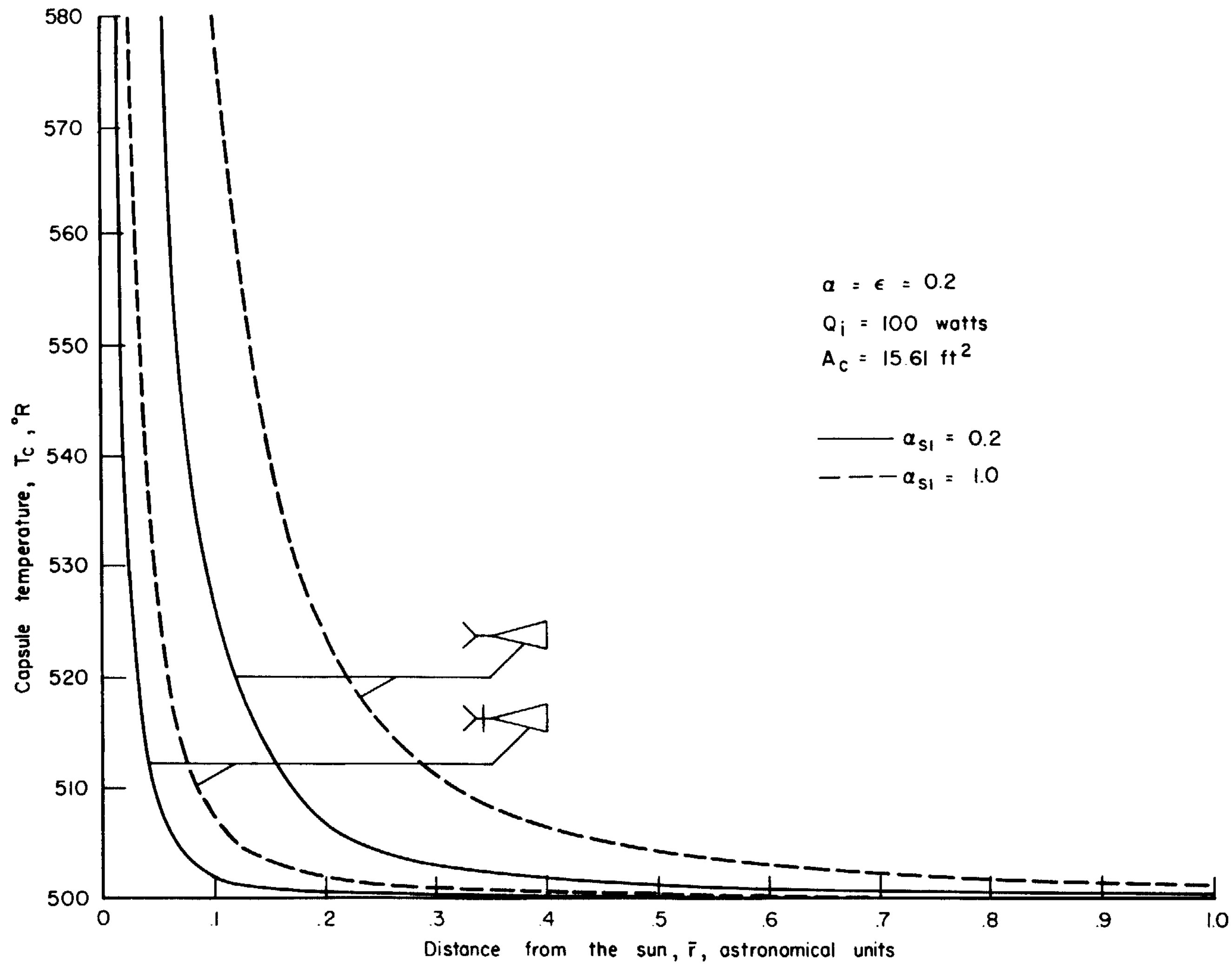

Figure 8.- Capsule temperature for the shielded solar probe configurations as a function of distance from the sun.

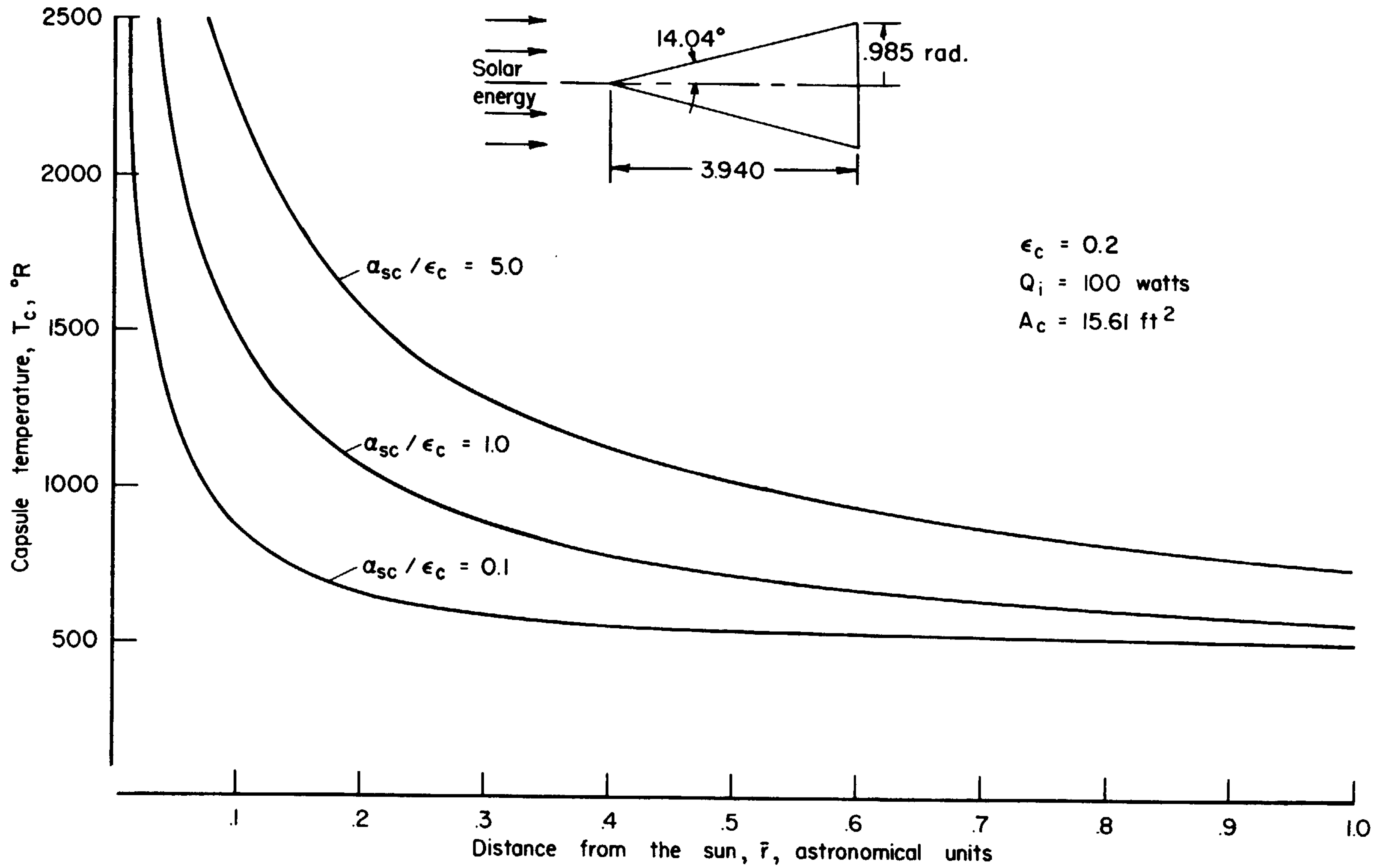

Figure 9.- Temperature of an unshielded conical capsule as a function of distance from the sun.

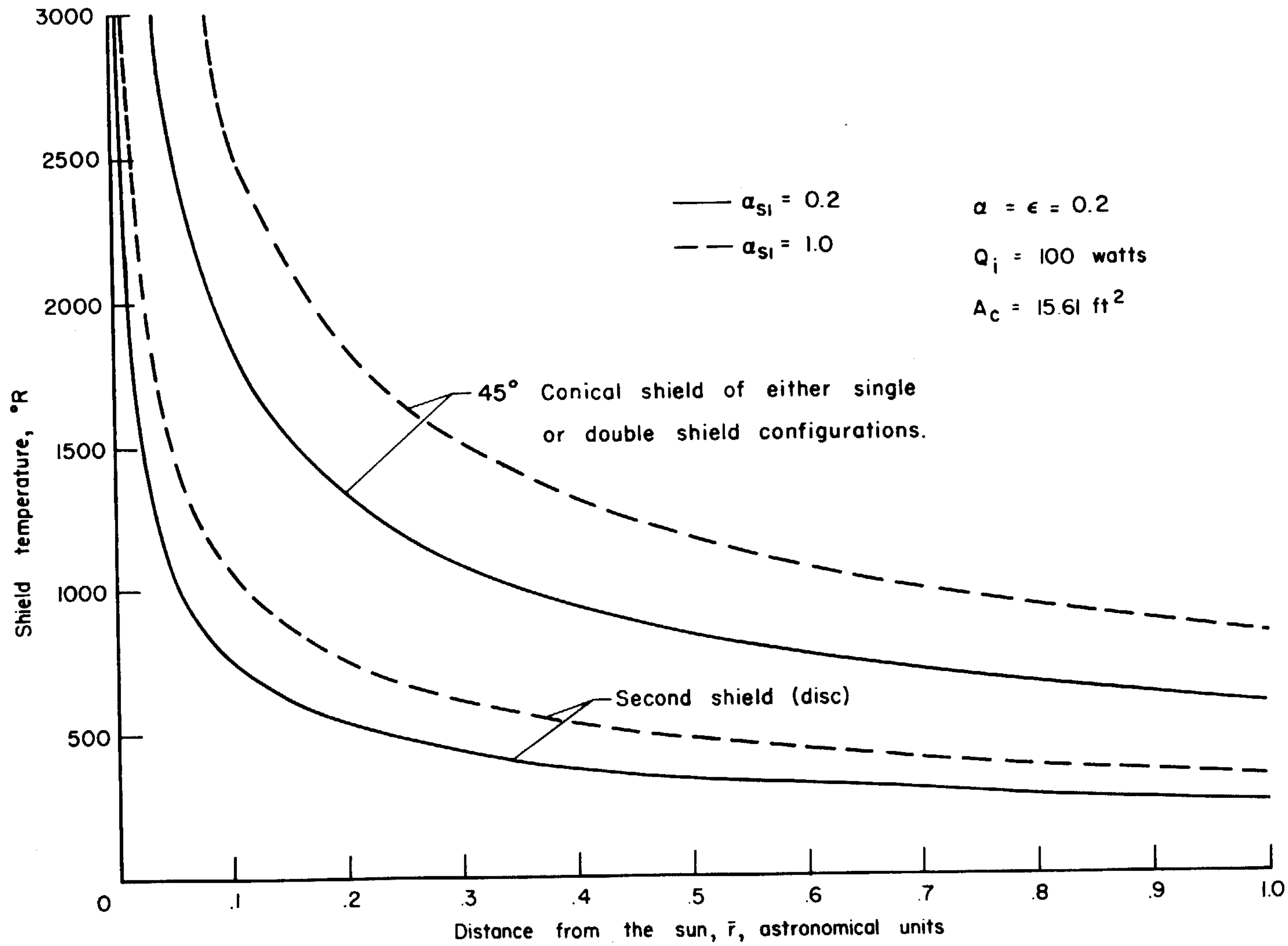

Figure 10.- Shield temperatures for the solar probe configurations as a function of distance from the sun.

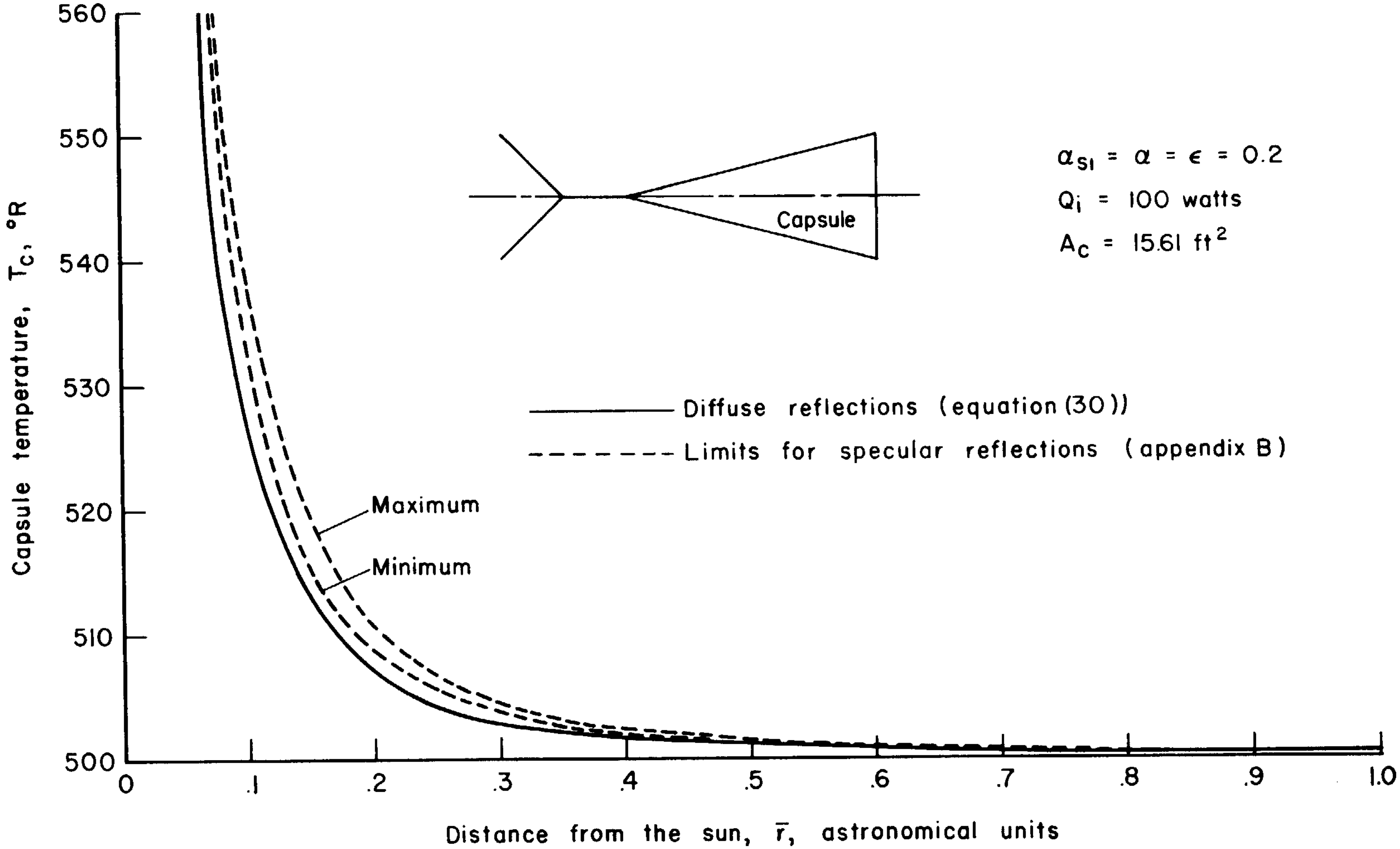

Figure 11.- Capsule temperatures for the single-shield solar-probe configuration comparing specular and diffuse reflections from all surfaces.

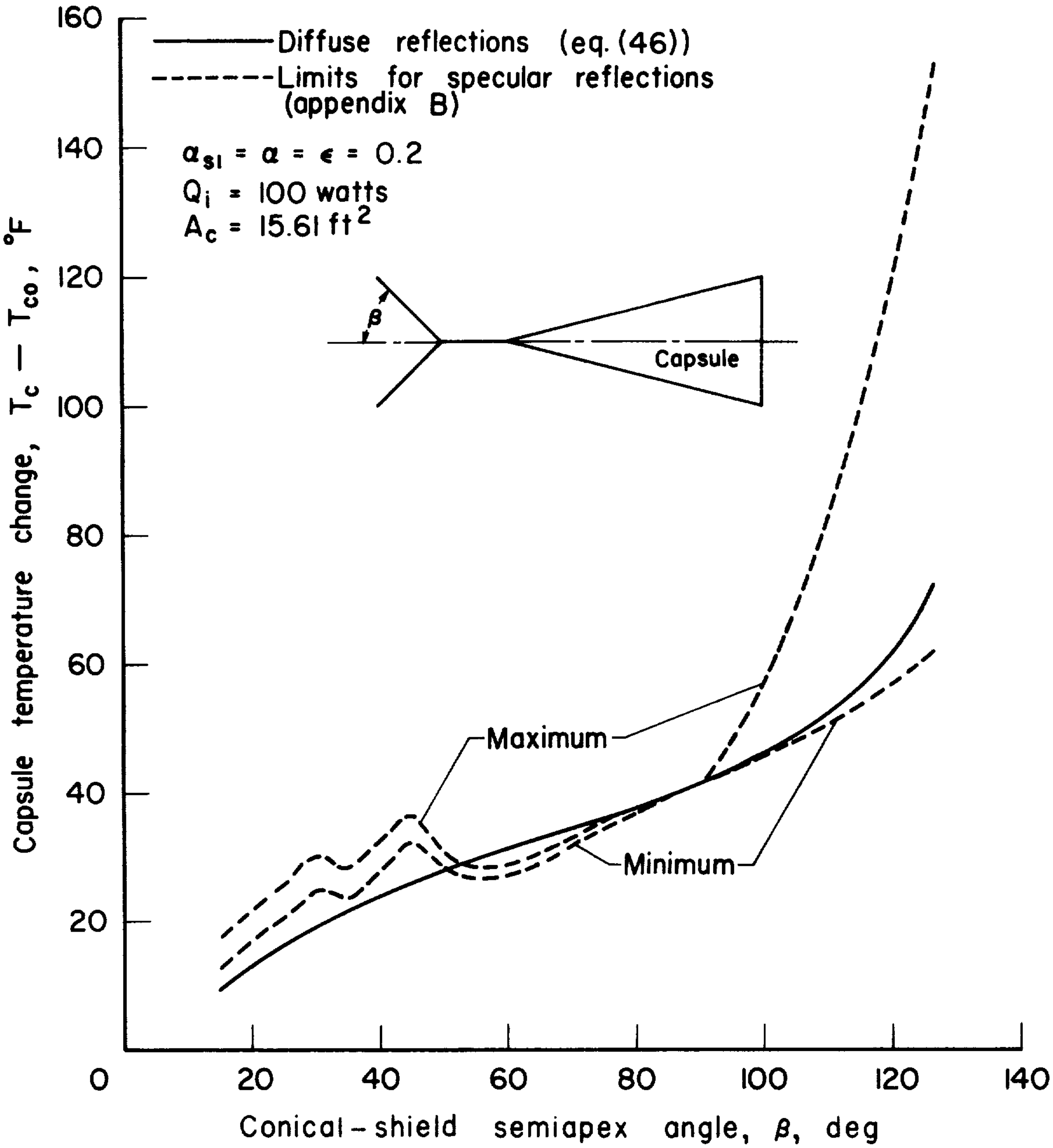

Figure 12.- Capsule temperature change as capsule travels from $\bar{r}$ = 1.0 to 0.1 as a function of shield, semiapex angle for diffuse and specular reflection analyses; single-shield solar-probe configuration.

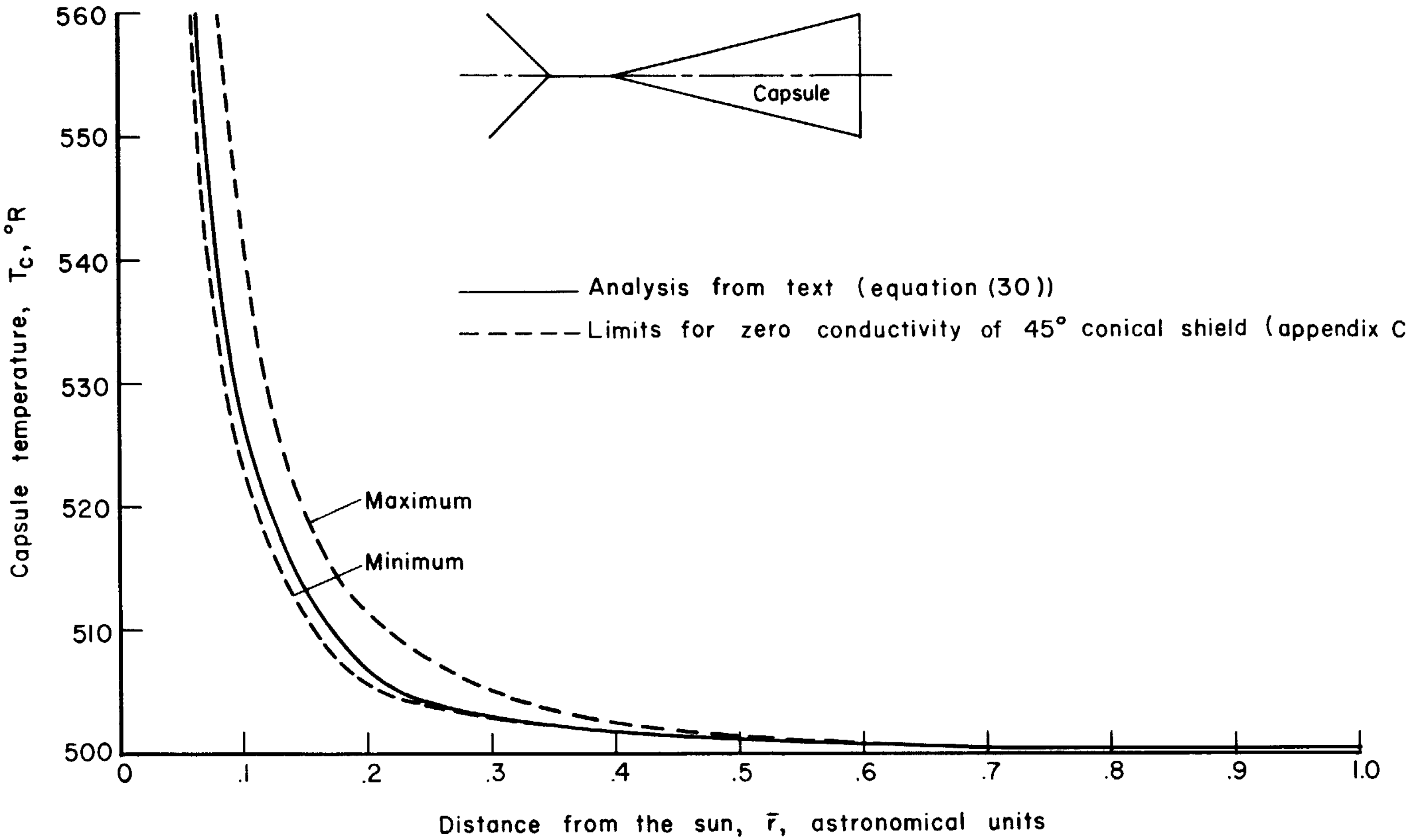

Figure 13.- Capsule temperatures for the single-shield solar-probe configuration comparing zero and infinite shield conductance.

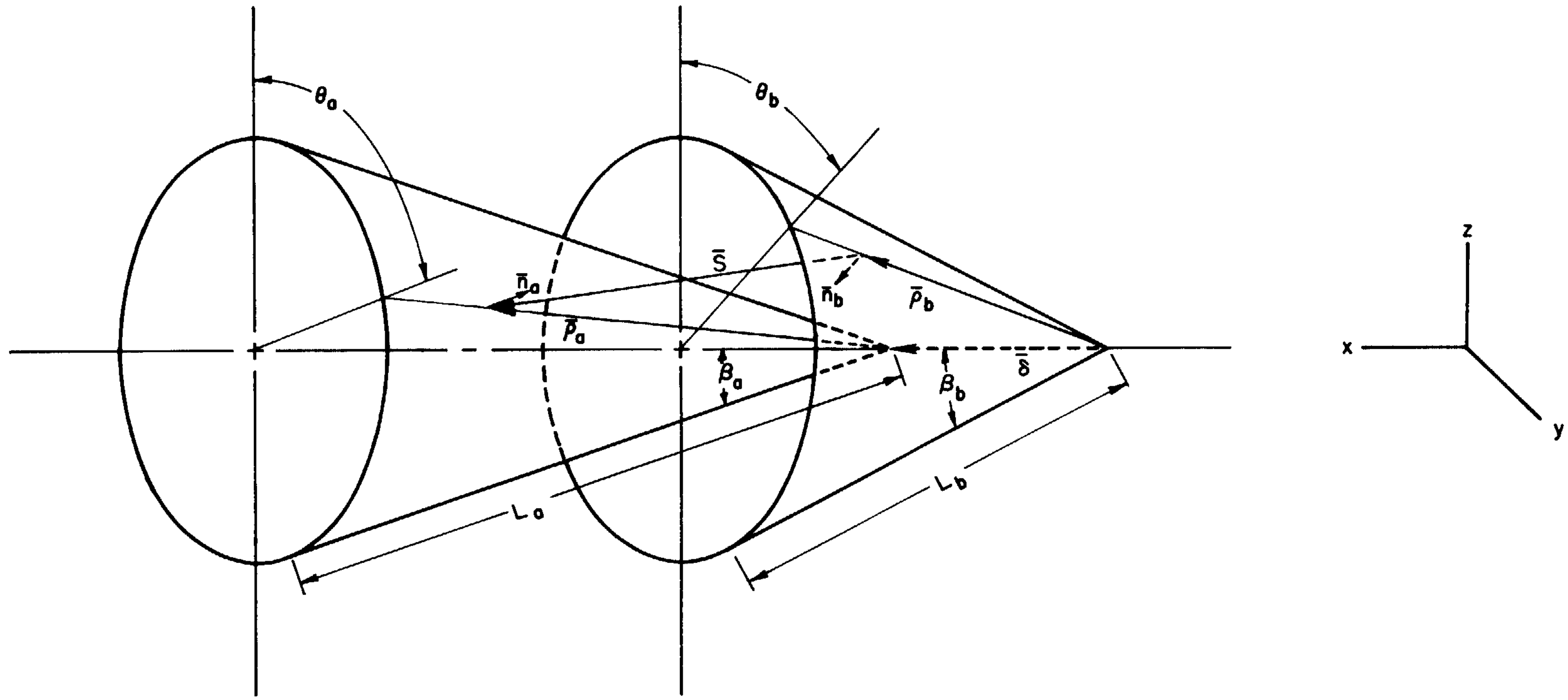

Figure 14.- Coordinate system for radiation configuration factors between two cones.

A535

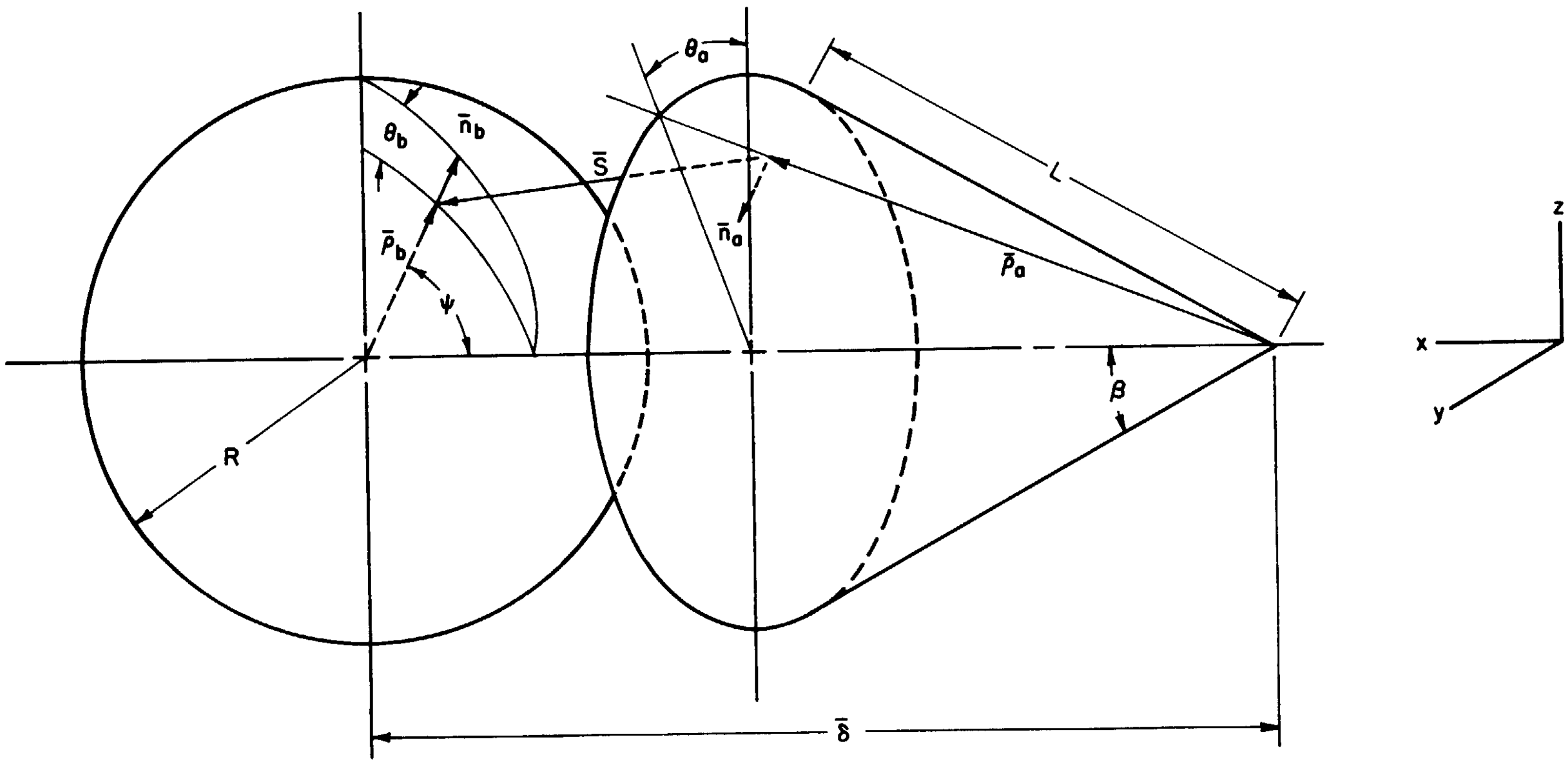

Figure 15.- Coordinate system for radiation configuration factors between a sphere and a cone.

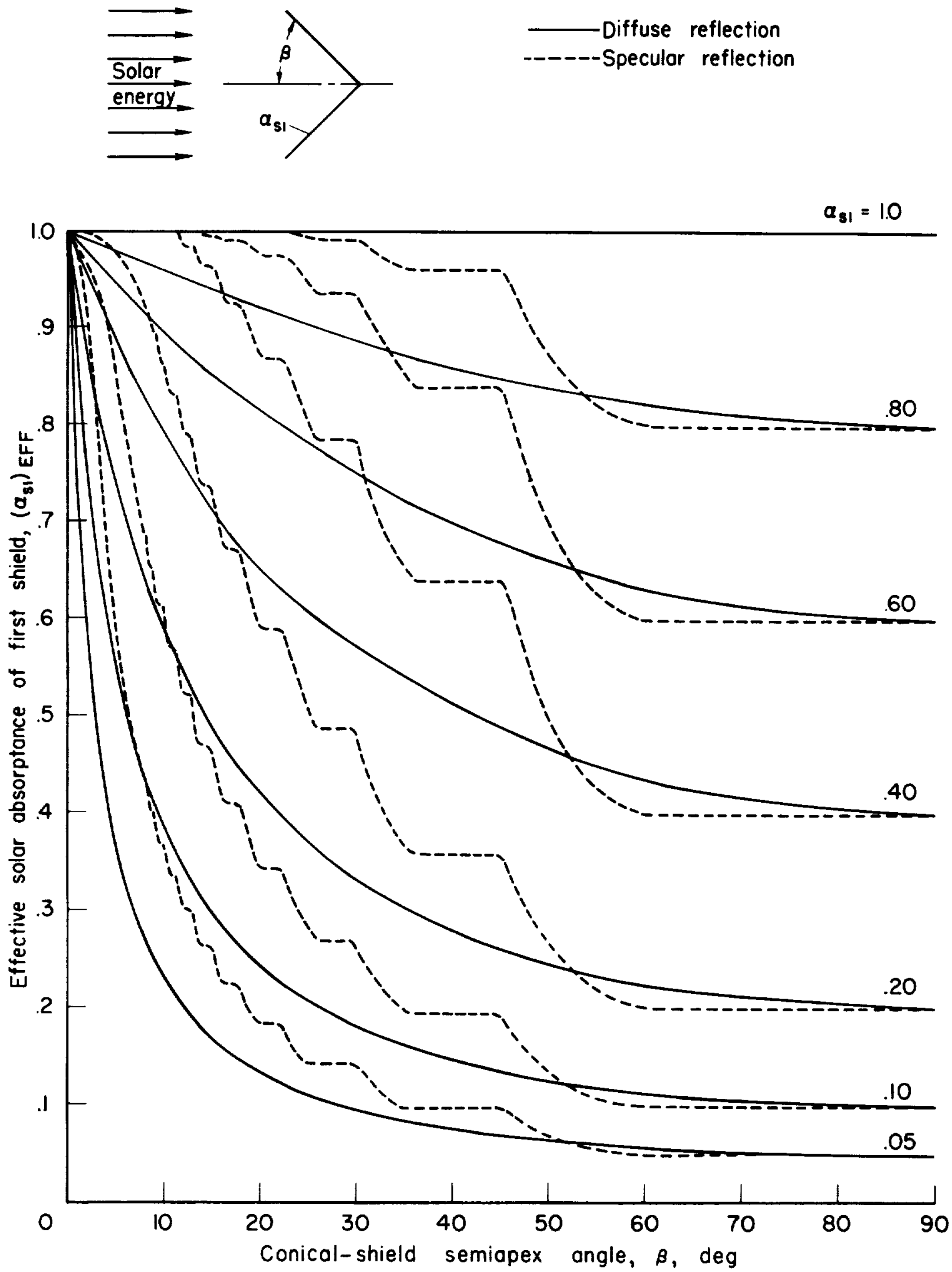

Figure 16.- Variation of effective solar absorptance for conical shields; diffuse and specular reflections.

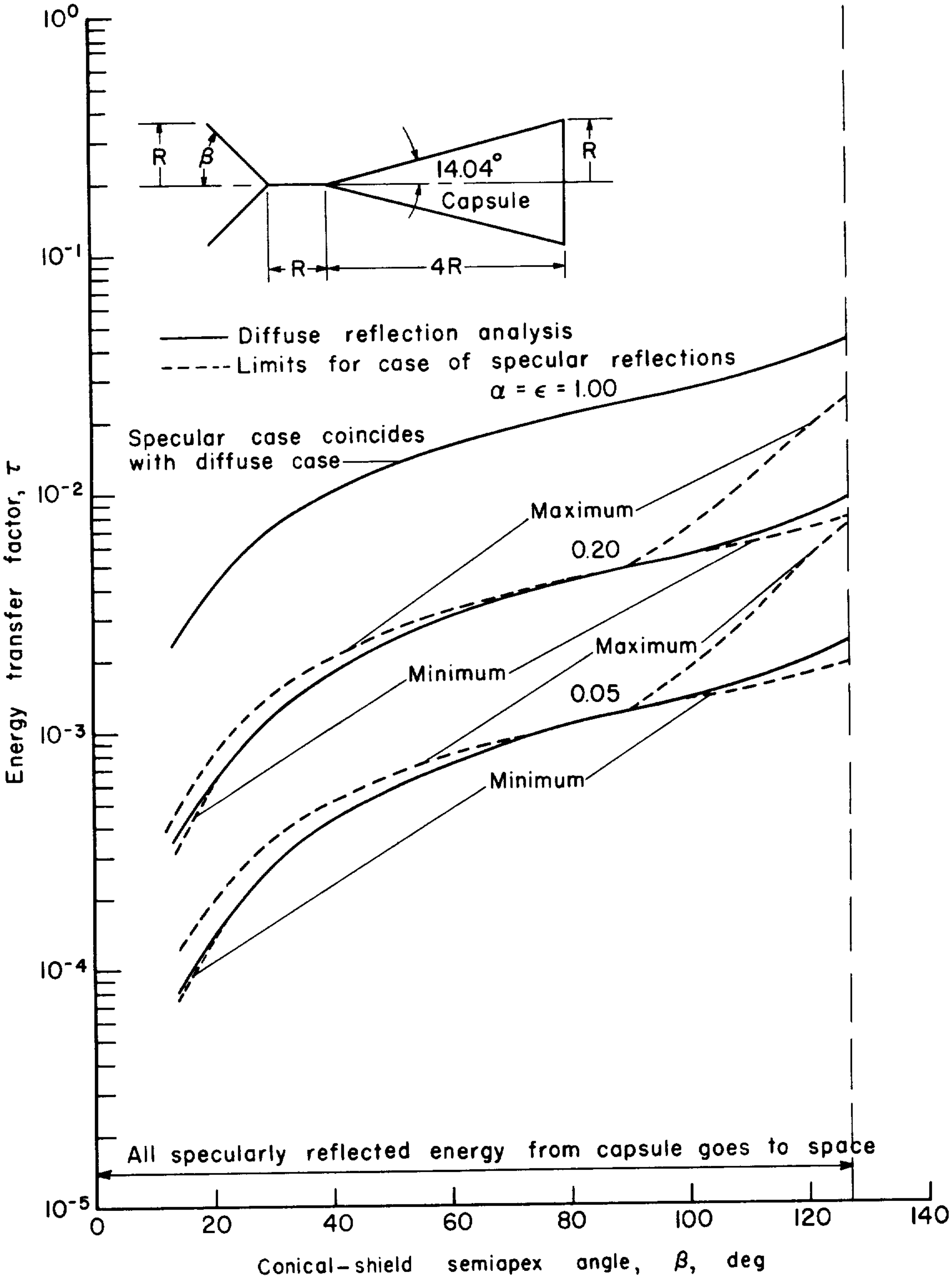

Figure 17.- Energy transfer factors for the diffuse reflection analysis and the limiting values for specular reflections.

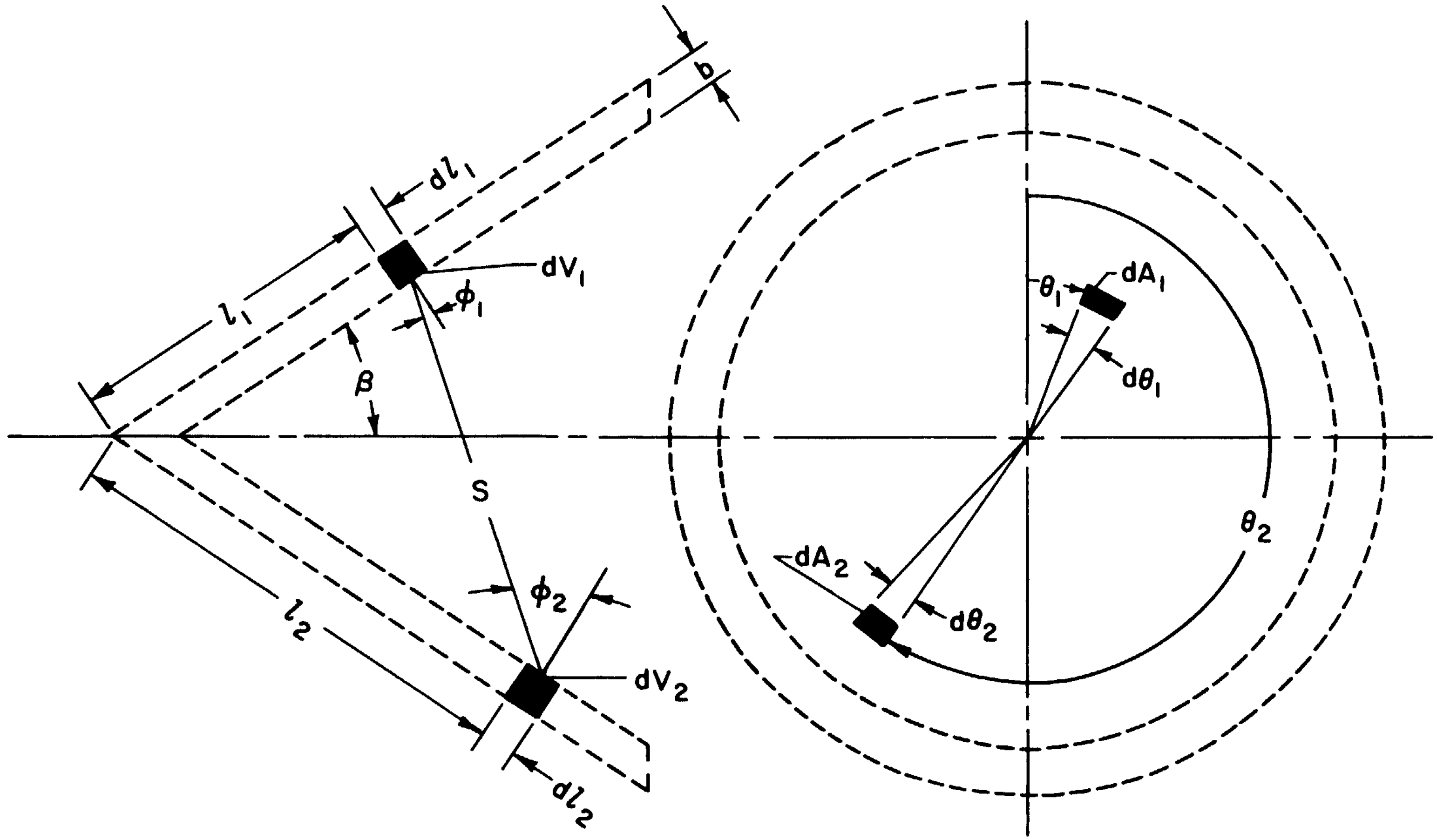

Figure 18.- Configuration for finite conductance analysis.

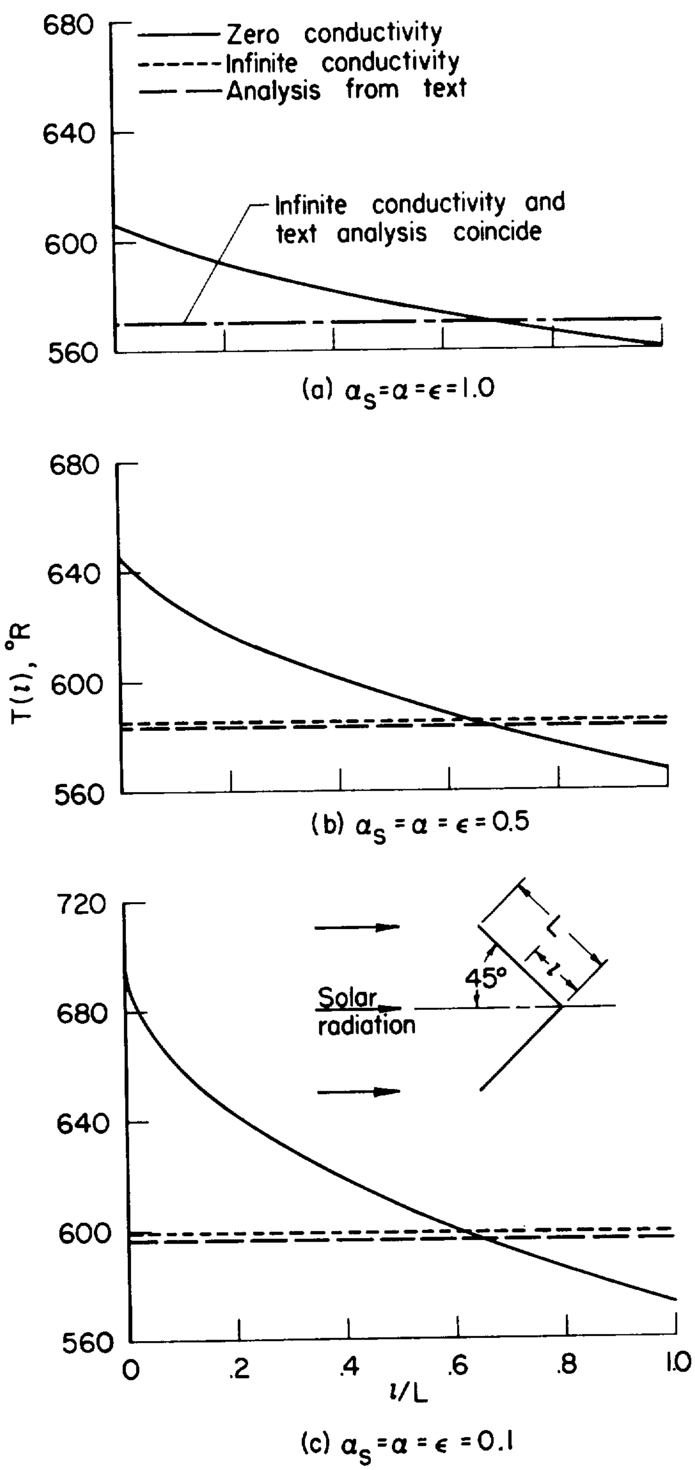

Figure 19.- Effects of thermal conductivity upon the temperature distribution of a 45° conical shield for incident solar radiation; $\bar{r}$ = 1.0 A.U.

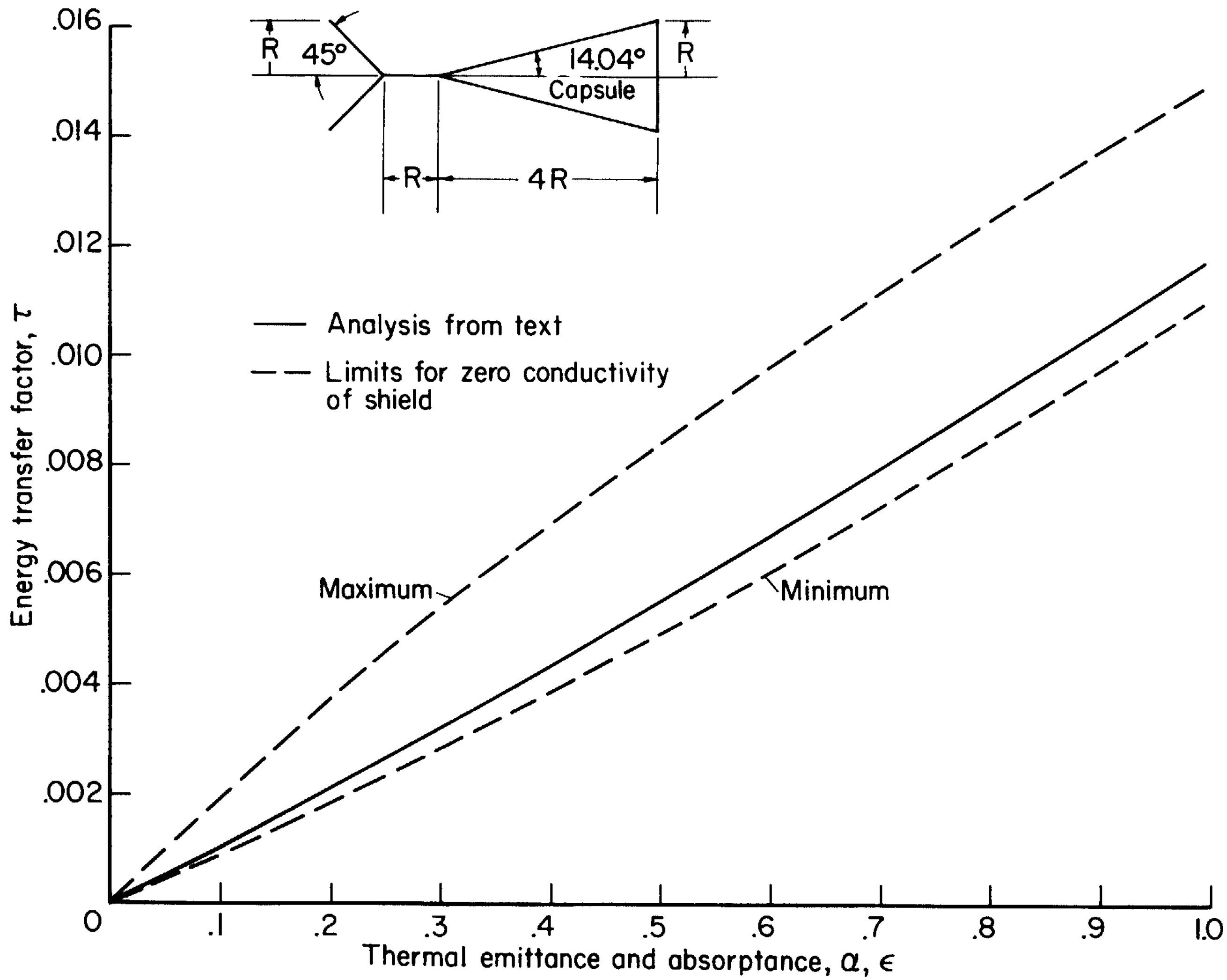

Figure 20.- Limiting values of energy transfer factor for zero conductivity of the shield.

NASA TN D-1209
National Aeronautics and Space Administration.
ANALYSIS OF SOLAR-RADIATION SHIELDS FOR TEMPERATURE CONTROL OF SPACE VEHICLES SUBJECTED TO LARGE CHANGES IN SOLAR ENERGY. George J. Nothwang, John C. Arvesen, and Frank M. Hamaker. March 1962. 76p. OTS price, $2.00. (NASA TECHNICAL NOTE D-1209)

A passive temperature control system which effectively isolates a capsule from variable solar energy by the use of solar radiation shields and utilizes the internal heat load of the capsule to maintain the desired capsule temperature level was studied by means of a radiative heat-transfer analysis. Parameters were established which indicated the important criteria for achieving the desired temperature control. The analysis is applied to two typical solar probe configurations for which shield and capsule temperatures are presented as a function of distance from the sun. The effects of diffusely and specularly reflecting

Copies obtainable from NASA, Washington (over)

I. Nothwang, George J.
II. Arvesen, John C.
III. Hamaker, Frank M.
IV. NASA TN D-1209

(Initial NASA distribution: 25, Materials, engineering; 28, Missiles and satellite carriers; 31, Physics, nuclear and particle; 35, Power sources, supplementary; 48, Space vehicles; 52, Structures.)

NASA

NASA TN D-1209
National Aeronautics and Space Administration.
ANALYSIS OF SOLAR-RADIATION SHIELDS FOR TEMPERATURE CONTROL OF SPACE VEHICLES SUBJECTED TO LARGE CHANGES IN SOLAR ENERGY. George J. Nothwang, John C. Arvesen, and Frank M. Hamaker. March 1962. 76p. OTS price, $2.00. (NASA TECHNICAL NOTE D-1209)

A passive temperature control system which effectively isolates a capsule from variable solar energy by the use of solar radiation shields and utilizes the internal heat load of the capsule to maintain the desired capsule temperature level was studied by means of a radiative heat-transfer analysis. Parameters were established which indicated the important criteria for achieving the desired temperature control. The analysis is applied to two typical solar probe configurations for which shield and capsule temperatures are presented as a function of distance from the sun. The effects of diffusely and specularly reflecting

Copies obtainable from NASA, Washington (over)

I. Nothwang, George J.
II. Arvesen, John C.
III. Hamaker, Frank M.
IV. NASA TN D-1209

(Initial NASA distribution: 25, Materials, engineering; 28, Missiles and satellite carriers; 31, Physics, nuclear and particle; 35, Power sources, supplementary; 48, Space vehicles; 52, Structures.)

NASA

NASA TN D-1209
National Aeronautics and Space Administration.
ANALYSIS OF SOLAR-RADIATION SHIELDS FOR TEMPERATURE CONTROL OF SPACE VEHICLES SUBJECTED TO LARGE CHANGES IN SOLAR ENERGY. George J. Nothwang, John C. Arvesen, and Frank M. Hamaker. March 1962. 76p. OTS price, $2.00. (NASA TECHNICAL NOTE D-1209)

A passive temperature control system which effectively isolates a capsule from variable solar energy by the use of solar radiation shields and utilizes the internal heat load of the capsule to maintain the desired capsule temperature level was studied by means of a radiative heat-transfer analysis. Parameters were established which indicated the important criteria for achieving the desired temperature control. The analysis is applied to two typical solar probe configurations for which shield and capsule temperatures are presented as a function of distance from the sun. The effects of diffusely and specularly reflecting

Copies obtainable from NASA, Washington (over)

I. Nothwang, George J.
II. Arvesen, John C.
III. Hamaker, Frank M.
IV. NASA TN D-1209

(Initial NASA distribution: 25, Materials, engineering; 28, Missiles and satellite carriers; 31, Physics, nuclear and particle; 35, Power sources, supplementary; 48, Space vehicles; 52, Structures.)

NASA

NASA TN D-1209
National Aeronautics and Space Administration.
ANALYSIS OF SOLAR-RADIATION SHIELDS FOR TEMPERATURE CONTROL OF SPACE VEHICLES SUBJECTED TO LARGE CHANGES IN SOLAR ENERGY. George J. Nothwang, John C. Arvesen, and Frank M. Hamaker. March 1962. 76p. OTS price, $2.00. (NASA TECHNICAL NOTE D-1209)

A passive temperature control system which effectively isolates a capsule from variable solar energy by the use of solar radiation shields and utilizes the internal heat load of the capsule to maintain the desired capsule temperature level was studied by means of a radiative heat-transfer analysis. Parameters were established which indicated the important criteria for achieving the desired temperature control. The analysis is applied to two typical solar probe configurations for which shield and capsule temperatures are presented as a function of distance from the sun. The effects of diffusely and specularly reflecting

Copies obtainable from NASA, Washington (over)

I. Nothwang, George J.
II. Arvesen, John C.
III. Hamaker, Frank M.
IV. NASA TN D-1209

(Initial NASA distribution: 25, Materials, engineering; 28, Missiles and satellite carriers; 31, Physics, nuclear and particle; 35, Power sources, supplementary; 48, Space vehicles; 52, Structures.)

NASA

NASA TN D-1209

surfaces and of infinite and zero thermal conductance of the shield material are discussed.

Copies obtainable from NASA, Washington

NASA

NASA TN D-1209

surfaces and of infinite and zero thermal conductance of the shield material are discussed.

Copies obtainable from NASA, Washington

NASA

NASA TN D-1209

surfaces and of infinite and zero thermal conductance of the shield material are discussed.

Copies obtainable from NASA, Washington

NASA

NASA TN D-1209

surfaces and of infinite and zero thermal conductance of the shield material are discussed.

Copies obtainable from NASA, Washington

NASA

NASA TN D-1209
National Aeronautics and Space Administration.
ANALYSIS OF SOLAR-RADIATION SHIELDS FOR TEMPERATURE CONTROL OF SPACE VEHICLES SUBJECTED TO LARGE CHANGES IN SOLAR ENERGY. George J. Nothwang, John C. Arvesen, and Frank M. Hamaker. March 1962. 76p. OTS price, $2.00. (NASA TECHNICAL NOTE D-1209)

A passive temperature control system which effectively isolates a capsule from variable solar energy by the use of solar radiation shields and utilizes the internal heat load of the capsule to maintain the desired capsule temperature level was studied by means of a radiative heat-transfer analysis. Parameters were established which indicated the important criteria for achieving the desired temperature control. The analysis is applied to two typical solar probe configurations for which shield and capsule temperatures are presented as a function of distance from the sun. The effects of diffusely and specularly reflecting

Copies obtainable from NASA, Washington (over)

I. Nothwang, George J.
II. Arvesen, John C.
III. Hamaker, Frank M.
IV. NASA TN D-1209

(Initial NASA distribution: 25, Materials, engineering; 28, Missiles and satellite carriers; 31, Physics, nuclear and particle; 35, Power sources, supplementary; 48, Space vehicles; 52, Structures.)

NASA

NASA TN D-1209
National Aeronautics and Space Administration.
ANALYSIS OF SOLAR-RADIATION SHIELDS FOR TEMPERATURE CONTROL OF SPACE VEHICLES SUBJECTED TO LARGE CHANGES IN SOLAR ENERGY. George J. Nothwang, John C. Arvesen, and Frank M. Hamaker. March 1962. 76p. OTS price, $2.00. (NASA TECHNICAL NOTE D-1209)

A passive temperature control system which effectively isolates a capsule from variable solar energy by the use of solar radiation shields and utilizes the internal heat load of the capsule to maintain the desired capsule temperature level was studied by means of a radiative heat-transfer analysis. Parameters were established which indicated the important criteria for achieving the desired temperature control. The analysis is applied to two typical solar probe configurations for which shield and capsule temperatures are presented as a function of distance from the sun. The effects of diffusely and specularly reflecting

Copies obtainable from NASA, Washington (over)

I. Nothwang, George J.
II. Arvesen, John C.
III. Hamaker, Frank M.
IV. NASA TN D-1209

(Initial NASA distribution: 25, Materials, engineering; 28, Missiles and satellite carriers; 31, Physics, nuclear and particle; 35, Power sources, supplementary; 48, Space vehicles; 52, Structures.)

NASA

NASA TN D-1209
National Aeronautics and Space Administration.
ANALYSIS OF SOLAR-RADIATION SHIELDS FOR TEMPERATURE CONTROL OF SPACE VEHICLES SUBJECTED TO LARGE CHANGES IN SOLAR ENERGY. George J. Nothwang, John C. Arvesen, and Frank M. Hamaker. March 1962. 76p. OTS price, $2.00. (NASA TECHNICAL NOTE D-1209)

A passive temperature control system which effectively isolates a capsule from variable solar energy by the use of solar radiation shields and utilizes the internal heat load of the capsule to maintain the desired capsule temperature level was studied by means of a radiative heat-transfer analysis. Parameters were established which indicated the important criteria for achieving the desired temperature control. The analysis is applied to two typical solar probe configurations for which shield and capsule temperatures are presented as a function of distance from the sun. The effects of diffusely and specularly reflecting

Copies obtainable from NASA, Washington (over)

I. Nothwang, George J.
II. Arvesen, John C.
III. Hamaker, Frank M.
IV. NASA TN D-1209

(Initial NASA distribution: 25, Materials, engineering; 28, Missiles and satellite carriers; 31, Physics, nuclear and particle; 35, Power sources, supplementary; 48, Space vehicles; 52, Structures.)

NASA

NASA TN D-1209
National Aeronautics and Space Administration.
ANALYSIS OF SOLAR-RADIATION SHIELDS FOR TEMPERATURE CONTROL OF SPACE VEHICLES SUBJECTED TO LARGE CHANGES IN SOLAR ENERGY. George J. Nothwang, John C. Arvesen, and Frank M. Hamaker. March 1962. 76p. OTS price, $2.00. (NASA TECHNICAL NOTE D-1209)

A passive temperature control system which effectively isolates a capsule from variable solar energy by the use of solar radiation shields and utilizes the internal heat load of the capsule to maintain the desired capsule temperature level was studied by means of a radiative heat-transfer analysis. Parameters were established which indicated the important criteria for achieving the desired temperature control. The analysis is applied to two typical solar probe configurations for which shield and capsule temperatures are presented as a function of distance from the sun. The effects of diffusely and specularly reflecting

Copies obtainable from NASA, Washington (over)

I. Nothwang, George J.
II. Arvesen, John C.
III. Hamaker, Frank M.
IV. NASA TN D-1209

(Initial NASA distribution: 25, Materials, engineering; 28, Missiles and satellite carriers; 31, Physics, nuclear and particle; 35, Power sources, supplementary; 48, Space vehicles; 52, Structures.)

NASA

NASA TN D-1209

surfaces and of infinite and zero thermal conductance of the shield material are discussed.

Copies obtainable from **NASA**, **Washington**

NASA

NASA TN D-1209

surfaces and of infinite and zero thermal conductance of the shield material are discussed.

Copies obtainable from **NASA**, **Washington**

NASA

NASA TN D-1209

surfaces and of infinite and zero thermal conductance of the shield material are discussed.

Copies obtainable from **NASA**, **Washington**

NASA

NASA TN D-1209

surfaces and of infinite and zero thermal conductance of the shield material are discussed.

Copies obtainable from **NASA**, **Washington**

NASA